AN ABSTRACT OF THE THESIS OF

Daniel P. Jordheim for the degree of Master of Science in Nuclear Engineering presented on October 5, 1990. Title: CHAIN.238DJ: A Computer Code for Calculating Pu-238 Production, Quality, and Impurity Levels in the Np-237 Transmutation Chain

Redacted for Privacy

Abstract Approved: _____
Dr. Stephen E. Binney

The computer code CHAIN.238DJ calculates ^{238}Pu production, plutonium quality, and ^{236}Pu impurity levels in the chain of nuclides that results from neutron and photon irradiation of ^{237}Np target material. The code contains methods for accounting for burnup dependent resonance and spatial self shielding and local fission neutron sources. The isotopic compositions of the chain are calculated as a function of burnup and printed out for a user-specified cycle history of intermittent irradiation and decay periods.

The code requires group fluxes, effective cross sections, half lives, initial nuclide amounts, C-factors, and irradiation/decay cycle information as input. The code is small, quick, and easy to use. Its input file is only slightly more than one page long and is easy to set up. The code can be adapted to run on almost any computer, the main concern being the number of digits of accuracy kept in the representation of FORTRAN real variables. When used properly, the CHAIN.238DJ code accurately calculates isotopic compositions in the ^{237}Np transmutation chain.

CHAIN.238DJ: A Computer Code for Calculating Pu-238 Production, Quality, and Impurity Levels in the Np-237 Transmutation Chain

by

Daniel P. Jordheim

A THESIS

submitted to

Oregon State University

in partial fulfillment of
the requirements for the
degree of

Master of Science

Completed October 5, 1990

Commencement June, 1991

APPROVED:

Redacted for Privacy

Professor of Nuclear Engineering in charge of major

Redacted for Privacy

Head of department of Nuclear Engineering

Redacted for Privacy

Dean of Graduate School

Date thesis is presented October 5, 1990

Typed by the researcher for Daniel P. Jordheim

WHC-MR-0220

CHAIN.238DJ: A Computer Code for Calculating ^{238}Pu Production, Quality, and Impurity Levels In the ^{237}Np Transmutation Chain

D. P. Jordheim

Date Published
September 1990

To be presented at
Masters Thesis Defense
Corvallis, Oregon
October 5, 1990

Prepared for the U.S. Department of Energy
Assistant Secretary for Nuclear Energy

Westinghouse Hanford Company
P.O. Box 1970
Richland, Washington 99352

Hanford Operations and Engineering Contractor for the
U.S. Department of Energy under Contract DE-AC06-87RL10930

This document was prepared in partial fulfillment of the requirements for a Master of Science degree in Nuclear Engineering from Oregon State University, Corvallis, Oregon.

Approved for Public Release

ACKNOWLEDGEMENTS

Several people have been particularly helpful and supportive during the preparation of this document and the completion of my Master's degree studies. Dr. S. E. Binney of Oregon State University has provided guidance and moral support not only in the preparation of this document and the completion of my Master's program, but throughout my entire academic career at OSU. Dr. R. E. Schenter of Westinghouse Hanford Company (WHC) has provided technical guidance as my WHC advisor and has been a constant advocate for me to WHC management and staff. Dr. J. W. Daughtry and R. E. Schenter of WHC, and my ever-supportive sister R. J. Macdonald of the law firm of Hazel, Thomas, Fiske, Beckhorn & Hanes have all been important in providing financial support during the preparation of this document. Dr. F. A. Schmittroth of WHC has provided valuable technical consultation about the AKM and TRANX computer subroutines developed by him, and provided computer software used in the preparation of this document. Dr. F. M. Mann of WHC has been a consultant on matters of cross section data and has provided computer software used to generate plots of that data. Dr. L. L. Carter and D. W. Wootan of WHC have provided guidance on the use of the MCNP computer code. Dr. J. A. Rawlins of WHC has been helpful because of his clear understanding of resonance and spatial self-shielding. All of those mentioned above have been most helpful by providing constant challenge and encouragement, even insistence, that I complete this document and the requirements for the degree.

Printed in the United States of America

DISCLM-2.CHP (7-90)

TABLE OF CONTENTS

LIST OF FIGURES

LIST OF FIGURES - CONT.

LIST OF FIGURES - CONT.

LIST OF FIGURES - CONT.

LIST OF FIGURES - CONT.

LIST OF TABLES

CHAIN.238DJ: A COMPUTER CODE FOR CALCULATING Pu-238 PRODUCTION, QUALITY, AND IMPURITY LEVELS IN THE Np-237 TRANSMUTATION CHAIN

1.0 INTRODUCTION

The computer code CHAIN.238DJ is used to calculate the isotopic concentrations of various nuclides of importance in the transmutation chain that results from neutron and photon irradiation of ^{237}Np. The code requires fluxes, effective microscopic cross sections, half lives, initial nuclide concentrations, and irradiation/decay cycle information as input. Given this information, CHAIN.238DJ calculates time-dependent concentrations of the nuclides in the chain at a point in space.

The basic transmutation calculations performed by the CHAIN.238DJ code could easily be accomplished using any of several other existing computer codes, but the CHAIN.238DJ code has additional features that are important. The CHAIN.238DJ code is relatively small, simple, and easy to use. It is specific to the transmutation chain that arises from the irradiation of ^{237}Np for production of ^{238}Pu, whereas most other transmutation codes are much more general. An important part of this transmutation chain is the production of ^{236}Pu, which is an undesirable impurity because one of its daughter products, ^{208}Tl, produces a very high energy γ ray that is difficult to shield. The ^{236}Pu arises as a daughter product of ^{236}Np, which is produced by $^{237}Np(\gamma,n)^{236}Np$ and $^{237}Np(n,2n)^{236}Np$ reactions. The CHAIN.238DJ code calculates the production of the ^{236}Pu impurity through both paths. The CHAIN.238DJ code prints a small summary output that includes the ^{236}Pu impurity level in units of parts per million (ppm) $^{236}Pu/Pu$. The CHAIN.238DJ code also contains methods that account for changing resonance and spatial self-shielding in the transmutation chain. The code accomplishes this by compensating, as a function of time of irradiation, for changes in group fluxes and in effective resonance integrals for individual nuclides.

The most basic operation performed by the CHAIN.238DJ code is to solve the set of differential equations that describe the reactions taking place during transmutation. The solutions to these types of equations were first given by Bateman[1]. Since then, several solution methods have been devised and some have been implemented in computer codes. Some of these existing codes are capable of performing the basic task of solving the transmutation equations for the $^{237}Np/^{238}Pu$ chain, but none is known to incorporate the features, specificity to ^{238}Pu production from irradiation of ^{237}Np, and simplicity that are found in the CHAIN.238DJ code. The ORIGEN2[2] code is widely used for transmutation calculations but it is very general, it does not calculate $^{237}Np(\gamma,n)^{236}Np$ reactions, and it does not contain the simple features for treatment of self-shielding that are found in CHAIN.238DJ. The fission product inventory code RIBD[3] follows fission products and their transmutation, but does not treat actinides other than ^{235}U, ^{238}U, and ^{239}Pu. The CINDER[4] and EPRI-CINDER[5] fission product inventory codes consider the transmutation of actinides, but they lack the simplicity and the treatment of $^{237}Np(\gamma,n)^{236}Np$ reactions found in CHAIN.238DJ. The CRUNCH[6] code is used for calculating the transmutation of actinides and contains a treatment of self-shielding similar to that found in CHAIN.238DJ, but it is not specific to the $^{237}Np/^{238}Pu$ chain. In the CHAIN.238DJ code, the transmutation equations are solved by use of a somewhat simpler method than is found in some of these other codes, but for the situations in which the CHAIN.238DJ code is used, the method is sufficient.

Like any other computer code, the CHAIN.238DJ code cannot be used like a magic "black box". If used improperly and given the wrong input, the code will calculate incorrect answers. Even if given correct input data, the code can give incorrect answers if not used properly. The user must understand the various methods and models built into the code and must use the code in a way that applies to the situation at hand. Spatial effects are not explicitly treated by the CHAIN.238DJ code and must be considered separately. Occasional comparison of results with those from a calculation that models the

same situation with other methods may be useful, especially when applying the code to new situations with which the user has little or no experience.

The CHAIN.238DJ code is small, quick, and easy to use. Its input file is only slightly more than one page and is easy to set up. Appendix A contains a listing of the CHAIN.238DJ source code, an example input file, and example output. The code can be adapted to run on most computers, the main concern being the number of digits of numerical accuracy kept by the machine. If used properly, the CHAIN.238DJ code is capable of accurately calculating the buildup of isotopes in the ^{237}Np transmutation chain.

2.0 THE AKM METHOD FOR SOLVING SETS OF DIFFERENTIAL EQUATIONS

The CHAIN.238DJ code uses an exponential method for solving the set of differential equations that describe the reactions that occur in the $^{237}Np/^{238}Pu$ transmutation chain. The method uses the theory and the "AKM" computer code subroutine developed by Schmittroth[7] for the SDCAY computer code system used at Westinghouse Hanford Company. This method is fairly general, and can be applied to many situations where there are transmutation and decay chains.

Given some arbitrary transmutation and decay chain such as the example depicted in Figure 2.1, the equations that describe the time-dependent concentrations of the nuclides in the chain are:

$$dN_1/dt = - N_1(t)\sigma_{a,1}\phi \qquad (2.1)$$

$$dN_2/dt = N_1(t)\sigma_{\gamma,1}\phi - N_2(t)\sigma_{a,2}\phi - N_2(t)\lambda_2 \qquad (2.2)$$

$$dN_3/dt = N_2(t)\sigma_{\gamma,2}\phi - N_3(t)\sigma_{a,3}\phi - N_3(t)\lambda_3 \qquad (2.3)$$

$$dN_4/dt = N_2(t)\lambda_2 - N_4(t)\sigma_{a,4}\phi \qquad (2.4)$$

$$dN_5/dt = N_3(t)\lambda_3 + N_4(t)\sigma_{\gamma,4}\phi - N_5(t)\sigma_{a,5}\phi \qquad (2.5)$$

where $N_1(t)$ = the amount of ^{169}Tm at time t

$N_2(t)$ = the amount of ^{170}Tm at time t

$N_3(t)$ = the amount of ^{171}Tm at time t

$N_4(t)$ = the amount of ^{170}Yb at time t

$N_5(t)$ = the amount of ^{171}Yb at time t

λ_i = the radioactive decay constant for nuclide i

$\sigma_{a,i}\phi = \int_o^\infty \sigma_{a,i}(E)\phi_E(E)dE$ = the microscopic total neutron absorption reaction rate for nuclide i

$\sigma_{\gamma,i}\phi = \int_o^\infty \sigma_{\gamma,i}(E)\phi_E(E)dE$ = the microscopic total radiative neutron capture reaction rate for nuclide i

$\phi_E(E)$ = the energy dependent neutron flux per unit energy

$\sigma_{a,i}(E)$ = the microscopic total neutron absorption cross section for nuclide i

$\sigma_{\gamma,i}(E)$ = the microscopic radiative neutron capture cross section for nuclide i

All energy dependence has been integrated out of the equations, and the determination of the absorption and radiative capture reaction rates is done outside of the AKM method. The equations actually apply at a point in space, so there is no spatial dependence.

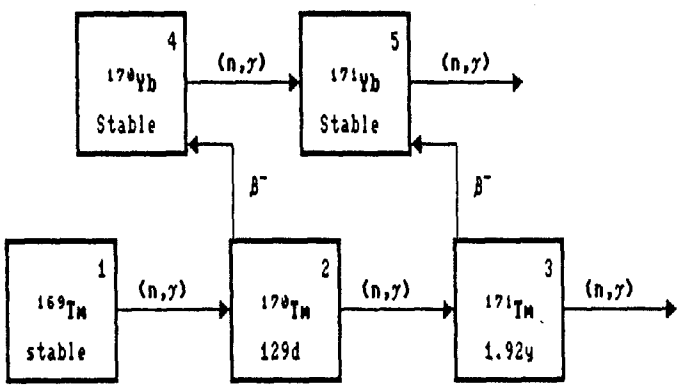

Figure 2.1 Thulium Transmutation Chain

Equations 2.1-2.5 can be stated in a simpler form by writing them in terms of nuclide loss coefficients, β_k, and nuclide gain coefficients, $\alpha_{i,k}$. The β_k terms always consist of the sum of the radioactive decay constant (λ_k) and the microscopic total neutron absorption reaction rate $\sigma_{a,k}\phi$. The $\alpha_{i,k}$ terms depend on what mechanisms exist for producing nuclide k. Each $\alpha_{i,k}$ term represents the rate of nuclide i "feeding" or producing nuclide k. The new form of Equations 2.1 through 2.5 becomes:

$$dN_1/dt = - N_1(t)\beta_1 \qquad (2.6)$$

$$dN_2/dt = N_1(t)\alpha_{1,2} - N_2(t)\beta_2 \qquad (2.7)$$

$$dN_3/dt = N_2(t)\alpha_{2,3} - N_3(t)\beta_3 \qquad (2.8)$$

$$dN_4/dt = N_2(t)\alpha_{2,4} - N_4(t)\beta_4 \qquad (2.9)$$

$$dN_5/dt = N_3(t)\alpha_{3,5} + N_4(t)\alpha_{4,5} - N_5(t)\beta_5 \qquad (2.10)$$

where $\beta_k = \lambda_k + \sigma_{a,k}\phi$

$\alpha_{1,2} = \sigma_{\gamma,1}\phi$

$\alpha_{2,3} = \sigma_{\gamma,2}\phi$

$\alpha_{2,4} = \lambda_2$

$\alpha_{3,5} = \lambda_3$

$\alpha_{4,5} = \sigma_{\gamma,4}\phi$

If all the coefficients (the $\alpha_{i,k}$ and β_k factors) in the equations above are constants, this set of equations can be solved analytically by seeking solutions in the form of a sum of exponentials. These solutions may assume the form:

$$N_k(t) = \sum_{m=1}^{k} [A_{k,m} e^{-\beta_m t}] \qquad (2.11)$$

where $A_{1,1} = N_1(0)$

$$A_{k,m} = \frac{1}{\beta_k - \beta_m} \sum_{i=m}^{k-1} [A_{i,m}\alpha_{i,k}] \quad \text{for } m < k \qquad (2.12)$$

$$A_{k,k} = N_k(0) - \sum_{j=1}^{k-1} A_{k,j} \quad \text{for } m = k \qquad (2.13)$$

The detailed solutions for Equations 2.6 and 2.7 give the time-dependent concentrations of the first two nuclides in the chain:

$$N_1(t) = A_{1,1} e^{-\beta_1 t} \qquad (2.14)$$

where $A_{1,1} = N_1(0)$

$$N_2(t) = A_{2,1} e^{-\beta_1 t} + A_{2,2} e^{-\beta_2 t} \qquad (2.15)$$

where $A_{2,1} = (A_{1,1}\alpha_{1,2})/(\beta_2 - \beta_1)$

$A_{2,2} = N_2(0) - A_{2,1}$

The solutions for the rest of the nuclides in the chain take on a similar form, but become increasingly long and cumbersome to write out on paper.

This solution method can be applied to many different decay or transmutation chains, with the limitation that the nuclides must always feed up the chain, that is, the $\alpha_{i,k}$ only exist for $k > i$. This restriction rules out using this method to analyze chains in which significant alpha decay from the upper end of the transmutation chain may feed back to the lower end of the chain.

All of the above equations for $N_k(t)$ can easily be solved for any time (t) when they are programmed into a digital computer. In the CHAIN.238DJ code, the AKM subroutine first calculates all of the coefficients (the $A_{k,m}$ values) sequentially, then the TRANX subroutine uses these values to calculate the sum of the applicable exponentials, yielding values of $N_k(t)$ for each nuclide. All that is needed are initial amounts of each nuclide, the values of the constant coefficients β_k and $\alpha_{i,k}$, and the time t. The radioactive decay constants (λ_k) are simply taken from known data. The time step size, t, is chosen as desired. This leaves a set of microscopic total reaction rates ($\sigma_{a,k}\phi$ and $\sigma_{\gamma,k}\phi$) as the only other data needed. These reaction rates can be calculated using any of several computer codes common in the nuclear reactor physics community and can often be estimated by simple hand calculations.

2.1 Pitfalls of the AKM Method

Although the AKM method outlined above gives analytically correct solutions to the differential equations, there are situations in which the method will fail.

One fairly obvious situation in which the AKM method fails is when the β_k's in the denominator of Equation 2.12 are equal to one another. This happens in situations where there are two stable nuclides in a chain that describes strictly radioactive decay. It would be unusual for this to happen in a chain that describes transmutation, since two of the nuclides in the chain would need to have neutron cross sections and radioactive decay constants such that

their β_k values would be equal, and this would be somewhat of a remarkable coincidence. When this problem does occur, it is usually possible to alter one of the β_k values slightly, allowing the code to work without significantly impacting the results.

Other, less obvious problems can occur when using the AKM method. Consider the example transmutation chain shown in Figure 2.2, a simple case of radiative neuton capture along an isotopic line where all the isotopes are stable. Assume that we start with one gram-atom of ^{114}Sn and irradiate it for 100 days. Also assume the realistic values shown in Table 2.1 for the total microscopic radiative neuton capture reaction rates (the products $\sigma_{\gamma,k}\phi$). The transmutation calculation has been performed on two different computers, but with the exact same FORTRAN source code (using the AKM method) compiled on each machine. The ORIGEN2 code was also run as a comparison with AKM. The exact same input data are used in all three calculations. The results are shown in Table 2.1. The AKM calculation on the SUN 4/260 begins to give incorrect answers at the third isotope. The same code compiled on the CRAY X-MP/18 becomes incorrect by the fifth isotope.

Nuclide	Reaction Rate	Nuclide Amounts (Gram-Atoms)			
		Initial Amount	100 Days AKM SUN 4/260	100 Days AKM CRAY X-MP/18	100 Days ORIGEN2 CRAY X-MP/18
^{114}Sn	6.33e+15	1.00	0.947	0.947	0.947
^{115}Sn	6.31e+15	0.0	5.18e-2	5.18e-2	5.18e-2
^{116}Sn	6.29e+15	0.0	2.98e-3	1.41e-3	1.41e-3
^{117}Sn	6.27e+15	0.0	-0.3121	2.56e-5	2.56e-5
^{118}Sn	6.25e+15	0.0	24.4	2.50e-9	3.46e-7
^{119}Sn	6.23e+15	0.0	7.04	-3.6e-4	3.74e-9
Total	-	1.00	32.13	1.00	1.00

Table 2.1 Results of Erroneous AKM Calculation

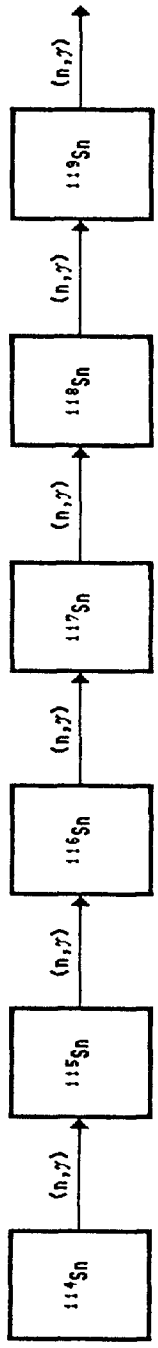

Figure 2.2 Tin Transmutation Chain

The problem in this example calculation is that the machines do not keep enough digits of accuracy in their representation of real numbers, even when using double precision FORTRAN variables. Recall that the AKM method expresses the solution to the differential equations as a sum of some exponential terms. Table 2.2 shows the values of these terms and their cumulative sums for this example.

k	m	$A_{k,m}e^{-\beta_m t}$	$\sum_{n=1}^{m} A_{k,n}e^{-\beta_n t}$
1	1	0.946777467699025265801537898	0.946777467699025265801537898
2	1	-299.655068526741496626186745	-299.655068526741496626186745
2	2	299.706853396667197486635814	0.051784869925700860449069296
3	1	4.72705870600936915315881 6e+4	4.72705870600936915315881 6e+4
3	2	-9.455751224664894176083 82e+4	-4.728692518655525022925 01e+4
3	3	4.728692659829128705812672e+4	0.001411736036828876639018907
4	1	-4.955533210133160435727 19e+6	-4.955533210133160435727 19e+6
4	2	1.486916880078558963608002e+7	9.913635590652429200352828e+6
4	3	-1.487173841516265333149 41e+7	-4.958102824510224131141 32e+6
4	4	4.958102824535811229381475e+6	2.558709824015751473459608e-5
5	1	3.883899153441878493774220e+8	3.883899153441878493774220e+8
5	2	-1.553828139682096769748 45e+9	-1.165438224337908920371 03e+9
5	3	2.331144996576742663730848e+9	1.165706772238833743359819e+9
5	4	-1.554365235491982424224 57e+9	-3.886584632531486808647 50e+8
5	5	3.886584632531486833624308e+8	2.497680375552840080499717e-9
6	1	-2.427436970901186157701 4e+10	-2.427436970901186157701 4e+10
6	2	1.213928234126640684155 88e+11	9.711845370365220683857 34e+10
6	3	-2.428276038100777052368 0e+11	-1.457091501064254983982 2e+11
6	4	2.428695680456227705216 22e+11	9.716041793919727212339 99e+10
6	5	-1.214557697666092761761 8e+11	-2.429535182741200405277 6e+10
6	6	2.429535182741163968161 52e+10	-3.643711611651264357936 15e-4

Table 2.2 Exponential Terms from Erroneous AKM Calculation on CRAY

Notice that the final answer consists of the sum of some relatively large numbers, some of which are negative and some of which are positive. The problem is essentially a case of trying to calculate very small differences between relatively large numbers. It is a computer round-off error problem. As the calculation is done for isotopes further down the transmutation chain, one is forced to go out to an increasingly large number of digits of accuracy before any difference shows up. Since the CRAY machine has a 64-bit word and the SUN machine has only a 32-bit word, the CRAY effectively keeps twice

as many digits of accuracy as the SUN does. The SUN machine does not keep enough digits of accuracy to calculate this particular problem correctly beyond the second isotope. The CRAY machine does about twice as well, but it fails to calculate the problem correctly beyond the fourth isotope.

The root of the problem in this example case lies in the small differences between the cross sections used for the isotopes. These cross sections result in β_k values that are not close enough to cause the denominator in Equation 2.12 to be too close to zero, but are close enough to make the differences in the terms in the sum of exponentials very small and hard to calculate. If we assume the different set of values for the reaction rates as shown in Table 2.3, the problem largely ceases to exist. The round-off error problem is

Nuclide	Reaction Rate	Nuclide Amounts (Gram-Atoms)			
		Initial Amount	100 Days AKM SUN 4/260	100 Days AKM CRAY X-MP/18	100 Days ORIGEN2 CRAY X-MP/18
^{114}Sn	6.33e+16	1.00	0.579	0.579	0.579
^{115}Sn	7.50e+15	0.0	0.407	0.407	0.407
^{116}Sn	9.11e+15	0.0	1.42e-2	1.42e-2	1.42e-2
^{117}Sn	2.22e+16	0.0	3.74e-4	3.74e-4	3.74e-4
^{118}Sn	8.34e+16	0.0	1.62e-5	1.63e-5	1.63e-5
^{119}Sn	6.55e+13	0.0	2.49e-6	2.47e-6	2.47e-6
Total	-	1.00	1.00	1.00	1.00

Table 2.3 Results of Correct AKM Calculation

also dependent on the length of the chain being calculated. The data in Table 2.1 show that the longer the chain is, the more digits of accuracy are required. For relatively short chains, this problem usually does not occur.

Notice that in both the AKM calculational results shown in Table 2.1 the code failed to give correct results one isotope up the chain

before it gave a negative amount. This is usually the case, so it is good practice to model the transmutation chain one nuclide beyond what is important. This practice serves as a check on the results. A negative amount strongly suggests that the calculated amount of the previous nuclide and all subsequent nuclides in the chain are incorrect.

Other potential problems in the AKM method come as a result of the use of exponentials. The calculation of exponentials with computers can become inaccurate when the absolute value of the exponent becomes very small. When the exponent is sufficiently small, the AKM method converts to a truncated series to evaluate the exponential. The series representation actually calculates the value of the exponential more accurately than some computers otherwise would. This avoids what would otherwise be a possible source of significant error. Another problem that comes as the result of calculating exponentials is a multiplication of errors or uncertainties in the input data. This is not a source of error in the same sense as the problems with division by zero or computer round-off are, but it is a problem users should be aware of. Some simple calculus shows that with exponentials the value of the exponent acts as an "error multiplication factor". For example, if the data that comprises the exponent has a relative error of 2%, then the relative error in the result of the evaluation of the exponential is equal to 2% multiplied by the value of the exponent. If one is performing a simple calculation of radioactive decay for some arbitrary time period, t, and the value used for the decay constant, λ, is in error by 2%, then the final result will be in error by $2\lambda t$%. Of course, if the value of the exponent λt is less than unity, this can actually be advantageous. This problem does not really constitute an error in the strictest sense since what it really does is just compound errors in the input data, but it is an important problem since it can adversely affect results. One should be concerned about this problem when there is considerable uncertainty in input data and when exponentials are being evaluated where the exponent is much greater than unity, such as

when calculating radioactive decay for a time period of several half-lives.

Other computer codes that perform transmutation calculations, such as the ORIGEN2 code, solve the differential equations using methods that are more sophisticated than the AKM method. These other methods are able to avoid some of the pitfalls of the AKM method and are less susceptible to round-off error. It will be shown in subsequent sections of this paper that the potential problems mentioned above do not cause significant errors where the AKM method is applied to practical problems for which the CHAIN.238DJ code is used. For this reason, the AKM method is sufficiently sophisticated for the CHAIN.238DJ code as it is commonly applied. It is important, however, that users be aware of these potential problems whether the application is the CHAIN.238DJ code or use of the AKM method in some other code to calculate transmutation or decay for a different chain.

3.0 THE Np-237/Pu-238 TRANSMUTATION CHAIN IN CHAIN.238DJ

The transmutation chain modeled in the CHAIN.238DJ code is shown in Figure 3.1. The level of ^{236}Pu impurity in the plutonium produced in the chain is important because one of its daughter products is ^{208}Tl, which, upon decay, gives off a very high energy γ ray which

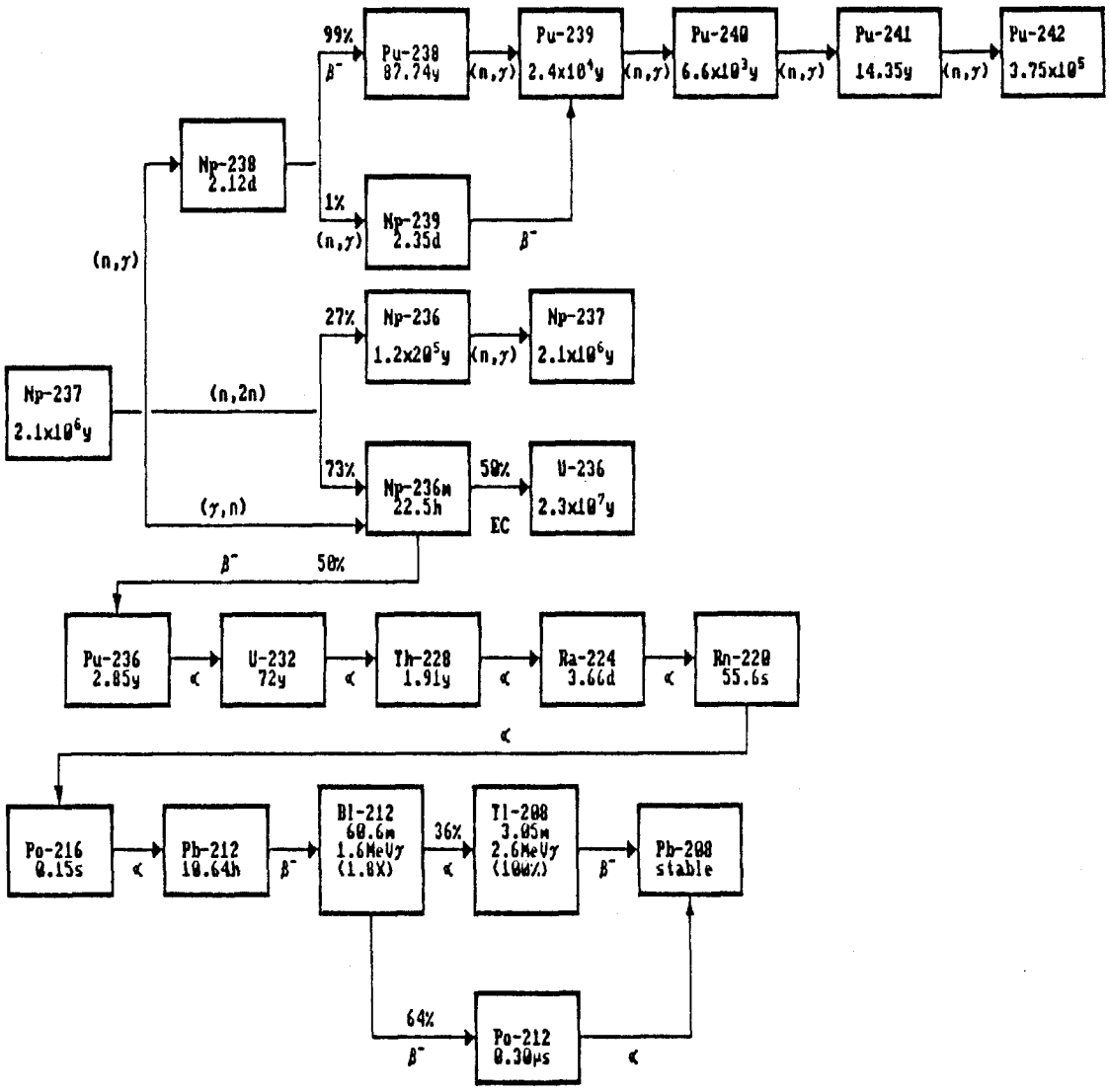

Figure 3.1 Np-237/Pu-238 Transmutation Chain

is difficult to shield. The bottom part of the chain can be simplified in the equations so that the $^{237}Np(\gamma,n)$ and $^{237}Np(n,2n)$ reactions appear to produce ^{236}Pu directly. This is basically just a matter of having the branching factors built into the cross sections and, therefore, the microscopic $^{237}Np(n,2n)$ and $^{237}Np(\gamma,n)$ reaction rates. For long irradiation times of hundreds of days, the effect of ignoring the few nuclides that are not included in the simplified chain is negligible. Figure 3.2 shows the simplified chain. This is the chain that is actually modeled in the CHAIN.238DJ code.

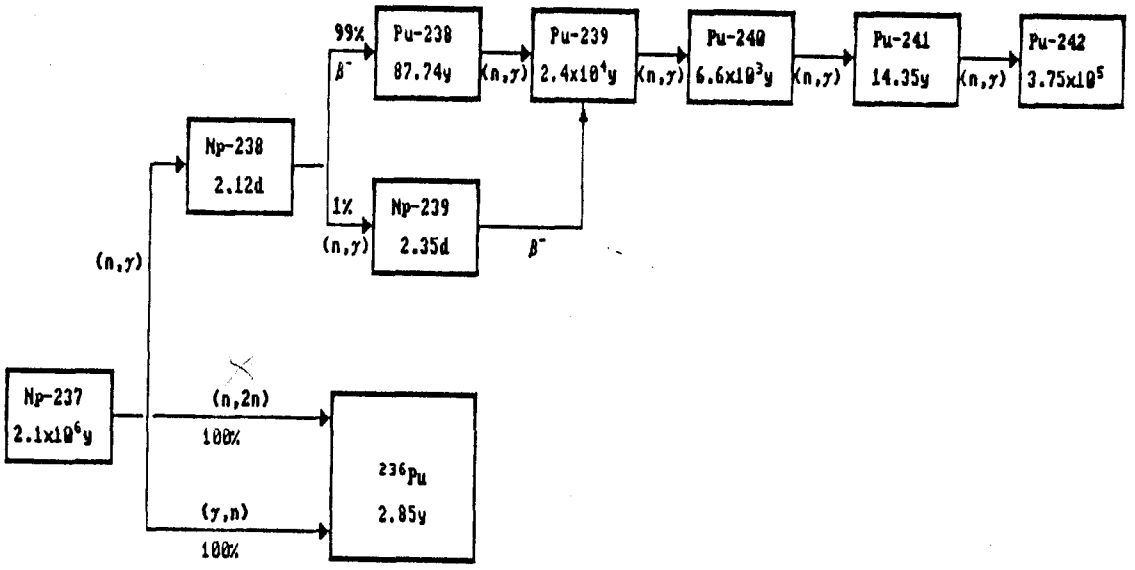

Figure 3.2 Simplified Np-237/Pu-238 Transmutation Chain

This chain is mathematically described by the following equations:

$$dN_1/dt = - N_1(t)\lambda_1 - N_1(t)\sigma_{a,1}\phi$$

$$dN_2/dt = N_1(t)\sigma_{\gamma,1}\phi - N_2(t)\lambda_2 - N_2(t)\sigma_{a,2}\phi$$

$$dN_3/dt = N_2(t)\sigma_{\gamma,2}\phi - N_3(t)\lambda_3 - N_3(t)\sigma_{a,3}\phi$$

$$dN_4/dt = N_1(t)\sigma_{\gamma,n}\phi + N_1(t)\sigma_{n,2n}\phi - N_4(t)\lambda_4 - N_4(t)\sigma_{a,4}\phi$$

$$dN_5/dt = N_2(t)\lambda_2 - N_5(t)\lambda_5 - N_5(t)\sigma_{a,5}\phi$$

$$dN_6/dt = N_5(t)\sigma_{\gamma,5}\phi + N_3(t)\lambda_3 - N_6(t)\lambda_6 - N_6(t)\sigma_{a,6}\phi$$

$$dN_7/dt = N_6(t)\sigma_{\gamma,6}\phi - N_7(t)\lambda_7 - N_7(t)\sigma_{a,7}\phi$$

$$dN_8/dt = N_7(t)\sigma_{\gamma,7}\phi - N_8(t)\lambda_8 - N_8(t)\sigma_{a,8}\phi$$

$$dN_9/dt = N_8(t)\sigma_{\gamma,8}\phi - N_9(t)\lambda_9 - N_9(t)\sigma_{a,9}\phi$$

$$dN_{10}/dt = \sum_{i=1}^{9} [N_i(t)\sigma_{f,i}\phi] - N_{10}(t)\lambda_{10} - N_{10}(t)\sigma_{a,10}\phi$$

where $N_1(t)$ = The amount of ^{237}Np at time t

$N_2(t)$ = The amount of ^{238}Np at time t

$N_3(t)$ = The amount of ^{239}Np at time t

$N_4(t)$ = The amount of ^{236}Pu at time t

$N_5(t)$ = The amount of ^{238}Pu at time t

$N_6(t)$ = The amount of ^{239}Pu at time t

$N_7(t)$ = The amount of ^{240}Pu at time t

$N_8(t)$ = The amount of ^{241}Pu at time t

$N_9(t)$ = The amount of ^{242}Pu at time t

$N_{10}(t)$ = The amount of fission product pairs at time t

$\sigma_{a,k}\phi = \int_o^\infty \sigma_{a,k}(E)\phi_E(E)dE$ = The microscopic total neutron absorption reaction rate for nuclide k

$\sigma_{a,k}(E)$ = The microscopic total neutron absorption cross section for nuclide k

$\sigma_{f,k}\phi = \int_o^\infty \sigma_{f,k}(E)\phi_E(E)dE$ = The microscopic total fission reaction rate for nuclide k

$\sigma_{f,k}(E)$ = The microscopic total fission cross section for nuclide k

$\sigma_{\gamma,k}\phi = \int_o^\infty \sigma_{\gamma,k}(E)\phi_E(E)dE$ = The microscopic total neutron radiative capture reaction rate for nuclide k

$\sigma_{\gamma,k}(E)$ = The microscopic radiative neutron capture cross section for nuclide k

$\sigma_{\gamma,n}\phi_\gamma = \int_o^\infty \sigma_{\gamma,n}(E)\phi_\gamma(E)dE$ = The microscopic total reaction rate for the effective reaction $^{237}Np(\gamma,n)^{236}Pu$

$\sigma_{\gamma,n}(E)$ = The effective microscopic cross section for the effective reaction $^{237}Np(\gamma,n)^{236}Pu$

$\phi_\gamma(E)$ = The energy dependent γ ray flux per unit energy

$\sigma_{n,2n}\phi = \int_o^\infty \sigma_{n,2n}(E)\phi_E(E)dE$ = The microscopic total reaction rate for the effective reaction $^{237}Np(n,2n)^{236}Pu$

$\sigma_{n,2n}(E)$ = The effective microscopic cross section for the effective reaction $^{237}Np(n,2n)^{236}Pu$

$\phi_E(E)$ = The energy dependent neutron flux per unit energy

λ_k = The radioactive decay constant for nuclide k

Determination of the effective cross sections, fluxes, and reaction rates is done outside of the CHAIN.238DJ code. The energy dependence of these parameters may be very complex, but it is not treated by CHAIN.238DJ except with some very simple methods of adjusting the effective microscopic reaction rates for changing self-shielding.

As was done with Equations 2.1-2.5, the equations above can be stated in a simpler form by writing them in terms of the nuclide loss coefficients, β_k, and nuclide gain coefficients, $\alpha_{i,k}$. The new form of the equations then becomes:

$$dN_1/dt = - N_1(t)\beta_1$$

$$dN_2/dt = N_1(t)\alpha_{1,2} - N_2(t)\beta_2$$

$$dN_3/dt = N_2(t)\alpha_{2,3} - N_3(t)\beta_3$$

$$dN_4/dt = N_1(t)\alpha_{1,4} - N_4(t)\beta_4$$

$$dN_5/dt = N_2(t)\alpha_{2,5} - N_5(t)\beta_5$$

$$dN_6/dt = N_3(t)\alpha_{3,6} + N_5(t)\alpha_{5,6} - N_6(t)\beta_6$$

$$dN_7/dt = N_6(t)\alpha_{6,7} - N_7(t)\beta_7$$

$$dN_8/dt = N_7(t)\alpha_{7,8} - N_8(t)\beta_8$$

$$dN_9/dt = N_8(t)\alpha_{8,9} - N_9(t)\beta_9$$

$$dN_{10}/dt = \sum_{i=1}^{9} [N_i(t)\alpha_{i,10}] - N_{10}(t)\beta_{10}$$

where $\beta_k = \lambda_k + \sigma_{a,k}\phi$

$$\alpha_{1,2} = \sigma_{\gamma,1}\phi$$

$$\alpha_{2,3} = \sigma_{\gamma,2}\phi$$

$$\alpha_{1,4} = \sigma_{\gamma,n}\phi_\gamma + \sigma_{n,2n}\phi$$

$$\alpha_{2,5} = \lambda_2$$

$$\alpha_{3,6} = \lambda_3$$

$$\alpha_{5,6} = \sigma_{\gamma,5}\phi$$

$$\alpha_{6,7} = \sigma_{\gamma,6}\phi$$

$$\alpha_{7,8} = \sigma_{\gamma,7}\phi$$

$$\alpha_{8,9} = \sigma_{\gamma,8}\phi$$

$$\alpha_{i,10} = \sigma_{f,i}\phi$$

If all the coefficients (the $\alpha_{i,k}$ and β_k factors) in the equations above are constant, this set of equations can be solved analytically by assuming solutions of the form shown in Equations 2.11, 2.12, and 2.13:

$$N_k(t) = \sum_{m=1}^{k} [A_{k,m} e^{-\beta_m t}]$$

where

$$A_{1,1} = N_1(0)$$

$$A_{k,m} = \frac{1}{\beta_k - \beta_m} \sum_{i=1}^{k-1} [A_{i,m}\alpha_{i,k}] \quad \text{for} \quad m < k$$

$$A_{k,k} = N_k(0) - \sum_{j=1}^{k-1} A_{k,j} \quad \text{for} \quad m = k$$

The solutions for the first four nuclides in the ^{237}Np transmutation chain are:

$$N_1(t) = A_{1,1} e^{-\beta_1 t}$$

where $A_{1,1} = N_1(0)$

$$N_2(t) = A_{2,1} e^{-\beta_1 t} + A_{2,2} e^{-\beta_2 t}$$

$$\text{where } A_{2,1} = (A_{1,1}\alpha_{1,2})/(\beta_2 - \beta_1)$$

$$A_{2,2} = N_2(0) - A_{2,1}$$

$$N_3(t) = A_{3,1}e^{-\beta_1 t} + A_{3,2}e^{-\beta_2 t} + A_{3,3}e^{-\beta_3 t}$$

$$\text{where } A_{3,1} = (A_{2,1}\alpha_{2,3})/(\beta_3 - \beta_1)$$

$$A_{3,2} = (A_{2,2}\alpha_{2,3})/(\beta_3 - \beta_2)$$

$$A_{3,3} = N_3(0) - A_{3,1} - A_{3,2}$$

$$N_4(t) = A_{4,1}e^{-\beta_1 t} + A_{4,2}e^{-\beta_2 t} + A_{4,3}e^{-\beta_3 t} + A_{4,4}e^{-\beta_4 t}$$

$$\text{where } A_{4,1} = \frac{1}{\beta_4 - \beta_1} \sum_{i=1}^{3} [A_{i,1}\alpha_{i,4}]$$

$$= (A_{1,1}\alpha_{1,4})/(\beta_4 - \beta_1)$$

$$A_{4,2} = \frac{1}{\beta_4 - \beta_2} \sum_{i=2}^{3} [A_{i,2}\alpha_{i,4}] = 0$$

$$A_{4,3} = (A_{3,3}\alpha_{3,4})/(\beta_4 - \beta_3) = 0$$

$$A_{4,4} = N_4(0) - A_{4,1} - A_{4,2} - A_{4,3}$$

The solutions for the rest of the nuclides in the chain take on a similar form, but become increasingly long and cumbersome to write out or to solve on paper.

3.1 CHAIN.238DJ Comparison With ORIGEN2

The CHAIN.238DJ code easily solves all of these equations by using the AKM method and computer subroutines described in Section 2.0. One way of verifying the application of this method to the Np-237/Pu-238 chain is to compare results with those from the well known ORIGEN2 code. Table 3.1 shows the results of this comparison for three practical cases. For each case, the transmutation calculation was performed on a CRAY X-MP/18 computer using the ORIGEN2 code, on a CRAY X-MP/18 computer using the CHAIN.238DJ code, and on a

Case #1	Reaction Rate ($\sigma_\gamma\phi$)	Initial Amount	Nuclide Amounts (Gram-Atoms) at 530 Days		
Nuclide			CRAY X-MP/18 CHAIN.238DJ	CRAY X-MP/18 ORIGEN2	SUN 4/260 CHAIN.238DJ
^{237}Np	5.39e+15	1.00	0.778	0.778	0.778
^{238}Np	9.73e+14	0.0	1.10e-3	1.10e-3	1.10e-3
^{236}Pu	4.01e+15	0.0	1.84e-6	1.84e-6	1.84e-6
^{238}Pu	3.98e+15	0.0	0.192	0.192	0.192
^{239}Pu	8.06e+15	0.0	0.014	0.014	0.014
^{240}Pu	5.22e+16	0.0	1.12e-3	1.13e-3	1.12e-3
^{241}Pu	3.35e+15	0.0	6.59e-4	6.65e-4	6.59e-4
^{242}Pu	1.33e+16	0.0	2.10e-5	2.12e-5	2.11e-5

Case #2	Reaction Rate ($\sigma_\gamma\phi$)	Initial Amount	Nuclide Amounts (Gram-Atoms) at 530 Days		
Nuclide			CRAY X-MP/18 CHAIN.238DJ	CRAY X-MP/18 ORIGEN2	SUN 4/260 CHAIN.238DJ
^{237}Np	4.57e+15	1.00	0.807	0.807	0.807
^{238}Np	1.31e+15	0.0	9.67e-4	9.67e-4	9.67e-4
^{236}Pu	4.45e+15	0.0	1.85e-6	1.84e-6	1.85e-6
^{238}Pu	5.19e+15	0.0	0.161	0.161	0.161
^{239}Pu	1.17e+16	0.0	1.35e-2	1.36e-2	1.35e-2
^{240}Pu	6.29e+16	0.0	1.47e-3	1.48e-3	1.47e-3
^{241}Pu	7.65e+15	0.0	9.85e-4	9.93e-4	9.85e-4
^{242}Pu	1.54e+16	0.0	7.34e-5	7.43e-5	7.34e-5

Case #3	Reaction Rate ($\sigma_\gamma\phi$)	Initial Amount	Nuclide Amounts (Gram-Atoms) at 265 Days		
Nuclide			CRAY X-MP/18 CHAIN.238DJ	CRAY X-MP/18 ORIGEN2	SUN 4/260 CHAIN.238DJ
^{237}Np	1.25e+16	1.00	0.750	0.750	0.750
^{238}Np	4.92e+15	0.0	2.41e-3	2.41e-3	2.41e-3
^{236}Pu	1.08e+16	0.0	1.51e-6	1.51e-6	1.51e-6
^{238}Pu	1.91e+16	0.0	0.189	0.189	0.189
^{239}Pu	4.26e+16	0.0	2.22e-2	2.23-2	2.22e-2
^{240}Pu	1.18e+17	0.0	4.86e-3	4.91e-3	4.86e-3
^{241}Pu	2.82e+16	0.0	2.65e-3	2.69e-3	2.65e-3
^{242}Pu	2.23e+16	0.0	4.06e-4	4.15e-4	4.06e-4

Table 3.1 Comparison of CHAIN.238DJ Results with ORIGEN2 Results

SUN 4/260 computer using the CHAIN.238DJ code. In each case, the same data were used in all three calculations. The total microscopic radiative neutron capture reaction rates used in each case are given in the tables as the product $\sigma_\gamma\phi$. Other data, such as the radioactive decay constants, the fission reaction rates, and the $^{237}Np(n,2n)$ and $^{237}Np(\gamma,n)$ reaction rates were the same for all three calculations of each case. The reaction rates were determined in a separate calculation. They are input data for the CHAIN.238DJ and ORIGEN2 codes. Cross section sets were created for ORIGEN2 such that the products of the one group cross sections and the fluxes resulted in the same microscopic reaction rates as those used in the calculations with the CHAIN.238DJ code. It was assumed that the reaction rates did not change as a function of time or burnup.

The reaction rates and other data used in the calculations were derived from the practical case studies to be discussed in detail in Section 7.0. The three cases have significantly different fluxes and effective microscopic cross sections in order to represent different irradiation environments. In the first two cases, the transmutation is carried out for 530 days. In the third case it is half as long, 265 days. Table 3.1 shows good agreement between CHAIN.238DJ and ORIGEN2 for all three cases, regardless of whether the CHAIN.238DJ code is run on the SUN machine or the CRAY.

4.0 THE PROBLEM OF NON-CONSTANT COEFFICIENTS

Implicit in the solutions from Section 3.0 for the time-dependent nuclide amounts $N_k(t)$ is the assumption that the coefficients β_k and $\alpha_{i,k}$ are all constant. In truth these coefficients are not quite constant, but vary slowly throughout the time of irradiation. The λ_k values are all constant, but the microscopic reaction rates ($\sigma_a\phi$, $\sigma_f\phi$, $\sigma_\gamma\phi$, $\sigma_{n,2n}\phi$, and $\sigma_\gamma\phi_\gamma$) vary slowly as the target material composition changes throughout the time of irradiation. These varying reaction rates lead to non-constant coefficients. In the problems to which the CHAIN.238DJ code is usually applied, the reaction rates change due to increasing spatial self-shielding, an increasing neutron source within the target material, and decreasing resonance self-shielding.

The spatial self-shielding increases as the target material undergoes irradiation. One of the practical case studies to be discussed in detail in Section 7.0 serves as an example. This case is a representative two year irradiation of $^{237}NpO_2$ target pins in a nuclear reactor. Figure 4.1 shows the effective total macroscopic thermal neutron absorption cross section of the target material and the average thermal neutron flux in the target pins. The absorption cross section increases by about 50% from fresh material to two-year (530 Effective Full Power Days) irradiated material. For the same situation, the average thermal neutron flux in the target pins in the same energy region decreases by about 20%. As the ^{237}Np is irradiated, it is depleted and there is a buildup of plutonium isotopes in the target material. Since some of these plutonium isotopes have a larger thermal neutron absorption cross section than the ^{237}Np they are in effect replacing, the macroscopic thermal neutron absorption cross section increases with the buildup of plutonium. This increasing macroscopic thermal neutron absorption cross section results in increasing spatial self-shielding, since the material in the inner part of the target pins "sees" increasingly less neutron flux due to increased absorption in the outer part of the

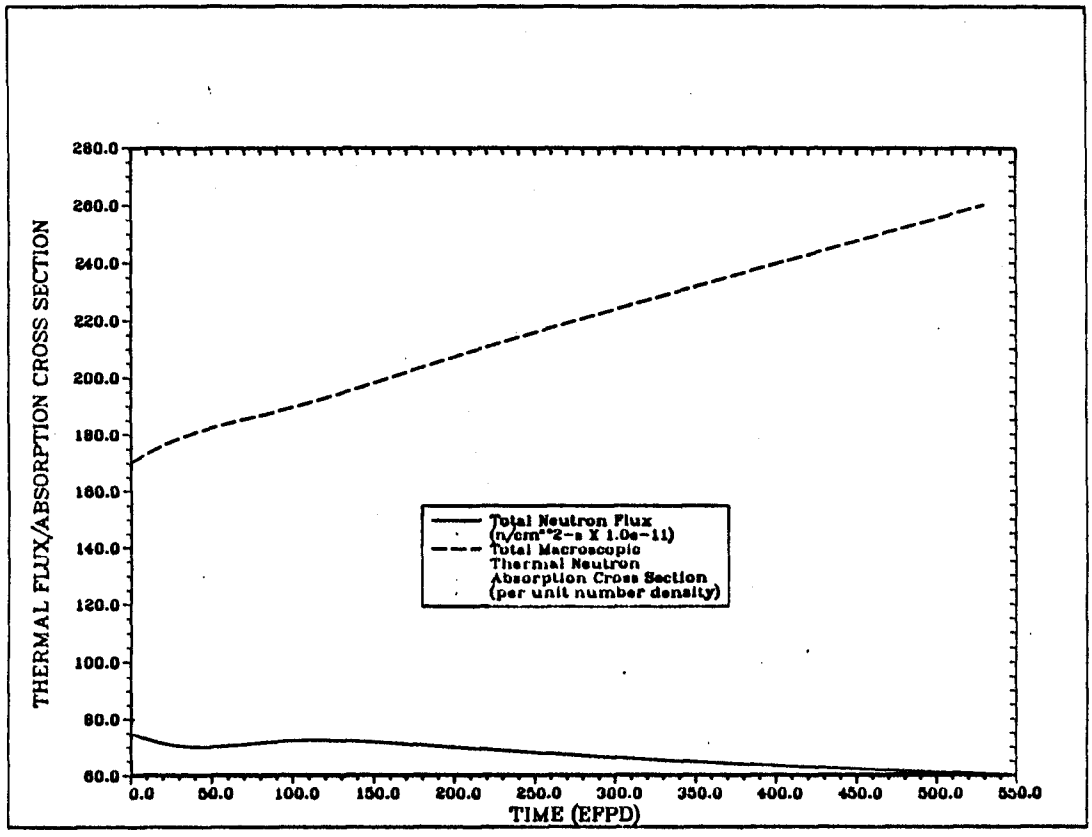

Figure 4.1 Thermal Flux and Macroscopic Neutron Absorption Cross Section vs Time

pins. The net effect is an increasing flux dip across the pin in the radial direction. This type of flux dip is usually referred to as spatial self-shielding.

As another consequence of the plutonium buildup, the internal neutron source in the target material increases with time of irradiation. Since the plutonium isotopes have higher microscopic fission cross sections than the ^{237}Np they are replacing, the total fission rate in the target material increases dramatically with irradiation. Figure 4.2 shows the time-dependent total fission rate in the target pins for the representative two year irradiation. The total fission rate increases by over a factor of four during the two year period. (The fluctuation in the curve at 50 EFPD is due to the

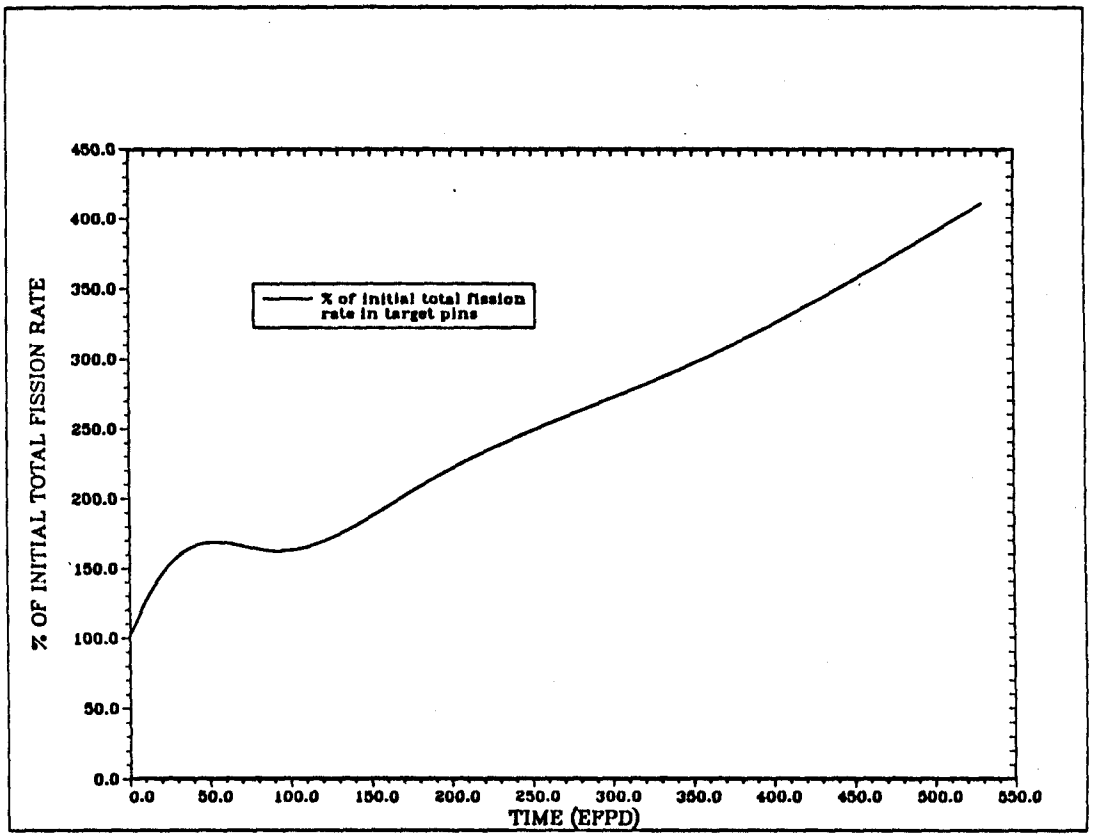

Figure 4.2 Total Fission Rate in Target Pins vs Time

rapid buildup of ^{238}Np to equilibrium.) One of the products of fission is fission neutrons, so the increasing fission rate causes an increasing fission neutron source. This has the opposite effect of the increasing spatial self-shielding (the fission source increases the neutron flux, whereas the increasing spatial self-shielding decreases it), and it can be difficult to detect the effects of one in the presence of the other. For target material that has no moderator in its composition, it may be possible to see the effect of the increased fission source separated from that of the increased spatial self-shielding by looking for an increase in the neutron flux in the fast region typified by the prompt neutron spectrum. Figures 4.3, 4.4, 4.5, and 4.6 show neutron flux shapes in the target pins at zero, 353, and 530 EFPD for the representative irradiation. The flux decreases with time in the thermal region and stays fairly constant

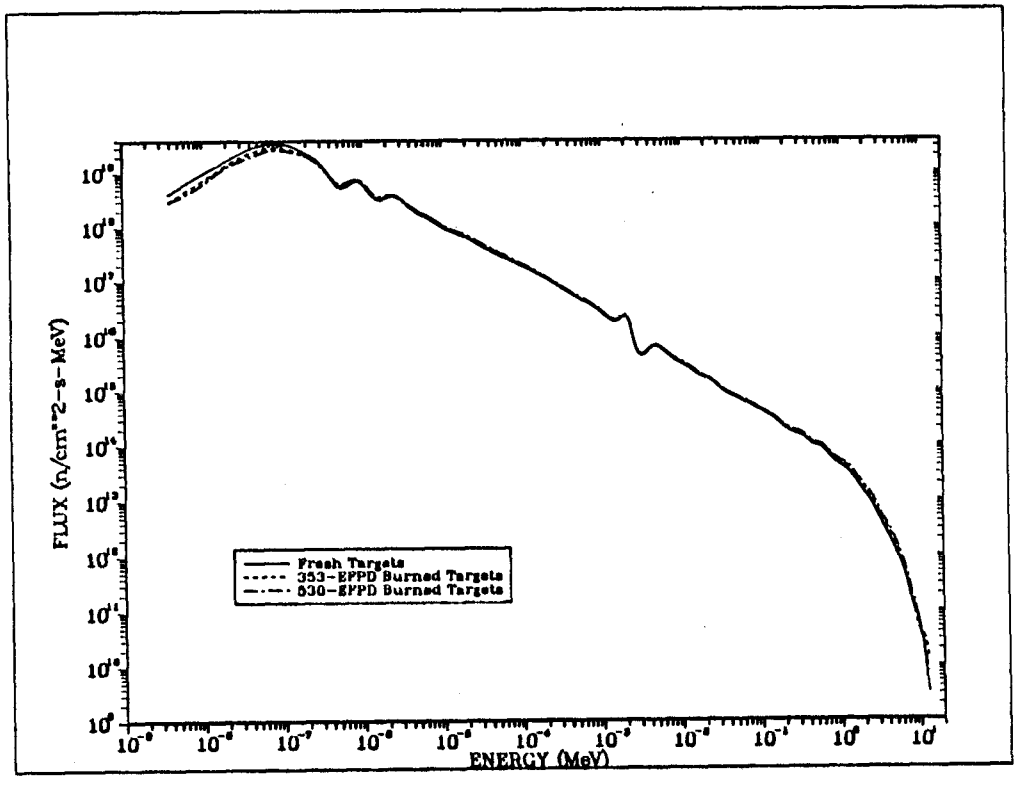

Figure 4.3 Total Neutron Flux Per Unit Energy in the Target Pins - Total Spectrum

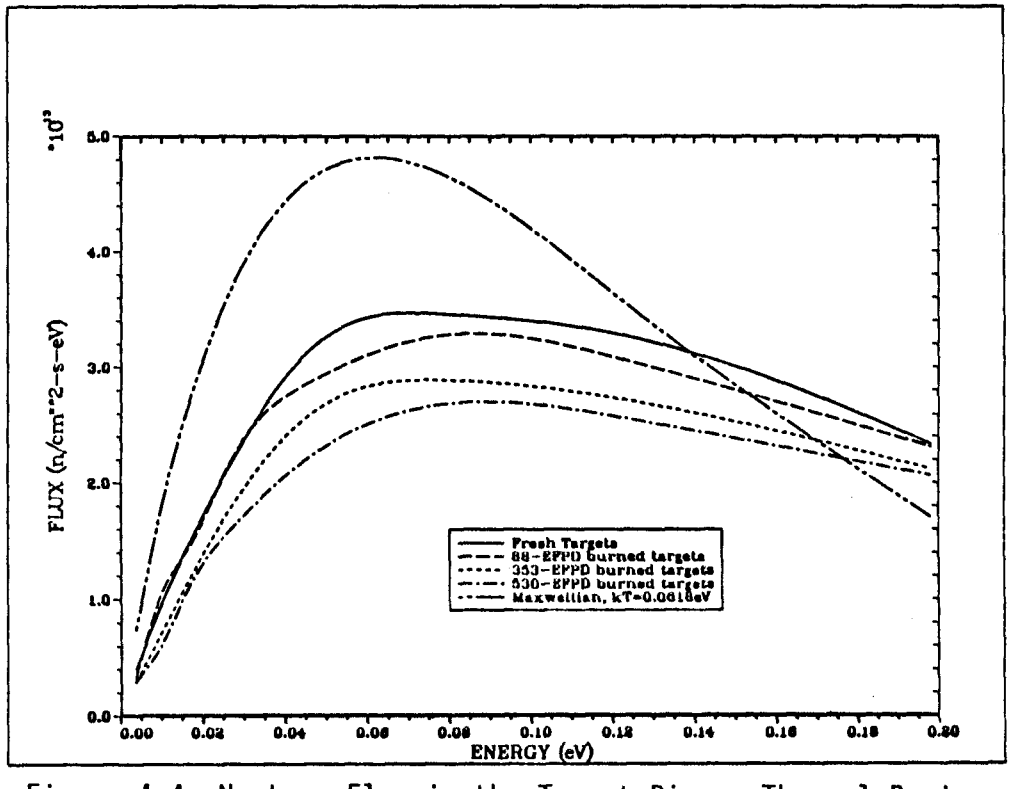

Figure 4.4 Neutron Flux in the Target Pins - Thermal Region

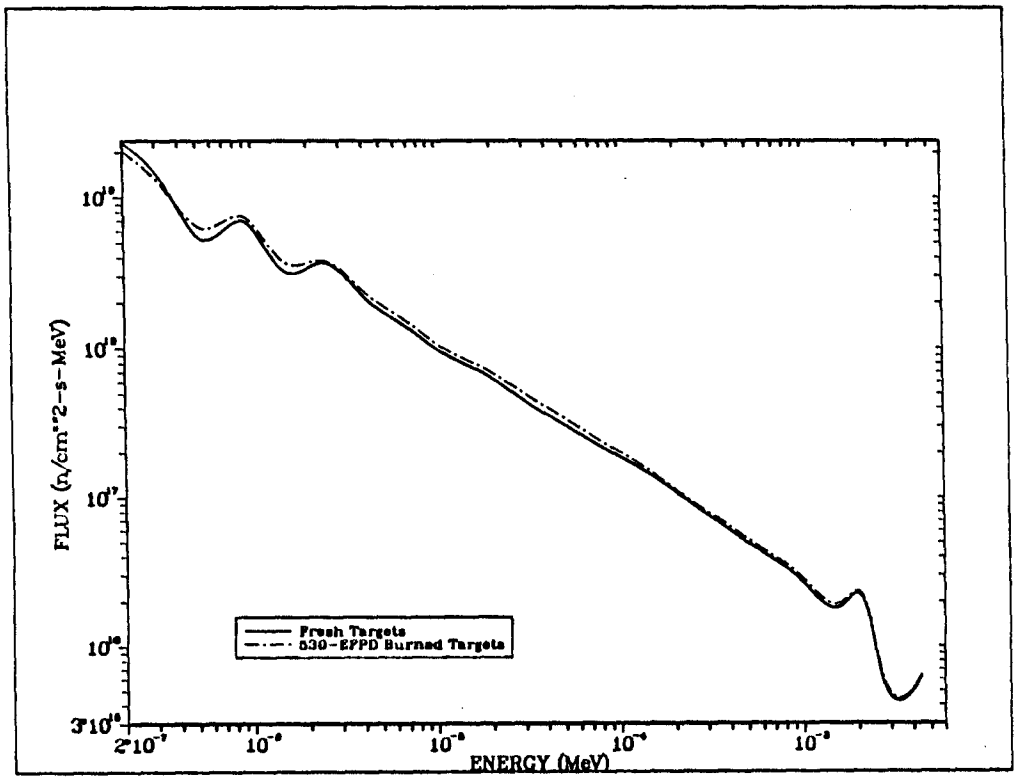

Figure 4.5 Total Neutron Flux Per Unit Energy in the Target Pins - Resolved Resonance Region

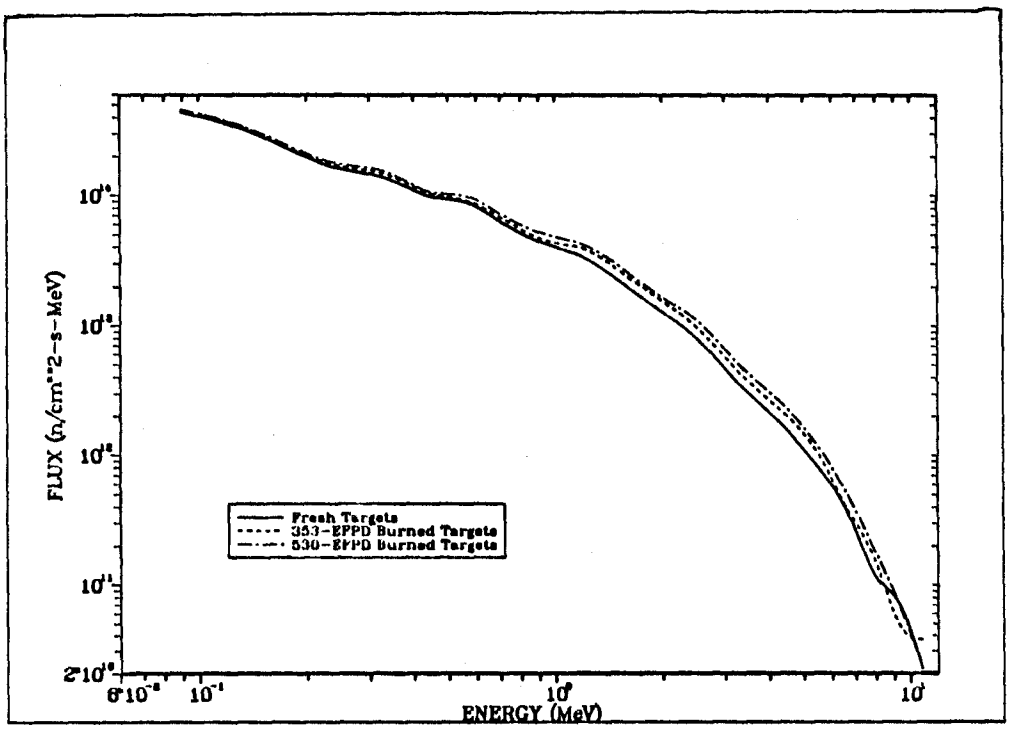

Figure 4.6 Total Neutron Flux Per Unit Energy in the Target Pins - Fast Region

throughout the resolved resonance region (except near and in the resonances) and into the lower part of the fast region, but Figure 4.6 shows that it increases significantly with time in the fast region around an energy of about 1 MeV. This is a manifestation of the dominance in this region of the increasing fission source over any increasing effective total neutron absorption cross section.

The effect of resonance self-shielding is different for each individual resonance of each nuclide. It is a function of the amount of the nuclide that is present and the resonance structure of that nuclide. For resonances that are very large, the target pin becomes very gray or even black at the resonance energy quite quickly as the nuclide concentration grows. In these situations, resonance self-shielding has reached its maximum and can no longer change with increasing concentration. Figure 4.7 shows the total microscopic radiative neutron capture reaction rate in the resolved resonance region as a function of irradiation time for ^{238}Pu for the representative irradiation case. The reaction rate drops rapidly as the ^{238}Pu concentration grows and resonance self-shielding takes effect during the first 200 days of irradiation (the initial ^{238}Pu concentration is zero). At about 200 days, the reaction rate levels off as resonance self-shielding has apparently approached its maximum and the target pins have become very grey at the energies of the resonances. Changes in resonance self-shielding are especially noticeable for several of the plutonium isotopes which have very large, dominant first resonances and which are not present in fresh, unirradiated target material. There is not nearly so noticeable a change for nuclides, such as ^{237}Np, that do not have large, dominant individual resonances or whose concentration in the target material does not change greatly during irradiation of the material.

The net effect of the increasing spatial self-shielding, the increasing internal fission neutron source, and the increasing resonance self-shielding is to cause time dependency in the reaction rates. Reaction rates that are dominated by the thermal region tend

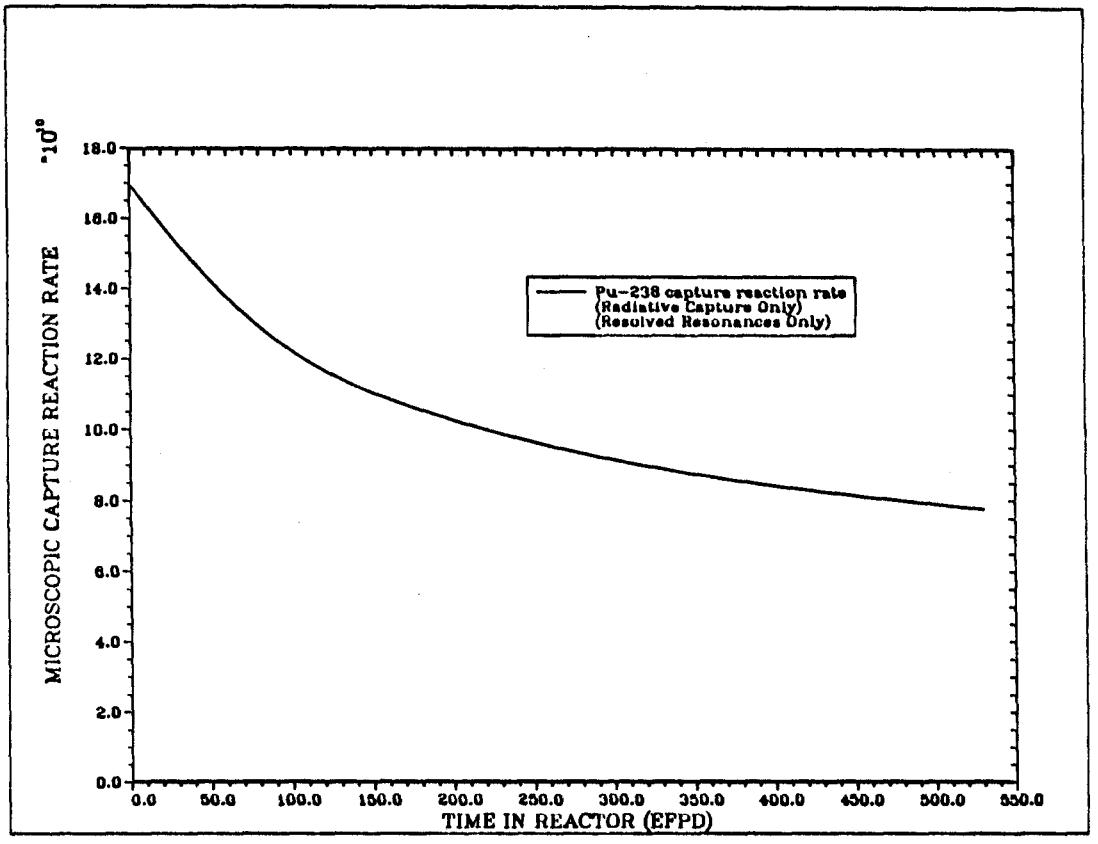

Figure 4.7 Microscopic Radiative Neutron Capture Reaction Rate in the Resolved Resonance Region for Pu-238

to have a time-dependent behavior that is a result of the increasing flux dip across the target pin. Those that have important resonance effects tend to follow the increasing resonance self-shielding. Some of the nuclides in the chain have threshold fission cross sections, so their fission rates tend to be affected by the increasing fission neutron source in the pins. The reaction rate that usually changes most rapidly during irradiation is $^{237}Np(n,2n)$. The $^{237}Np(n,2n)$ reaction rate is very strongly affected by the increase in the internal fission neutron source shown in Figure 4.2. The changing reaction rates result in similarly varying β_k and $\alpha_{i,k}$ coefficients. This time-dependency in the coefficients is too significant to ignore and is accounted for in the CHAIN.238DJ code. The next section presents the methods used in the CHAIN.238DJ code to treat the non-constant coefficients.

5.0 TREATMENT OF THE NON-CONSTANT COEFFICIENTS IN CHAIN.238DJ

In order to use the equations given in Section 3.0 for the time-dependent nuclide amounts $N_k(t)$, a method has been derived to account for the changing coefficients. Since the reaction rates, and therefore the β_k and $\alpha_{i,k}$ coefficients, change relatively slowly, they may be assumed to be constant over a sufficiently short time period. If the β_k and $\alpha_{i,k}$ values are assumed to be constant, the equations can be solved for these short time periods. The equations are then solved repeatedly until the sum of the short time steps is equal to the total irradiation time period desired. At the end of each time step or iteration, the coefficients are adjusted to new values. This approach reduces the problem of having non-constant coefficients down to having to answer two questions. The first question is whether the time steps are sufficiently short. The second question is whether the coefficients are adjusted accurately for each time step. The first question is a convergence problem typical in numerical methods. Understanding the second question requires some knowledge of what mechanisms are important in causing the coefficients to change during irradiation. These mechanisms have been identified as changing resonance and spatial self-shielding and a changing neutron source strength.

Because of the complexity of the mechanisms that cause the changing reaction rates, it may be necessary to account for the different mechanisms using different methods. Whereas the effects of changing spatial self-shielding and internal neutron source strength are best characterized by changes in the neutron flux, the effects of changing resonance self-shielding are best characterized by changes in the effective neutron cross section in the resolved resonance region or in the effective resonance integral. Of course, for a finite, heterogeneous system of absorber pins, resonance self-shielding can have the same effect as extreme spatial self-shielding in that it causes a flux dip across the pin within the energy region of the resonance. The method available in the CHAIN.238DJ code to account

for changing resonance self-shielding is analytically based on an infinite homogeneous system, so for our purposes resonance self-shielding is treated as only having an impact on the effective resonance integrals while general resolved resonance region flux depression across the target pin is accounted for separately.

There are two methods available in the CHAIN.238DJ code for adjusting the reaction rates as a function of time and/or changing target material composition. The first method simply consists of using a linear interpolation of the reaction rate through time. The second method treats the flux changes using a linear interpolation through time, and treats effective cross section changes separately. Changes in the effective cross section are treated by adjusting them as a function of target material composition using what is called the "C-factor method"[8]. The two methods can be used together or separately, using a multi-energy-group approach employing different methods for different groups. Each nuclide in the chain is treated separately, allowing the user to tailor the treatment for each nuclide.

5.1 The Simple Linear Interpolation Method

The simple linear interpolation method consists of using a linear interpolation of the reaction rate through time. It assumes that the beginning-of-irradiation and end-of-irradiation reaction rates are known. The reaction rates for all times in between are assumed to change linearly with the time of irradiation. Given the complexity of the mechanisms that affect the reaction rates, this method may seem quite simple, but it often works well enough to provide sufficient accuracy.

5.2 The C-factor Method

The CHAIN.238DJ code allows individual treatment of each nuclide in the transmutation chain, with separate C-factor method treatment in

as many as seven energy groups. The C-factor method is based on an analytical tool for calculating resonance self-shielding. As such, it has obvious applicability in the resolved resonance region, but it also can be used as an empirical method in the thermal or the fast neutron regions. It employs a combination of treating the changing group flux by using a linear interpolation through time and treating resonance self-shielding by using C-factors.

The resolved resonance region is typically affected by all three mechanisms of spatial self-shielding, resonance self-shielding, and the changing neutron source strength. Figure 5.1 shows the total neutron flux per unit energy in the resolved resonance region for one of the practical case studies to be discussed in detail in Section

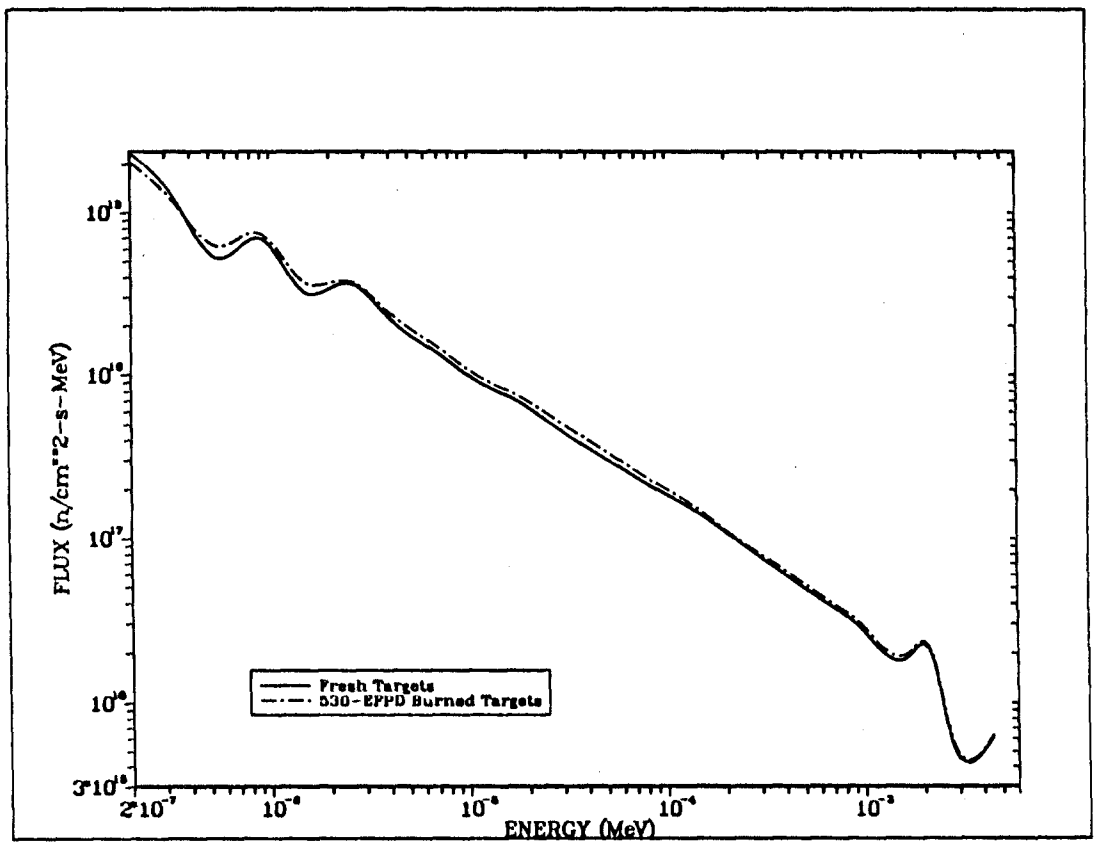

Figure 5.1 Total Neutron Flux Per Unit Energy in the Target Pins - Resolved Resonance Region

7.0. This is a typical case where spatial self-shielding together with the changing internal neutron source strength have the net effect of slightly increasing the neutron flux in the region through time. This does not hold, however, for the very narrow energy band around a large, isolated absorption resonance. Resonance self-shielding has the effect of decreasing the neutron flux in this narrow energy band in the immediate vicinity of the resonance. This narrow flux depression decreases the effective resonance integral but often does not manifest itself in the wider group flux. Actually, the effective resonance integral decreases for all the nuclides in the chain modelled in the CHAIN.238DJ code except ^{237}Np, for which it may increase. The ^{237}Np concentration is usually high enough that the target pins may be black at the energy of some resonances, but the effective resonance integrals can increase (resonance self-shielding decreases) with irradiation time for some other ^{237}Np resonances since the amount present is depleted. In any case, resonance self-shielding acts as a function of the concentration of the individual nuclide, assuming resonances of other nuclides in the chain do not overlap closely.

With the C-factor method, changes in group neutron fluxes are accounted for in the same simple manner as are reaction rate changes in the simple linear interpolation method. The group neutron flux is calculated at the beginning and at the end of target pin lifetime, and the flux at all intermediate times is calculated by using a simple linear interpolation. Changes in the effective resonance integrals are accounted for by using a fairly simple model called the "C-factor method". Bigelow[8] reports using a very simplified C-factor method to account for resonance self-shielding in analysis of isotope production in the High Flux Isotope Reactor (HFIR) at the Oak Ridge National Laboratory. He gives the following relationship as valid for a single absorber resonance peak, but also useful as an empirical correction for an energy region encompassing a multitude of absorber resonances:

$$I^{eff} = \frac{I^{\infty}}{\sqrt{1. + CN_a}}$$

where

I^{∞} = The infinitely dilute resonance integral

I^{eff} = The effective resonance self-shielded resonance integral

N_a = The amount of absorber nuclide present

C = The "C-factor"

The units of N_a can be atom density, mass density, weight density, mass or weight per target pin, or any units that characterize the amount of the nuclide present, as long as the units of N_a and C are consistent so that the product CN_a is unitless. It is obvious that if $N_a = 0$ (infinite dilution) the effective resonance integral and the infinitely dilute resonance integral are equal.

For the HFIR analysis, this relationship was used with a two-group approach. The thermal region was treated alone, and everything above the thermal region, including all the resolved resonances and the unresolved resonance (fast) region, was treated as one group employing one effective resonance integral and one C-factor for each reaction and each nuclide. Since it is really only valid for a single isolated resonance, the C-factor method has no analytical basis for application to the thermal or the unresolved resonance (fast) region, but it can often be used there as an empirical correction method. In the resolved resonance region, the C-factor method can be applied to individual isolated resonances wherever possible. The ability to isolate individual resonances is limited by the ability to calculate reaction rates in these often relatively narrow energy groups and not have excessively large uncertainties in the result. Where it is not possible to isolate individual resonances, the C-factor method can be used as an empirical correction for resonance self-shielding over a group of resonances.

The analytical basis of the C-factor method arises from the Narrow Resonance Infinite Mass Absorber (NRIM)[9] approximation to the effective resonance integral. The following assumptions are made in the development of the NRIM approximation:

a) An infinite medium consists of an absorber uniformly distributed throughout a moderator.

b) The neutron flux has achieved a 1/E behavior asymptotic to the resonance.

c) The moderator macroscopic neutron scattering cross section (Σ_s) is constant over the narrow energy range of the absorber resonance.

d) The macroscopic total neutron absorption cross section (Σ_a) is negligible.

e) The practical width of the absorber resonance is much smaller than the average energy loss in a scattering collision with a moderator nucleus.

f) The practical width of the absorber resonance is much greater than the average energy loss in a scattering collision with an absorber nucleus.

The first assumption may appear to never be valid in any heterogeneous, finite geometrical system, but the effects of treating a heterogeneous system as if it were homogeneous are generally negligible whenever the diameter of the absorber pin is less than the mean free path of a neutron in the pin material. This is often the case at the energy of the resolved resonance regions in the target material being irradiated. The effects of making the first assumption when it may not be strictly valid are generally reflected in spatial self-shielding, which for our situation is accounted for by the linear approximation to the flux.

The second assumption is commonly made in a variety of reactor systems with negligible error. If the flux has a 1/E behavior, a log-log plot of the flux per unit energy will be a straight line with a slope of -1. Figure 5.1 shows the resolved resonance region flux shape in typical ^{237}Np target pins. The flux appears to exhibit a

general 1/E behavior throughout the resolved resonance region. It can be difficult to judge how close the slope in Figure 5.1 is to -1. Another way of showing a 1/E behavior is to make a log-log plot of the flux per unit lethargy. If the flux is 1/E, the flux per unit lethargy will be constant in the resolved resonance region and the plot will be a horizontal line. Figure 5.2 shows the same flux as that shown in Figure 5.1, but it is per unit lethargy instead of per unit energy. Figure 5.2 shows that the second assumption is really not being met very well in this example. In Section 7.0 the CHAIN.238DJ code will be applied to some example cases. None of these cases actually meets this second assumption very well either, but it will be shown that this does not cause serious problems.

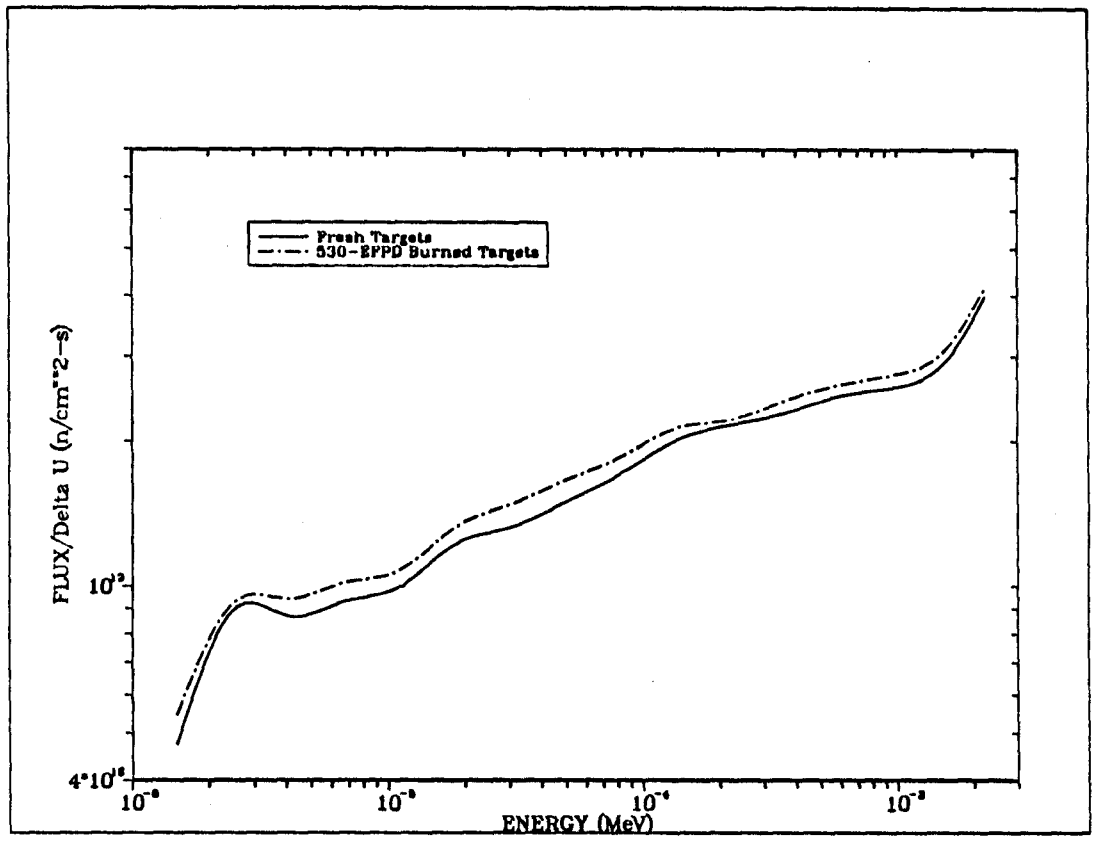

Figure 5.2 Total Neutron Flux Per Unit Lethargy in the Target Pins - Resolved Resonance Region

The third assumption is generally valid for a hydrogenous moderator. It is always valid for any moderator that has a scattering cross section dominated by potential ("billiard-ball") scattering.

The fourth assumption is also generally valid for hydrogen, especially in the presence of strong absorbers such as the plutonium isotopes and ^{237}Np, and especially within the resonances.

For the case of a hydrogen moderator, the fifth assumption can be effectively re-stated by the expression:

$$\overline{\Delta E_M} = \frac{1 - \alpha_M}{2} E_o = E_o/2 >> \Gamma_P$$

where

$\alpha_M = ((A-1)/(A+1))^2 = 0$ for hydrogen as the moderator

E_o = the energy at which the neutron scattering occurs

Γ_P = the "practical width" of the absorber resonance

$$\sim \sqrt{\frac{\Sigma_o}{\Sigma_P}}\,\Gamma$$

Σ_0 = the macroscopic total neutron absorption cross section of the absorber, at the energy of the absorption resonance peak

Σ_p = the total macroscopic potential scattering cross section

Γ = the total line width of the absorber resonance

This is a valid assumption for hydrogen moderator, even for the lowest-lying resonances of the ^{237}Np and plutonium absorbers. This

assumption is what leads to the "NR" part of the acronym "NRIM", since it suggests that the absorber resonances are relatively narrow.

The last assumption can be effectively re-stated by the expression:

$$\overline{\Delta E_a} = \frac{1 - \alpha_a}{2} E_o << \Gamma_p$$

$$\text{or} \quad 0.0084 E_o << \Gamma_p \quad \text{for } ^{237}\text{Np}$$

$$\text{where } \alpha_a = ((A-1)/(A+1))^2 = 0.9833 \text{ for } ^{237}\text{Np}$$

This assumption is valid for the lowest-lying resonances of the plutonium isotopes and of ^{237}Np. It is usually possible to isolate and calculate the reaction rate and the flux in only the first few resonances anyway, so where the NRIM approximation (and, therefore, the C-factor method) may not strictly apply for higher energy resonances, it is used only as an empirical correction. This assumption is what leads to the "IM" part of the acronym "NRIM", since it is equivalent to assuming that the absorber atom is infinitely massive or acts infinitely massive when a neutron scatters off of it. In the limit, as the absorber mass approaches infinity, $\alpha_a = 1$, then $\overline{\Delta E_a} = 0$ and the assumption is absolutely correct.

If all the assumptions discussed above can be met reasonably well, the following equation can be written for the NRIM resonance integral of a single absorber resonance (ignoring temperature effects):

$$I^{eff} = \frac{\sigma_0 \Gamma_\gamma \pi}{2 E_o a} = \frac{I^\infty}{\sqrt{1. + CN_a}}$$

where

$$a^2 = 1 + \frac{N_a \sigma_0 \Gamma_\gamma}{N_M \sigma_s^M \Gamma}$$

I^{eff} = The effective resonance self-shielded resonance integral

σ_0, Γ, and Γ_γ are resonance parameters

N_a = The absorber number density

N_M = The moderator number density

σ_s^M = The moderator scattering cross section

I^∞ = The infinitely dilute resonance integral

$$I^\infty = \frac{\sigma_0 \Gamma_\gamma \pi}{2E_o}$$

$$C = \text{The "C-factor"} = \frac{\sigma_0 \Gamma_\gamma}{N_M \sigma_s^M \Gamma} \qquad (5.1)$$

Figures 5.3 through 5.8 show the cross sections[10], as a function of energy, for the nuclides that exhibit significant resonance self-shielding. In looking at these figures, it is noticeable that several of the plutonium isotopes have very large first resonances. Typically, these first resonances will dominate the overall microscopic reaction rates for each nuclide. The effect of this dominance is that if the C-factor method works well for these dominant first resonances, the overall method should be accurate since the reaction rates in the other regions are far less important.

The C-factors can actually be calculated from resonance parameters and material densities using Equation 5.1, but that is cumbersome and is not the usual procedure. It is much easier to determine the beginning and ending fluxes, reaction rates, and nuclide amounts, then use the following equation to calculate C-factors:

$$I_1^{eff} = \frac{I^\infty}{\sqrt{1. + CN_{a,1}}} = \frac{RR_1}{\phi_1}$$

$$I_2^{eff} = \frac{I^{\infty}}{\sqrt{1. + CN_{a,2}}} = \frac{RR_2}{\phi_2}$$

where 1 and 2 refer to two different times, material compositions, and nuclide amounts. Then the C-factor is given by:

$$C = \frac{(I_2^{eff}/I_1^{eff})^2 - 1}{N_{a,1} - N_{a,2}\,(I_2^{eff}/I_1^{eff})^2} \qquad (5.2)$$

The fluxes and reaction rates can be calculated in whatever energy groups are desired. Once they have been calculated, Equation 5.2 can be applied to determine the applicable C-factors. Determination of the fluxes and reaction rates is done outside of the CHAIN.238DJ code, usually using any of several computer codes common in the nuclear industry. Within the CHAIN.238DJ code, the total reaction rates over all energy groups are calculated before the transmutation equations are solved. The subroutine that executes the AKM method to solve the transmutation equations receives one-group reaction rates from the main program. The AKM subroutine never uses multi-group data.

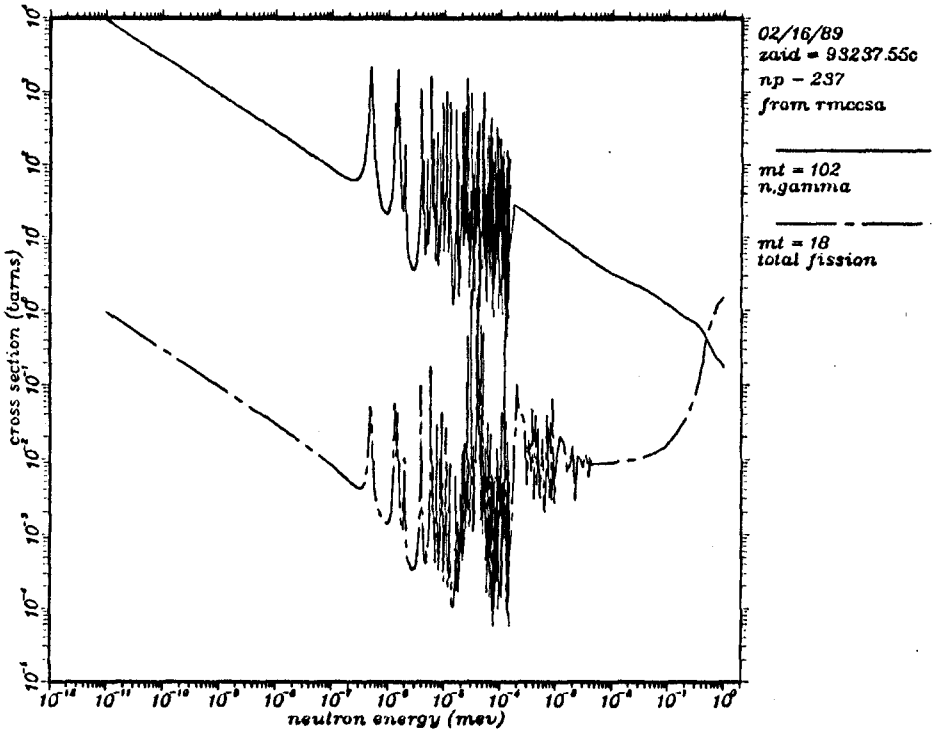

Figure 5.3 ^{237}Np Fission and Radiative Capture Cross Sections

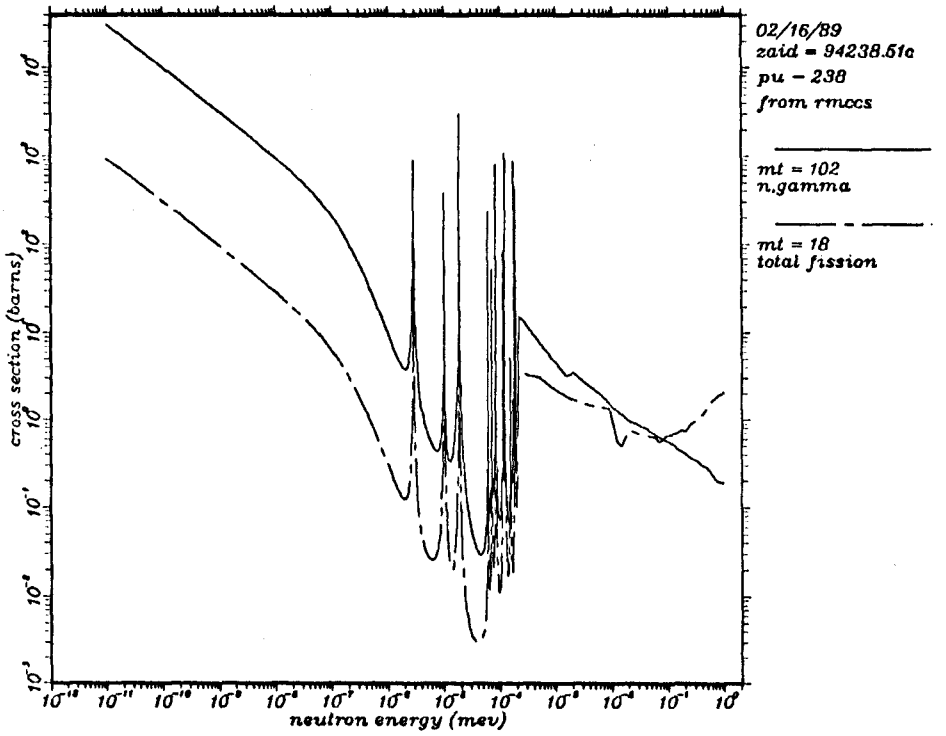

Figure 5.4 ^{238}Pu Fission and Radiative Capture Cross Sections

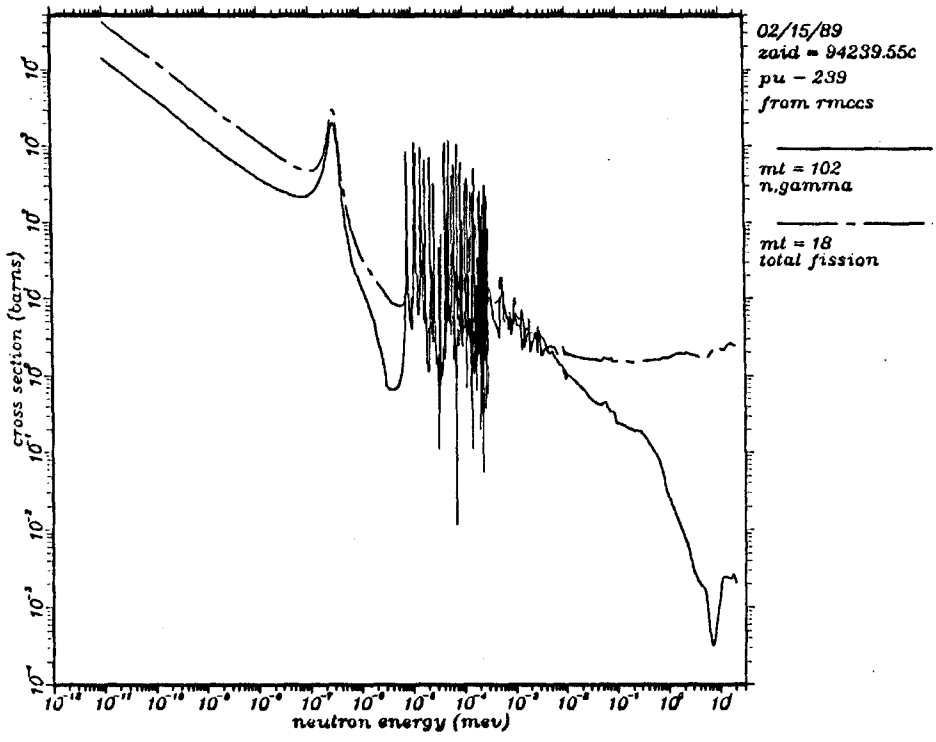

Figure 5.5 ^{239}Pu Fission and Radiative Capture Cross Sections

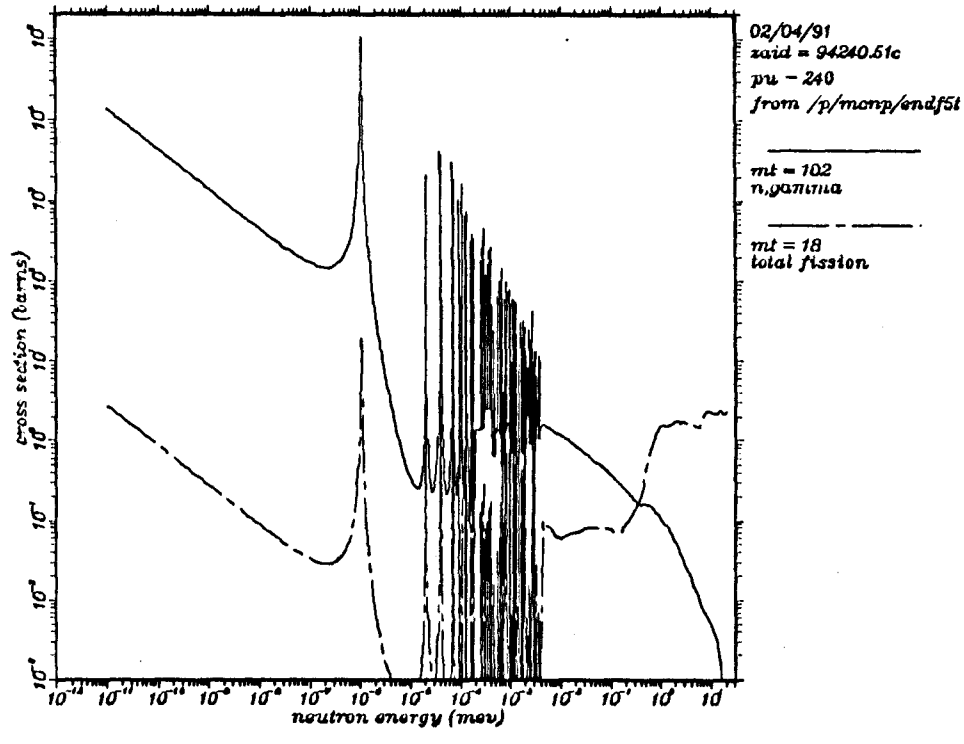

Figure 5.6 ^{240}Pu Fission and Radiative Capture Cross Sections

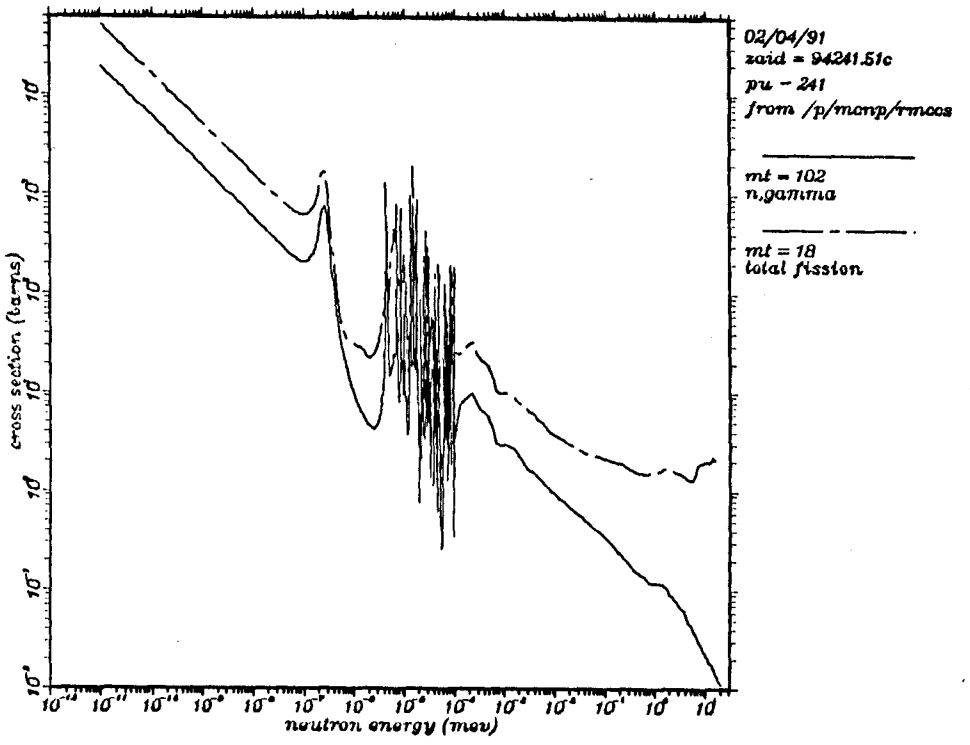

Figure 5.7 ^{241}Pu Fission and Radiative Capture Cross Sections

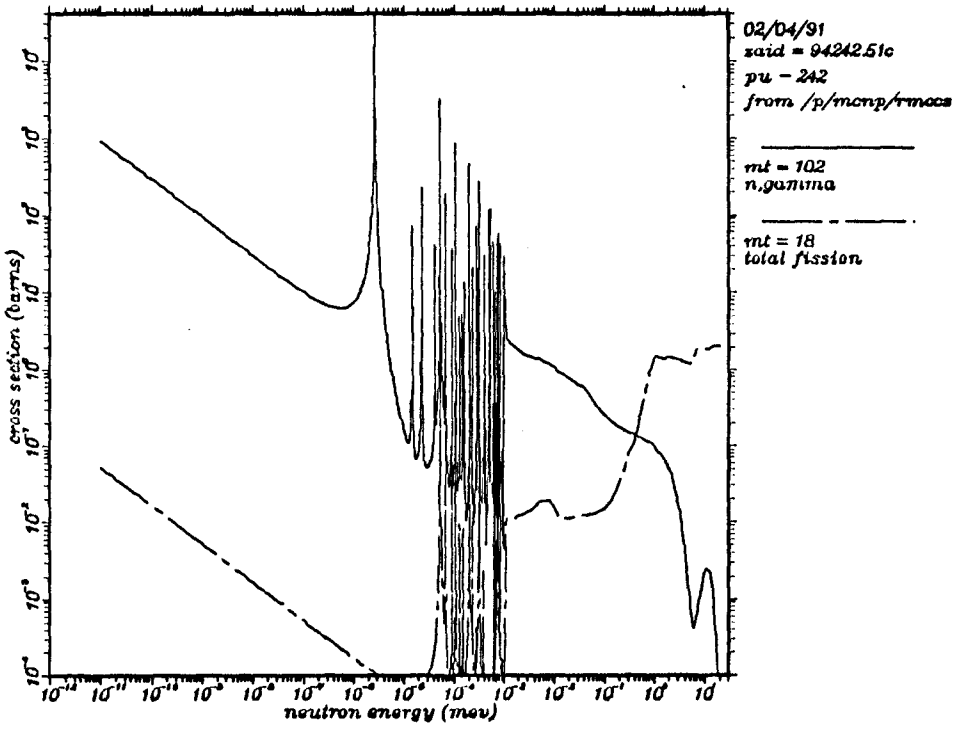

Figure 5.8 ^{242}Pu Fission and Radiative Capture Cross Sections

6.0 USING THE CHAIN.238DJ COMPUTER CODE

The CHAIN.238DJ code is written to allow for intermittent irradiation and decay time periods. This allows the user to model periods of reactor or accelerator operation and downtime. During the downtime, the reaction rates are all set to zero and only radioactive decay is modeled in the transmutation equations. Since the coefficients in the equations then consist only of decay constants, they are all constants, and the equations only need to be solved once for the period. Within an irradiation period, the code is written to allow time to be broken up into a user-chosen number of steps. The reaction rates are re-evaluated and the coefficients re-adjusted at the end of each time step using the methods discussed in Section 5.0.

The CHAIN.238DJ code has been compiled and used on a SUN 4/260 computer and on a CRAY X-MP/18. In both cases, Fortran 77 compilers were used. If an input file is in the local directory and is named unit 11 (fort.11), the CHAIN.238DJ code can be executed by invoking the name of the executable module. The user is prompted for the irradiation time period, the decay time period, the number of irradiation/decay cycles, and the number of time steps to be used in the irradiation periods. An example of these prompts (in bold), with user responses, is:

Enter the irradiation time period (days).
100
Enter the shutdown/decay time period (days).
40
Enter the number of time periods (integer).
6
Enter the number of steps in the irradiation period (integer).
200

A calculation such as this example case will run almost instantly on the CRAY X-MP/18 and will run in just a few seconds on the SUN 4/260. If more time periods and/or more time steps in the

irradiation period are used, running time will increase accordingly. For most practical problems, running time is similar to that for the example case above.

The code will create two output files, named unit 12 (fort.12) and unit 13 (fort.13). Copies of output for an example case are contained in Appendix A. Unit 12 gives initial and final amounts of each nuclide for each irradiation period and each decay period. In addition, total fission and capture reaction rates as well as the total of each being treated by the C-factor method are given for the end of each irradiation period. The total of the reaction rates being treated by the C-factor method is labelled as "Resonance Fission" and "Resonance Capture". This labelling convention can be confusing, since the user is not necessarily constrained to treating only resonance region reaction rates with the C-factor method. Unit 13 gives the plutonium quality (gram-atoms Pu-238 per gram-atom total Pu), the ^{236}Pu impurity level (gram-atoms Pu-236 per million gram-atoms Pu), and the total plutonium production level (gram-atoms total Pu) at the end of each irradiation and each decay period. The impurity level is labelled as "ppm" (parts-per-million). The calculated ppm level is on an atom basis. The ppm level on a weight basis would not be very different, since the range of atomic weights is only 236 to 242. The production level is labelled as "Kg total Pu per initial Kg Np-237". This is not strictly correct, since the code does the calculations on an atom basis, but the correction for the slight difference in atomic masses would be very small. A more serious danger with this production level labelling convention is that it assumes the initial target consists of one gram-atom of ^{237}Np, which is really not something to which the user is restricted.

6.1 The CHAIN.238DJ Input File

An input file for an example case is contained in Appendix A. It contains information for each of nine nuclides in the chain and for lumped fission products, which acts like a tenth nuclide. Each block

of information contains the nuclide name, its initial amount (gram-atoms), its half life in days, and one or eleven lines of information regarding microscopic fission and capture reaction rates. For ^{237}Np there are thirteen lines, since two additional lines of information are required for the $^{237}Np(\gamma,n)^{236}Pu$ and $^{237}Np(n,2n)^{236}Pu$ effective microscopic reaction rates. All reaction rates in the input file must have units of s^{-1}.

At the very top of the input file, the first three lines (one is blank) give information about the time, in Effective Full Power Days (EFPD's), for the ending reaction rates. This is important because the code needs to know, for purposes of setting up the linear interpolation models, the time (EFPD) that corresponds to the ending reaction rates.

The initial amounts can be atom densities, total atoms, or, as in the example shown, atoms per initial atom of ^{237}Np. It is important to realize that the final answers will have the same units as those used in the initial concentrations. For the example shown, the output of the code will give gram-atoms of each nuclide per initial gram-atom of ^{237}Np.

For fission and for capture in ^{237}Np, ^{238}Pu, ^{239}Pu, ^{240}Pu, ^{241}Pu, and ^{242}Pu, the code allows group treatment in as many as eleven groups. The first line for each nuclide contains the nuclide name, the initial amount, the half life, and beginning and ending reaction rates for fission and for capture. The time-dependent behavior of the reaction rates entered on this line will be treated using the linear interpolation method. The next seven lines allow individual treatment of as many as seven groups to be treated using the C-factor method. Each line contains the C-factor for capture and the initial microscopic capture reaction rate, the C-factor for fission and the initial microscopic fission reaction rate, and finally the beginning and ending neutron flux in the group. The time behavior of the flux is treated with a simple linear interpolation, while the C-factors are

used to determine effective group cross sections that are dependent on the amount of the nuclide present. The last three lines allow treatment of as many as three groups that are treated the same as the first group, that is, they are simply treated with a linear interpolation. These groups are provided for possible cases where the user may want to follow the reaction rates in certain energy groups and wants to use the linear interpolation method.

The twelfth and thirteenth lines in the block of information for ^{237}Np contain reaction rate information for the $^{237}Np(\gamma,n)^{236}Pu$ and $^{237}Np(n,2n)^{236}Pu$ reactions. Both of these reactions are treated using the simple linear interpolation method. At times it is desirable to separate the contribution of the $^{237}Np(\gamma,n)^{236}Pu$ reaction to the production of ^{236}Pu from that of the $^{237}Np(n,2n)^{236}Pu$ reaction. This can be done simply by running the code twice, once with each of these reaction rates put in as zero in the input file.

For fission and for capture in ^{238}Np, ^{239}Np, ^{236}Pu, and lumped fission products, the code allows only a one-group treatment of the reaction rates. Beginning and ending reaction rates must be given for capture and for fission, and the reaction rates at all intermediate times are calculated using simple linear interpolation. The ^{239}Np almost always decays at a rate orders of magnitude higher than it burns out by fission or capture. For this reason, the ^{239}Np reaction rates are usually unimportant. That is why they are entered as essentially zero in the example input file shown. The fission and capture rates of lumped fission products are also zero in the example shown, simply because in this case the lumped fission products are not important.

The code user is free to set up the input file and execute the code in any of a variety of ways. The most simple situation is to use only a one group treatment for each reaction of each nuclide by lumping the entire reaction rate spectrum into the first group. This effectively models the time behavior of all the reaction rates using a

linear interpolation. In spite of its simplicity, this mode of operation has been sufficiently accurate in many applications. A slightly less simple situation is to put the entire reaction rate into one of the "C-factor" groups. This allows the use of a C-factor while still remaining quite simple. This method can be particularly effective when the reaction rates for a particular nuclide are thoroughly dominated by one resonance, which is often the case for some of the plutonium isotopes. The most complicated situation, and the one which requires the most effort to set up, is one in which all eleven groups are used, requiring the calculation of two C-factors (one for fission and one for capture) for each group. This mode of operation seldom gives enough improvement in the precision of the final answers to merit its use.

The most typical mode of operation is one in which the reaction rates below the first resonance are modeled in the first ("thermal") group, the first one or two resolved resonances are treated individually using the C-factor method, the rest of the resolved resonance region is grouped into one resonance region and characterized by the C-factor method, and everything above the last resolved resonance is lumped into one of the last three ("fast") groups. This is what has been done for the example case in Appendix A and for the case studies to be discussed in Section 7.0.

6.2 Convergence and Time Step Size in CHAIN.238DJ

Given that it is accurate to solve the transmutation equations for short time steps and then adjust the reaction rates after each step, how short do the time steps need to be? The user needs some assurance that the time steps are sufficiently short so that the method is calculating accurate results, i.e., that the problem is "converged". An easy test of this "convergence" problem is to execute the code several times using the same input data, except that an increasingly larger number of time steps (increasingly shorter time steps) in the irradiation period is chosen with each successive

calculation. When this procedure has been repeated until the final answers no longer change with smaller time steps, the problem is almost always "converged".

The example case shown in Appendix A has been used as a case study to show "convergence". Table 6.1 shows the results of the study. The amounts shown are the final amounts after six cycles with 100 days of irradiation followed by 40 days of decay. This makes a total of 840 days, 600 EFPD. The table strongly suggests that this case is "converged" with 1/2-day time steps on the CRAY X-MP/18, but does not "converge" on the SUN 4/260. The round-off error on the SUN machine is too great for the user to know with a reasonable degree of confidence, based on information from runs on the SUN only, that the problem is "converged". In fact, when the time steps are 1/10-day or smaller, the SUN machine fails to calculate the final amount of ^{242}Pu. It gets an overflow or an underflow for the real number variable, as indicated by printing "****" instead of a number. Since the amount of ^{242}Pu is not particularly important, it might appear that the calculation on the SUN gives nearly correct results with 10-day time steps, but one would never know this without benefit of the "convergence" study performed on the CRAY.

This type of "convergence" study does not necessarily provide a vigorous mathematical guarantee of convergence. It is a "convergence" process that is not internal to the code, but is undertaken by the user. It is possible that this type of study could show convergence when it really is not there. That is highly unlikely, however, and this method of checking for "convergence" is quick, easy, effective, and can almost always be trusted. There have been no cases thus far in which the CHAIN.238DJ code has been applied and incorrect results have been obtained because of a lack of "convergence".

6 Cycles - 100 Days Irradiation/40 Days Decay							
Steps in Irradiation Period	Time Step Size (Days)	Final Amounts at 840 Days (600 EFPD) - CRAY X-MP/18					
		^{237}Np	^{238}Pu	^{239}Pu	^{240}Pu	^{241}Pu	^{242}Pu
1	100	0.785	0.183	0.0129	0.00144	8.84e-4	7.07e-5
10	10	0.784	0.184	0.0128	0.00144	8.42e-4	6.61e-5
50	2	0.784	0.184	0.0128	0.00144	8.39e-4	6.58e-5
100	1	0.784	0.184	0.0128	0.00144	8.39e-4	6.58e-5
200	1/2	0.784	0.184	0.0128	0.00144	8.38e-4	6.57e-5
500	1/5	0.784	0.184	0.0128	0.00144	8.38e-4	6.57e-5
1000	1/10	0.784	0.184	0.0128	0.00144	8.38e-4	6.57e-5
Steps in Irradiation Period	Time Step Size (Days)	Final Amounts at 840 Days (600 EFPD) - SUN 4/260					
		^{237}Np	^{238}Pu	^{239}Pu	^{240}Pu	^{241}Pu	^{242}Pu
1	100	0.785	0.183	0.0129	0.00144	8.84e-4	7.07e-5
10	10	0.784	0.184	0.0128	0.00144	8.40e-4	6.56e-5
50	2	0.784	0.184	0.0129	0.00144	8.62e-4	5.49e-5
100	1	0.784	0.184	0.0129	0.00145	8.32e-4	7.87e-5
200	1/2	0.784	0.184	0.0128	0.00142	7.95e-4	3.78e-5
500	1/5	0.784	0.184	0.0129	0.00145	8.53e-4	8.01e-5
1000	1/10	0.784	0.182	0.0125	0.00136	6.72e-4	****
1500	1/15	0.784	0.181	0.0122	0.00129	5.70e-4	****
2000	1/20	0.784	0.182	0.0125	0.00136	6.66e-4	****

Table 6.1 Time Step Size and Convergence

7.0 APPLICATION OF CHAIN.238DJ TO REAL PROBLEMS

The CHAIN.238DJ code has been applied to some realistic situations which have been thoroughly analyzed. These situations consist of ^{238}Pu production target assemblies placed in the reflector region on the outside of a fast reactor. The target assemblies feature yttrium hydride ($YH_{1.7}$) moderator pins to moderate the neutron spectrum somewhat, enhancing the neutron capture in ^{237}Np and the ^{238}Pu production. The example cases that follow are realistic design studies, but they do not represent any particular final design for a ^{238}Pu production system. The ^{236}Pu impurity levels in the example cases that follow are not correct, since the $^{237}Np(n,2n)^{236}Pu$ and $^{237}Np(\gamma,n)^{236}Pu$ effective cross sections used are known to be inaccurate. Since the ^{236}Pu concentration is never high enough for it to perturb the flux, it does not affect the time/burnup-dependency of the reaction rates and the following example cases serve as useful studies of the accuracy of the code in spite of the inaccurate $^{237}Np(n,2n)$ and $^{237}Np(\gamma,n)$ reaction rates being used.

Three example cases have been analyzed. The three cases are all significantly different, each having a unique target assembly geometry, unique target assembly material loadings, and a unique neutron spectrum. A significant shift in the neutron flux spectrum can provide new challenges for any code system. The three example cases analyzed here will all have significantly different spectral responses in order to show the accuracy of the CHAIN.238DJ code for a variety of spectra.

The first case consists of a homogeneous mixture of the $^{237}NpO_2$ target material and the $YH_{1.7}$ moderator. The second case has the same amount of target and moderator material as the first, but the geometry model is more detailed, with a heterogeneous system of target and moderator pins. The third and final case has a heterogeneous geometry model similar to the second case, but the size of the target and

moderator pins has been varied considerably, allowing very different material loadings and, therefore, a very different neutron spectrum.

For each example case, an important goal of the analysis is to validate the time-dependent reaction rates as calculated by the CHAIN.238DJ code. This is accomplished by checking the reaction rates at intermediate times in the irradiation cycle. The method used to check the reaction rates at intermediate times is to calculate them with the MCNP[10] computer code, using the target material isotopic compositions given by the CHAIN.238DJ code for those times. These reaction rates as calculated by MCNP are then compared with those used at the particular time in question by CHAIN.238DJ. This "checking" procedure has been performed at several intermediate times and also at the end-of-irradiation for the example cases. Plots have been generated which show the various reaction rates in the transmutation chain as calculated by the CHAIN.238DJ code with the results of the MCNP calculations at the "check points" represented on the same plots by "+" signs. For many of these reaction rates, plots have been generated not only for the total reaction rate, but also for the portion of the reaction rate that comes out of the resolved resonance region. For plots of the total reaction rate, the height of the "+" sign represents the one-standard-deviation statistical uncertainty in the Monte Carlo calculation. Plots of the resolved resonance region reaction rates do not have an indication of the statistical uncertainty, but it is almost always at least as much (in percent) as it is for the total reaction rate.

The CHAIN.238DJ calculations for these example cases used five neutron energy groups for calculating the fission and radiative capture reaction rates for ^{237}Np and ^{238}Pu. Three of these energy groups were resolved resonance region groups that were treated with the C-factor method. For fission and radiative capture in ^{239}Pu, ^{240}Pu, ^{241}Pu, and ^{242}Pu a four energy group treatment was used, with two of the groups being in the resolved resonance region where the C-factor method was employed. All other reaction rates in the

CHAIN.238DJ calculations were calculated using the simple linear interpolation method. The irradiation scenario used in the first two example cases features six cycles of 88.3-day irradiations followed by 40-day shutdown/decay periods, for a two year or 530 Effective Full Power Days (EFPD) irradiation. In the third example case, the irradiation period is 88.3 days and the decay period is 50 days. There are three irradiation cycles, for a total of 265 EFPD representing a one year irradiation.

In cases where a reaction rate calculated by the CHAIN.238DJ code is not in close agreement with the intermediate check points generated by MCNP calculations, sensitivity studies have been performed to determine the error that might occur in the final results of the calculation. The CHAIN.238DJ code is not very sensitive to some of the reaction rates. For example, the $^{238}Np(n,\gamma)$ reaction rate is not very important because burnout of ^{238}Np is dominated by radioactive decay. Similarly, $^{237}Np(n,f)$ is not very important because burnout of ^{237}Np is dominated by radiative capture. On the other hand, some of the reaction rates, such as $^{237}Np(n,\gamma)$, $^{237}Np(n,2n)$, or $^{238}Pu(n,\gamma)$, are very important, and errors in these reaction rates can have a significant impact on the final results of the calculation.

The MCNP (Monte Carlo Neutron-Photon) computer code has been used to calculate the cross sections, fluxes, and reaction rates for the example cases. In these Monte Carlo calculations, statistical uncertainties in the answers are a constant source of concern. Every effort has been made to minimize these uncertainties. Most of the calculated parameters carry statistical uncertainties of only one or two percent, but some carry more. For most of the analysis, the Monte Carlo statistical uncertainties are shown in the data. The MCNP code has been chosen for these cases because of the characteristics of the irradiation vehicle. It is merely the choice for this study and need not necessarily be the choice in other situations where the CHAIN.238DJ code might be applied. Any of the numerous neutronics

analysis codes common in the nuclear industry could be used to calculate the fluxes and effective cross sections needed as input to the CHAIN.238DJ code.

7.1 An Iterative Scheme to Determine the Final Isotopic Composition

The initial composition of the $^{237}NpO_2$ target material to be irradiated in the following example cases is known. It is simply a function of the design and is assumed to be 100% $^{237}NpO_2$ at the target mass loadings chosen. This composition can be used in the MCNP code to calculate the initial reaction rates needed for the transmutation calculation performed with the CHAIN.238DJ code. The final end-of-irradiation (EOI) target material composition is not initially known, yet it must be known before the EOI MCNP calculation can be performed. Since this MCNP calculation provides data to be fed into the CHAIN.238DJ code, it needs to be completed before the transmutation calculation can be performed. It is as if the results of the CHAIN.238DJ code calculation are a prerequisite to running the CHAIN.238DJ code. Since the final target material isotopic composition is not known ahead of time, the change in the reaction rates from the fresh to the burned composition cannot be known either.

A solution to this problem is to make an initial guess at the time-dependent change in the reaction rates, use the CHAIN.238DJ code to calculate the final isotopic composition based on that guess, then run the MCNP code with that final composition to check the validity of the initial guess. If the initial guess proves inaccurate, the results of the MCNP calculation can be used as the basis for a new, improved guess. This scheme can be repeated iteratively until the guess proves reliable; then the problem is converged. Figure 7.1 shows a flowchart for this iterative scheme.

Convergence of the final target material composition together with some type of proof that the reaction rates are sufficiently accurate at intermediate times provides confidence that the

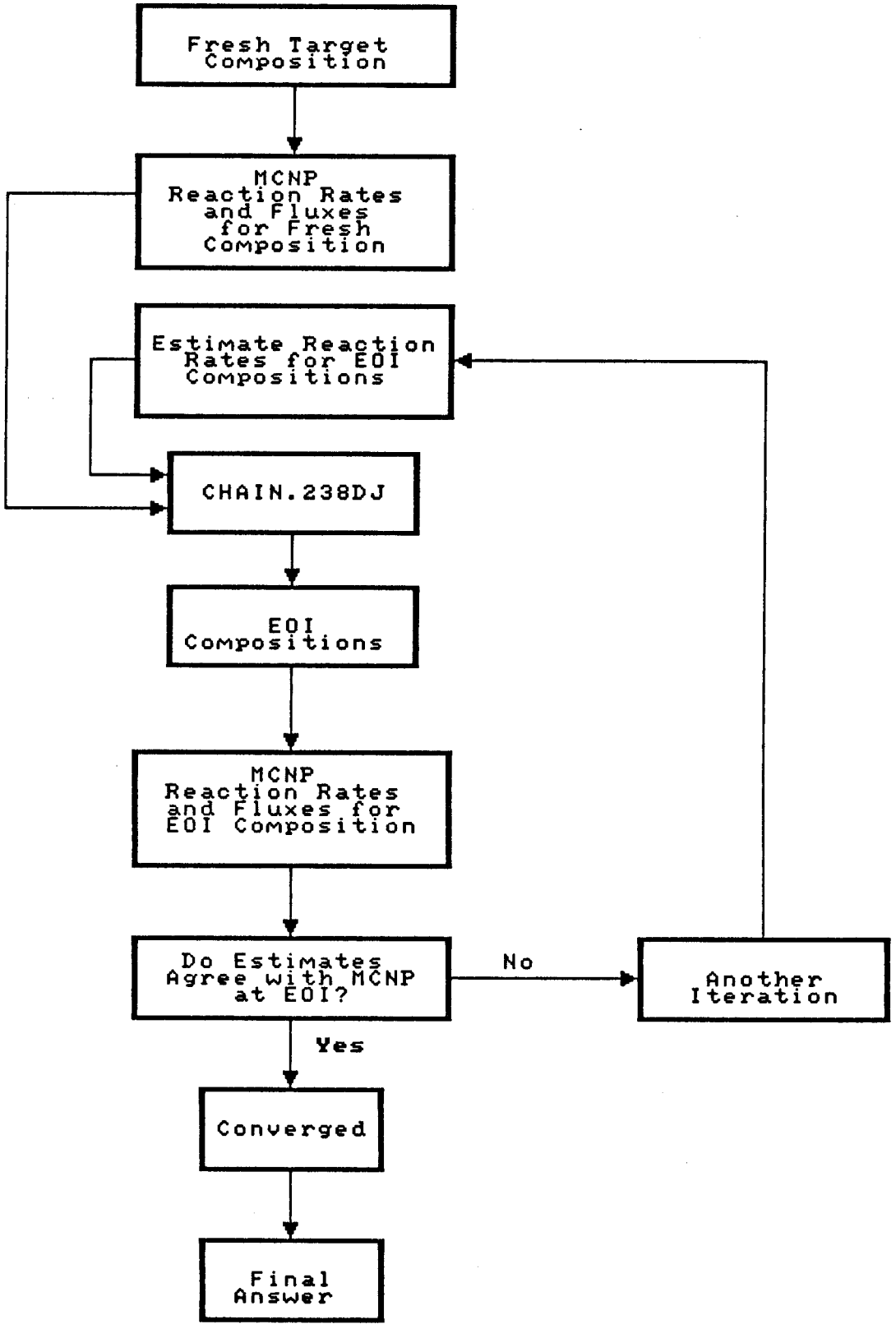

Figure 7.1 Iterative Scheme for EOI Compositions

CHAIN.238DJ code has calculated correct results. The rest of this subsection presents a thorough study of the convergence of the final composition for the first example case. The following three subsections present a study of the accuracy of the CHAIN.238DJ code models of the behavior of the reaction rates at intermediate times.

Table 7.1 shows the results of a study of the convergence of the final target material composition for example case 1. Exponents have been left off the numbers for the final amounts and microscopic reaction rates ($RR = \int_0^\infty \sigma(E)\phi_E(E)dE$), since it is their fractional change from one iteration to the next that is important. The ^{236}Pu has been ignored in this convergence study, since there is not enough of it produced for it to perturb the flux and affect the reaction rates. The initial guess for this case was to assume that the reaction rates calculated using MCNP with the fresh target composition do not change during irradiation. This is equivalent to assuming that the self-shielding and the internal fission neutron source strength do not change during the irradiation. Table 7.1 shows that convergence comes to the first nuclides in the chain in just two or three iterations. After that, convergence seems to progress down the chain with each successive iteration until the final amount of ^{242}Pu appears to be converged after six iterations. This does not suggest that one need perform six iterations for every case to be analyzed. The initial guess for this case was purposely simple and poor. Normally, one can make a better initial guess based on previous experience, as will be done for the second and third cases to be analyzed in the subsections that follow. Also, the number of iterations necessary for convergence is not the same as the number needed to provide reasonable evidence of convergence. In the case shown in Table 7.1, the final amounts after the third iteration are probably as good as those after the sixth, but without going out to the sixth iteration one would not know this with any degree of confidence.

Parameter	Iteration/Final Composition at 530 EFPD					
	First	Second	Third	Fourth	Fifth	Sixth
^{237}Np final amount:	0.778	0.768	0.767	0.767	0.768	0.767
% change in final amount from previous iteration:		-1.3%	-0.1%	< 0.1%	+0.1%	-0.1%
final (n,γ) RR:	5.392	5.95	5.97	5.99	5.95	5.99
final (n,f) RR:	1.019	1.274	1.258	1.252	1.260	1.263
^{238}Np final amount:	1.10	1.19	1.20	1.20	1.20	1.20
% change in final amount from previous iteration:		+8.2%	+0.8%	< 0.1%	< 0.1%	< 0.1%
final (n,γ) RR:	9.733	9.241	9.478	9.556	9.350	9.341
final (n,f) RR:	2.315	2.227	2.279	2.296	2.250	2.249
^{238}Pu final amount:	0.192	0.203	0.203	0.204	0.203	0.204
% change in final amount from previous iteration:		+5.7%	< 0.1%	+0.5%	-0.5%	+0.5%
final (n,γ) RR:	3.98	3.204	3.218	3.279	3.189	3.206
final (n,f) RR:	7.027	7.099	7.000	7.017	6.982	7.008
^{239}Pu final amount:	0.014	0.0125	0.0125	0.0127	0.0125	0.0125
% change in final amount from previous iteration:		-10.1%	< 0.1%	+1.6%	-1.6%	< 0.1%
final (n,γ) RR:	8.061	7.345	7.579	7.718	7.44	7.48
final (n,f) RR:	1.256	1.139	1.172	1.192	1.154	1.158
^{240}Pu final amount:	1.12	0.967	0.974	0.986	0.968	0.973
% change in final amount from previous iteration:		-13.7%	+0.7%	+1.2%	-1.8%	+0.5%
final (n,γ) RR:	5.217	4.873	5.134	5.288	4.99	5.02
final (n,f) RR:	1.402	1.672	1.662	1.655	1.658	1.667
^{241}Pu final amount:	6.59	5.58	5.75	5.94	5.60	5.67
% change in final amount from previous iteration:		-15.3%	+3.0%	+3.3%	-5.7%	+1.2%
final (n,γ) RR:	5.353	4.962	5.106	5.187	5.052	5.006
final (n,f) RR:	1.48	1.393	1.431	1.443	1.409	1.405
^{242}Pu final amount:	2.10	2.82	2.92	3.03	2.84	2.84
% change in final amount from previous iteration:		+34.3%	+3.5%	+3.8%	-6.3%	< 0.1%
final (n,γ) RR:	1.329	1.289	1.346	1.307	1.317	1.349
final (n,f) RR:	8.637	10.77	10.65	10.58	10.67	10.69

Table 7.1 Convergence of Final Composition for Case 1

7.2 Application to a Homogeneous Case: Example 1

The geometry of the example case used for the end-of-irradiation convergence study consists of a semi-infinite homogeneous mixture of $^{237}NpO_2$ target material and $YH_{1.7}$ moderator. It represents a homogeneous version of the case to be analyzed in subsection 7.3, which has a heterogeneous geometry of target and moderator pins. The homogeneous case is a good one to begin with, since it is the simplest. Given that the final composition of the target material has been shown to be converged for this case, it is now necessary to show that the reaction rates used at intermediate times are reasonably accurate.

Figure 7.2 shows the $^{237}Np(n,\gamma)$ reaction rate as a function of irradiation time, as calculated by the CHAIN.238DJ code. The "+" signs represent the same reaction rate as calculated with the MCNP code using the target composition for that time given by the CHAIN.238DJ code. The height of the "+" signs indicate the one-

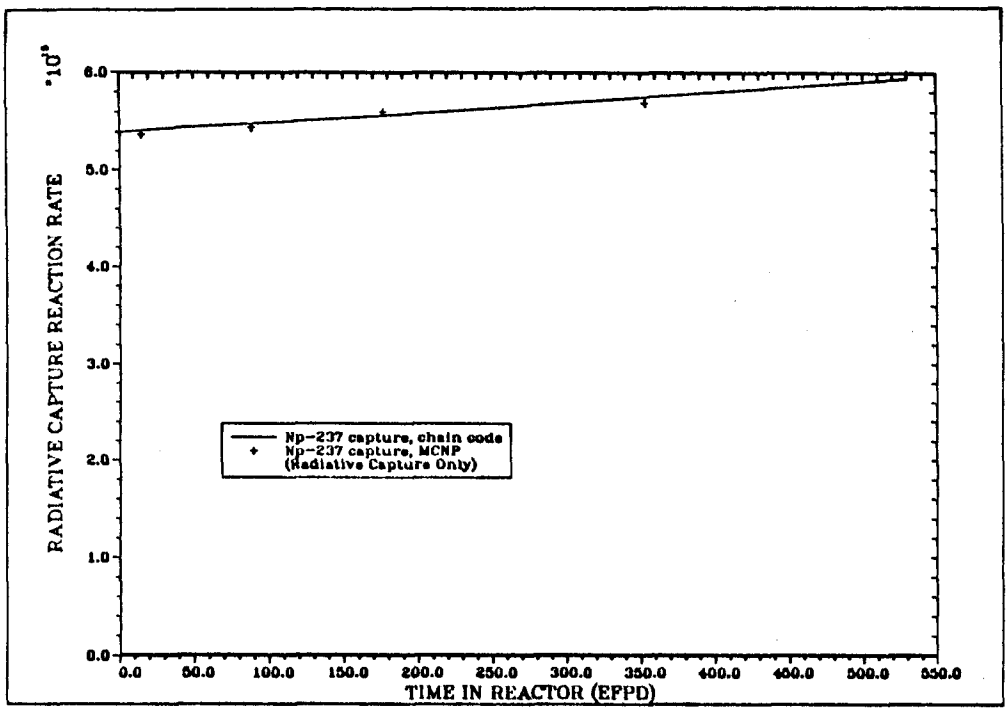

Figure 7.2 Total Microscopic Radiative Neutron Capture Reaction Rate vs Time for Np-237 - Example Case 1

standard-deviation statistical uncertainty from the Monte Carlo calculation. All five of the "+" signs lie either right on the line or very close to it, indicating that the CHAIN.238DJ code does a very good job of predicting the changes in that reaction rate during irradiation. Figure 7.3 shows a similar plot for the $^{238}Pu(n,\gamma)$

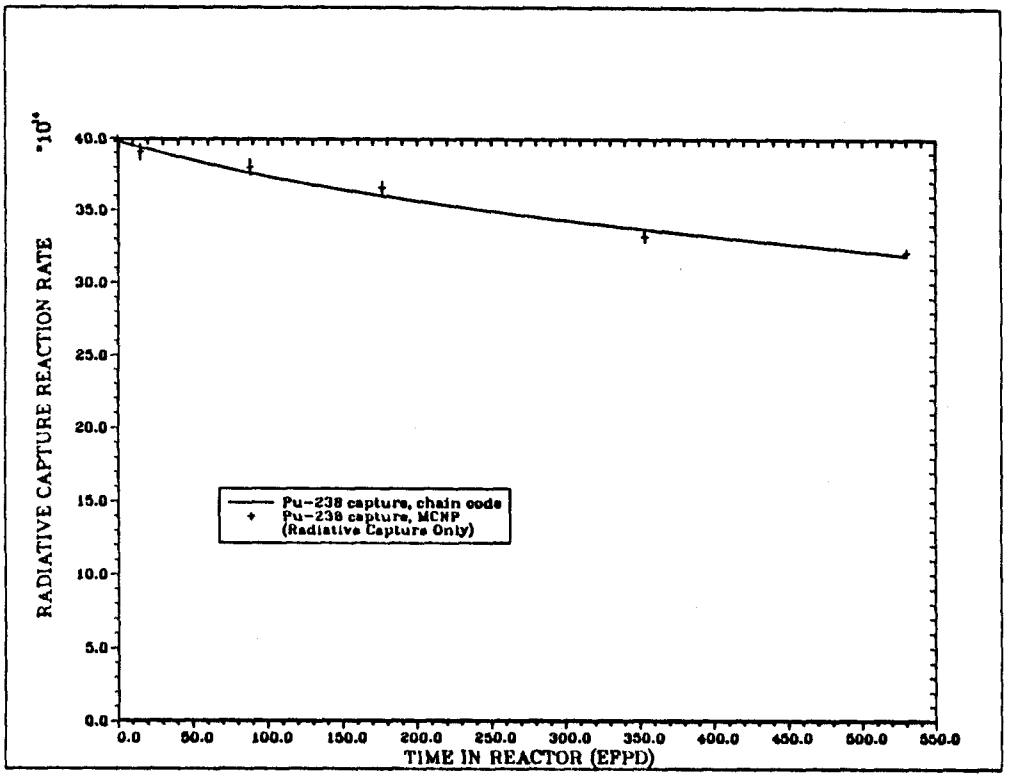

Figure 7.3 Total Microscopic Radiative Neutron Capture Reaction Rate vs Time for Pu-238 - Example Case 1

reaction rate. This case is more interesting because the reaction rate changes more through time. Again, the "check points" from the MCNP calculations at intermediate times verify the reaction rate being used at those times by the CHAIN.238DJ code. Figure 7.4 shows the same reaction rate, but only the fraction of it that occurs in the resolved resonance region. This serves as a particularly useful check of the C-factor method, since it has been used for the energy groups that make up this reaction rate. The C-factor method does a very good job of predicting the changing reaction rate in this case.

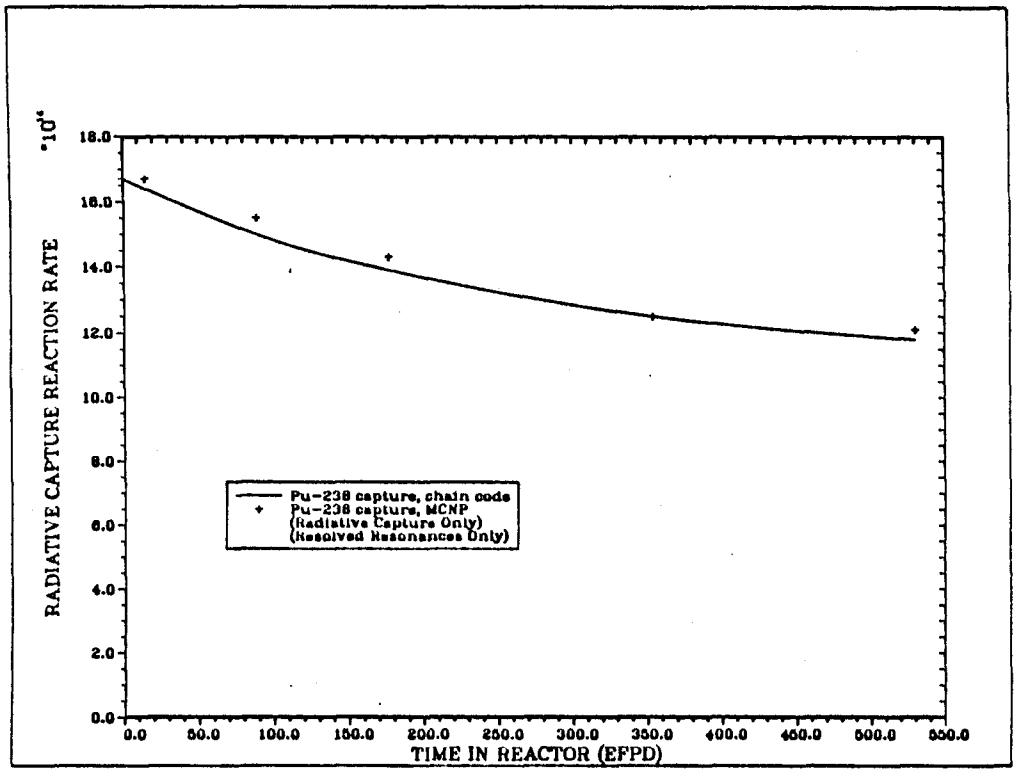

Figure 7.4 Microscopic Radiative Neutron Capture Reaction Rate in the Resolved Resonance Region vs Time for Pu-238 - Example Case 1

Figures 7.5 through 7.8 show plots of the total and resolved resonance region reaction rates for $^{241}Pu(n,\gamma)$ and $^{241}Pu(n,f)$. The CHAIN.238DJ code appears to consistently overpredict these reaction rates at intermediate times by an average of about 2% for the total and 3% for the resolved resonance region. These discrepancies between the CHAIN.238DJ code and the MCNP results lie outside the range of the one-sigma statistical uncertainties in the MCNP calculation. It is tempting to simply dismiss the error in the reaction rates calculated by the CHAIN.238DJ code because they are really quite small, being only two or three percent, but a sensitivity study has been done.

The sensitivity of the code to small errors such as this can be checked by adjusting these reaction rates downward by about 3% and then looking for a change in the final results of the calculation.

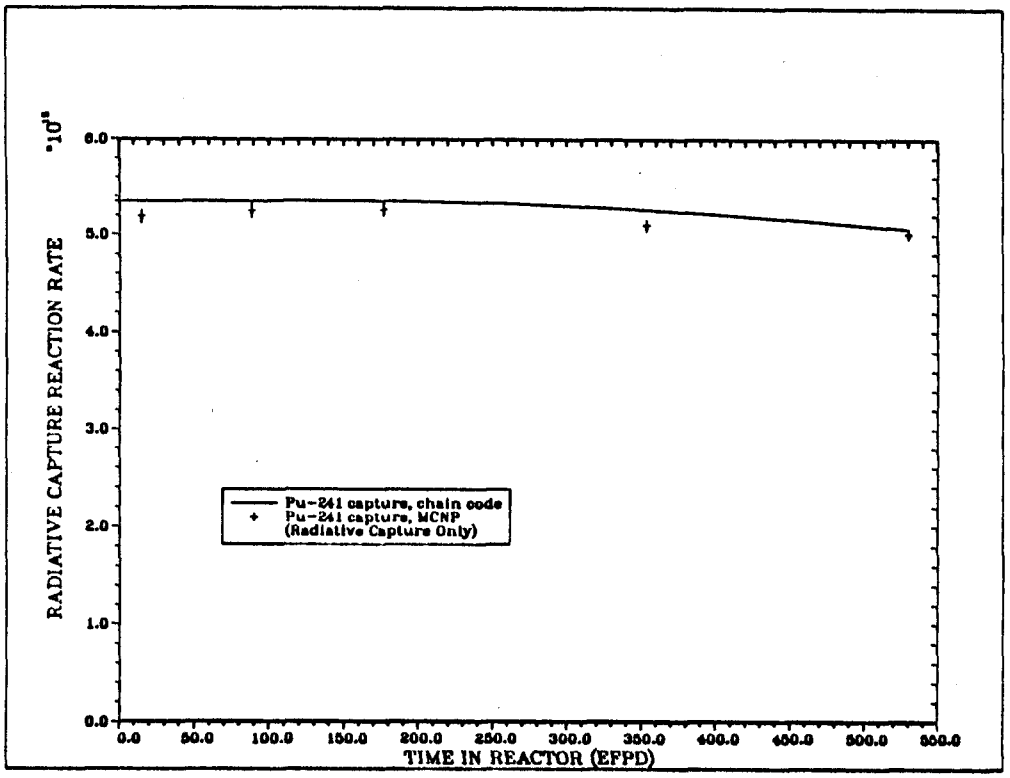

Figure 7.5 Total Microscopic Radiative Neutron Capture Reaction Rate vs Time for Pu-241 - Example Case 1

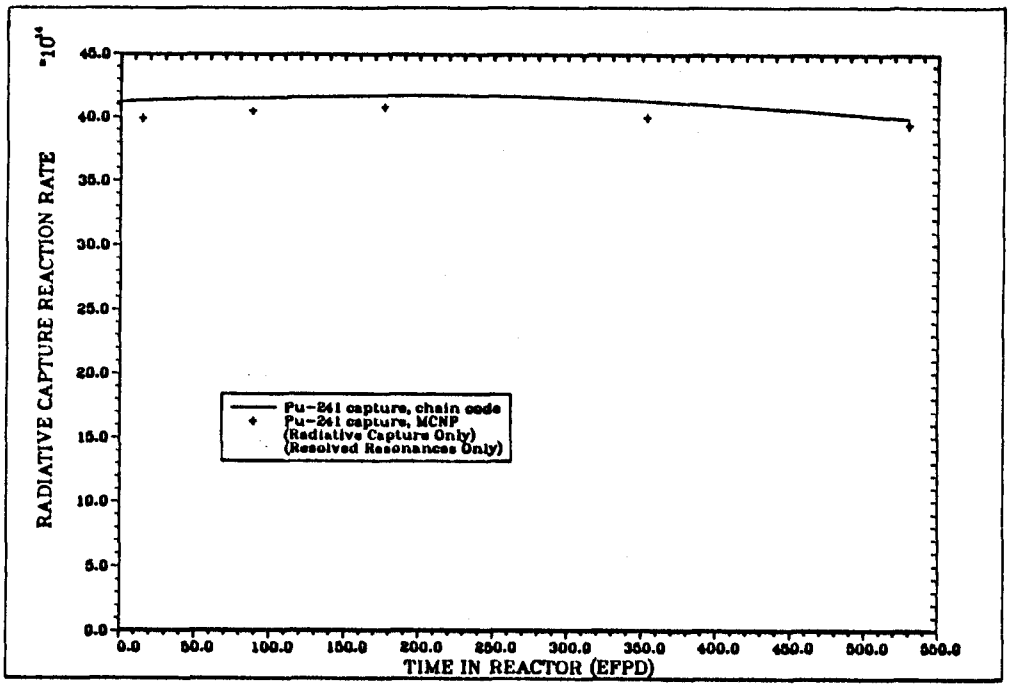

Figure 7.6 Microscopic Radiative Neutron Capture Reaction Rate in the Resolved Resonance Region vs Time for Pu-241 - Example Case 1

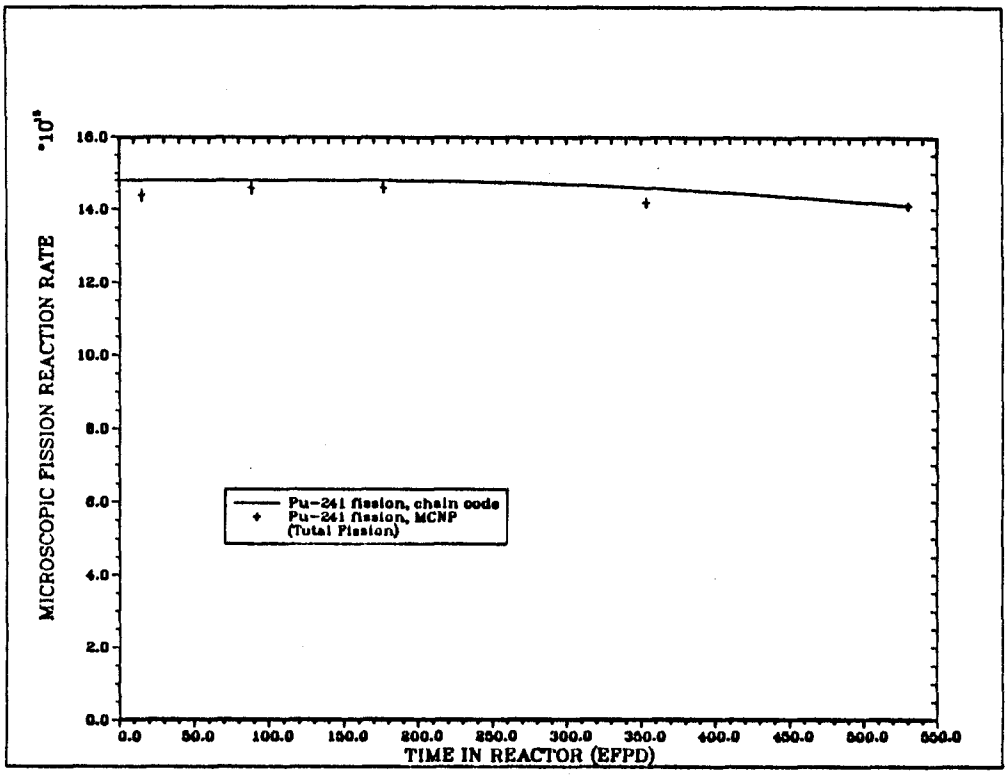

Figure 7.7 Total Microscopic Fission Reaction Rate vs Time for Pu-241 - Example Case 1

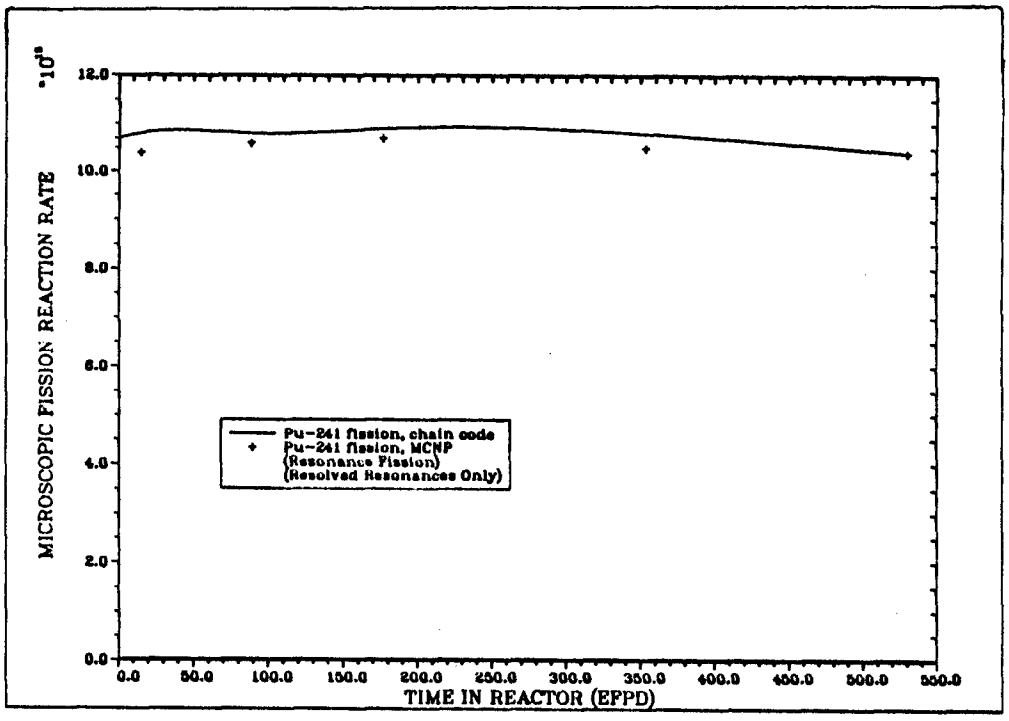

Figure 7.8 Microscopic Fission Reaction Rate in the Resolved Resonance Region vs Time for Pu-241 - Example Case 1

Figures 7.9 and 7.10 show the total ^{241}Pu reaction rates used by the CHAIN.238DJ code in a new calculation. These reaction rates are in closer agreement with those calculated for the intermediate times by the MCNP code. The results of the new calculation are shown in Table 7.2. These are obviously not significant changes from the results of the original CHAIN.238DJ calculation, especially considering the relative unimportance of the final amount of ^{242}Pu.

The ^{241}Pu reaction rates from the CHAIN.238DJ code are not as accurate as those of the other nuclides because the C-factor method is not working as well for ^{241}Pu. The reason for this is immediately evident in Figure 7.11. The first ^{241}Pu resonance is directly underneath the first resonance of ^{239}Pu. This causes the presence of ^{239}Pu to strongly resonance shield the ^{241}Pu. This effect is made even more important by the fact that the $^{241}Pu(n,\gamma)$ and $^{241}Pu(n,f)$ reaction rates are dominated by the first resonance.

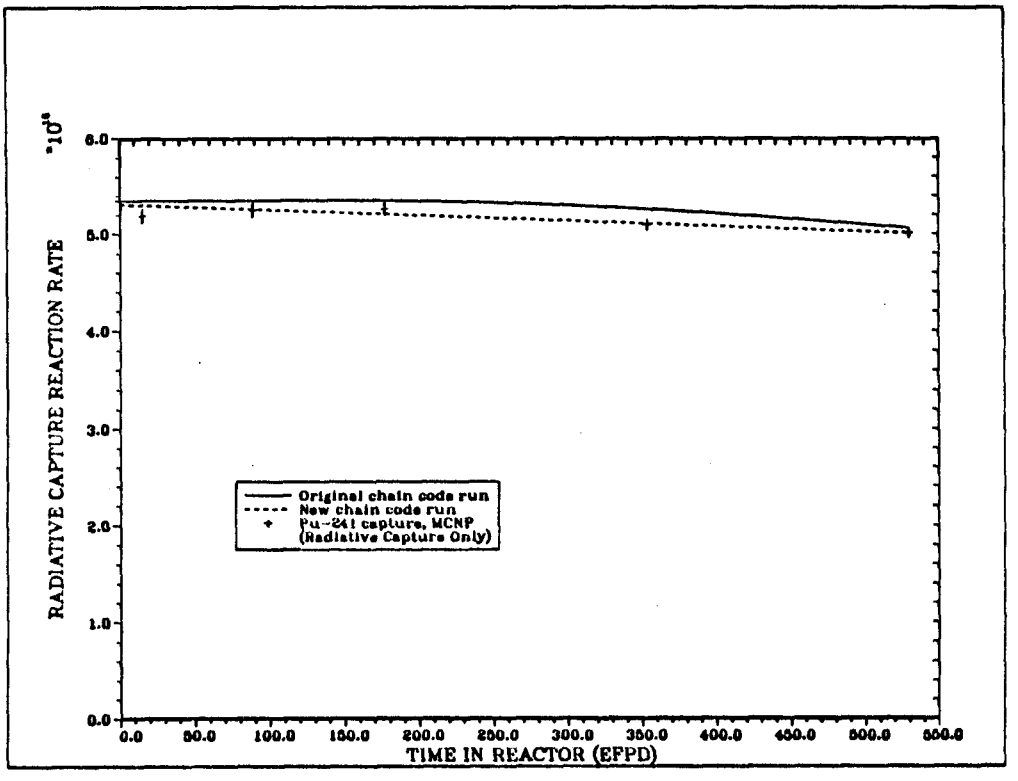

Figure 7.9 New Total Microscopic Radiative Neutron Capture Reaction Rate vs Time for Pu-241 - Example Case 1

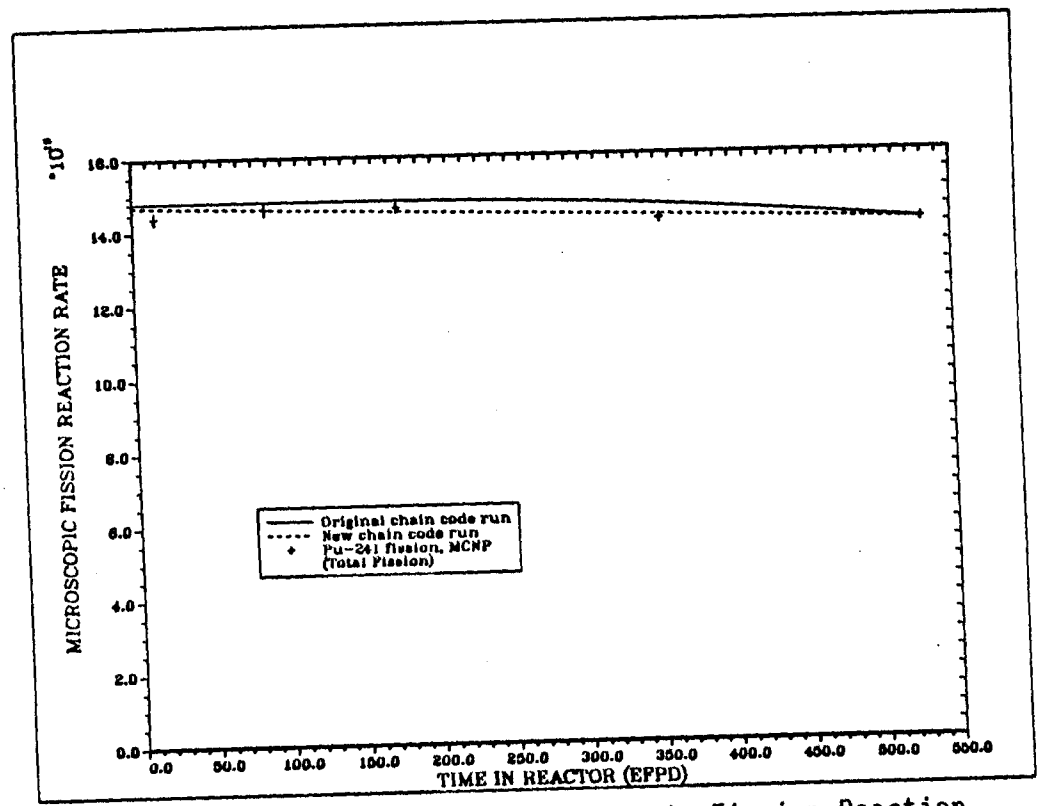

Figure 7.10 New Total Microscopic Fission Reaction Rate vs Time for Pu-241 - Example Case 1

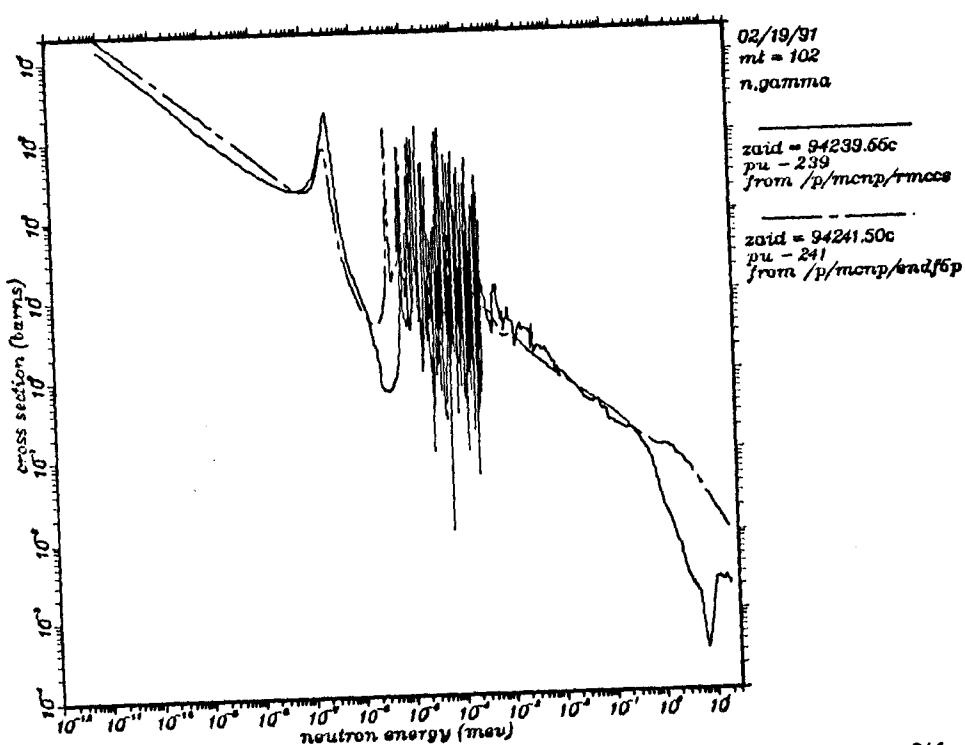

Figure 7.11 Radiative Capture Cross Sections for ^{239}Pu and ^{241}Pu

Nuclide	Final Amounts (gram-atoms) at 730 Days (530 EFPD)		
	Results From Original Calculation	Results With New Pu-241 Reaction Rates	Change From Original Calculation
^{237}Np	0.768	0.768	0
^{238}Np	0.0012	0.0012	0
^{238}Pu	0.203	0.203	0
^{239}Pu	0.0125	0.0125	0
^{240}Pu	9.68e-4	9.68e-4	0
^{241}Pu	5.60e-4	5.61e-4	+0.2%
^{242}Pu	2.84e-5	2.79e-5	-1.8%
Total Plutonium	0.21706	0.21706	< 0.1%
Quality ($^{238}Pu/Pu$)	93.5%	93.5%	< 0.1%

Table 7.2 ^{241}Pu Reaction Rate Sensitivity Study - Example Case 1

The CHAIN.238DJ code is not very sensitive to small errors in the ^{241}Pu reaction rates mostly because it is one of the last nuclides in the chain. If the $^{238}Pu(n,\gamma)$ and $^{238}Pu(n,f)$ reaction rates are changed by a similar fractional amount, the effects are more noticeable. Figures 7.12 and 7.13 show the total ^{238}Pu reaction rates as used in another new calculation. The ^{241}Pu reaction rates used in this calculation were the same as those in the original calculation. Table 7.3 shows a comparison of the results of the new calculation with those from the original calculation. The results are more noticeably affected than they were in the ^{241}Pu reaction rate sensitivity study, but the effect on the important results is still not very significant. The calculated ^{238}Pu production level is the same, and the plutonium quality ($^{238}Pu/Pu$ fraction) and ^{236}Pu ppm impurity concentration are changed very little if at all.

Other reaction rate plots for example case 1 show close agreement between the CHAIN.238DJ reaction rates and those calculated by MCNP. The differences are at most only a few percent and are often less than one percent. The sensitivity studies have shown that these

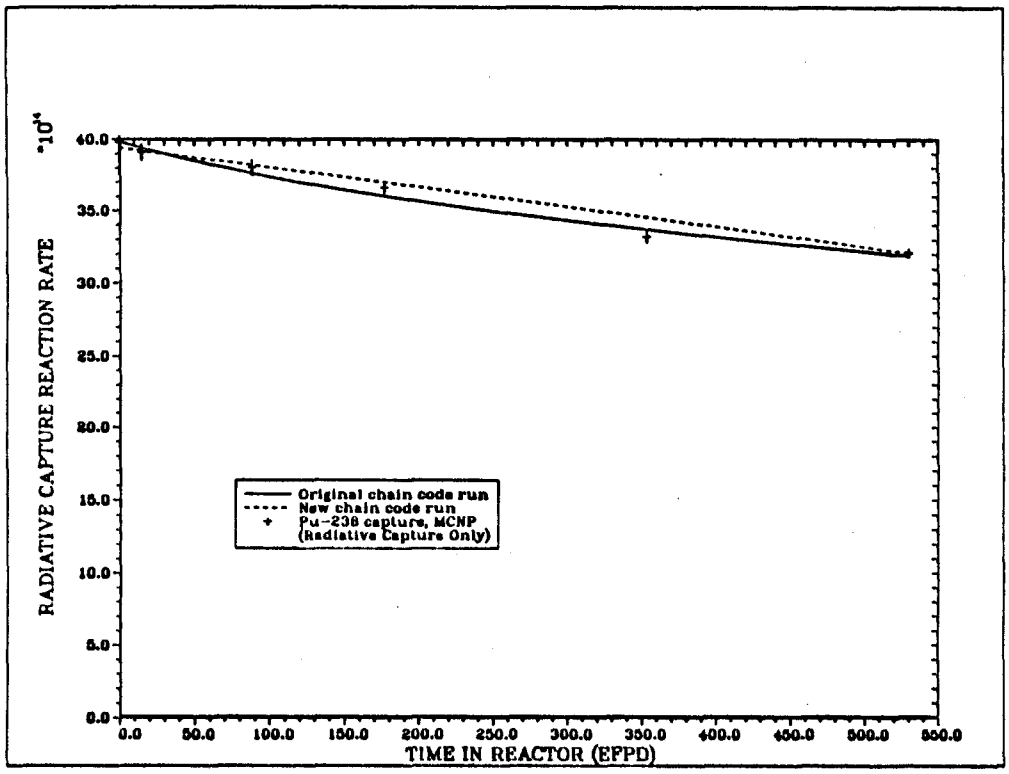

Figure 7.12 New Total Microscopic Radiative Neutron Capture Reaction Rate vs Time for Pu-238 - Example Case 1

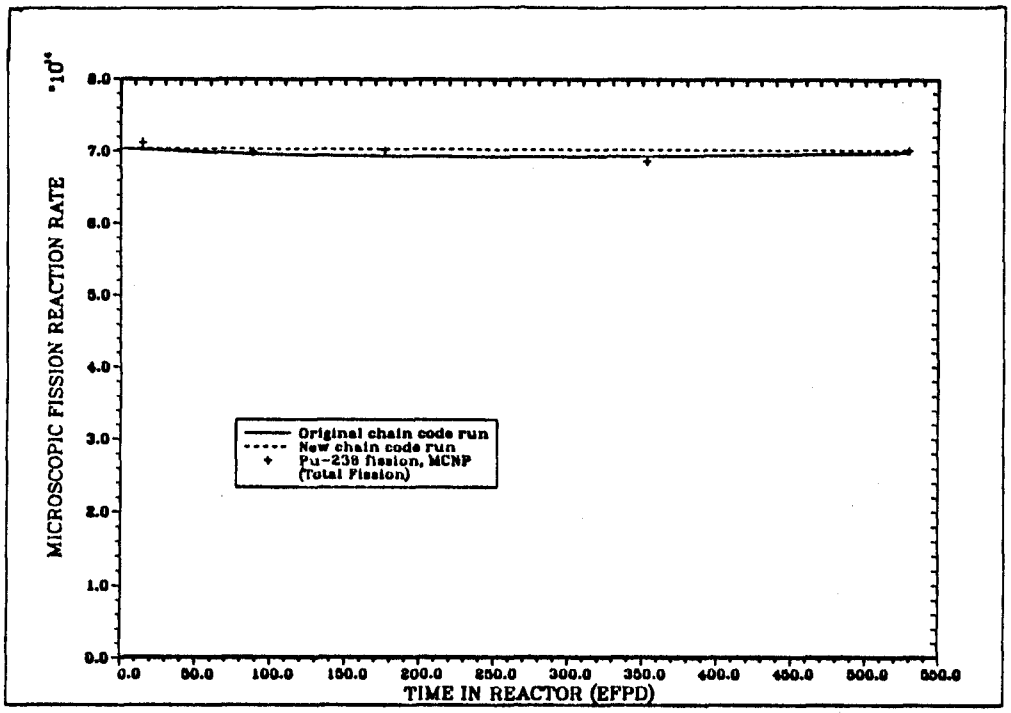

Figure 7.13 New Total Microscopic Fission Reaction Rate vs Time for Pu-238 - Example Case 1

Nuclide	Final Amounts (gram-atoms) at 730 Days (530 EFPD)		
	Results From Original Calculation	Results With New Pu-238 Reaction Rates	Change From Original Calculation
^{237}Np	0.768	0.768	0
^{238}Np	0.0012	0.0012	0
^{238}Pu	0.203	0.203	< 0.1%
^{239}Pu	0.0125	0.0127	+1.6%
^{240}Pu	9.68e-4	9.89e-4	+2.2%
^{241}Pu	5.60e-4	5.72e-4	+2.1%
^{242}Pu	2.84e-5	2.90e-5	+2.1%
Total Plutonium	0.21706	0.21729	+0.1%
Quality ($^{238}Pu/Pu$)	93.5%	93.4%	-0.1%

Table 7.3 ^{238}Pu Reaction Rate Sensitivity Study - Example Case 1

small differences have no important effect on the final results of the CHAIN.238DJ calculations

7.3 Application to a Heterogeneous Case: Example 2

The first example case analyzed was for a semi-infinite homogeneous mixture of absorber and moderator. The CHAIN.238DJ code worked well for the homogeneous geometry, but this could be partly because the analytical basis of the C-factor method assumes a homogeneous system. More realistic cases involve heterogeneous systems of absorber pins and moderator pins, for which the CHAIN.238DJ code needs to work equally well. This second example case features a detailed heterogeneous model. It represents the same design as the first case in that the assembly $YH_{1.7}$ moderator and $^{237}NpO_2$ target mass loadings are the same. The first case represented a homogenized version of this second case. The production of ^{236}Pu impurity will be included in the analysis of this second case.

Figure 7.14 shows a core mid-plane section of the geometry used in the second example case. It features 19 moderator pins (the large circles) and 36 target pins (the small circles). There are 45.3 kg of $YH_{1.7}$ moderator and 14.8 kg of initial $^{237}NpO_2$ target material per hexagonal assembly. In spite of their having the same material loadings, there is a significant difference in the neutron flux spectrum seen by the ^{237}Np target isotope in the first and the second example cases. Figure 7.15 shows the flux in the thermal region and Figure 7.16 the flux in the resolved resonance region for the first two cases. The homogeneous case has about half the thermal flux of the heterogeneous case, slightly more flux in the resolved resonance region, about the same fast flux, and about the same total flux. This shows one of several important effects of intimately mixing the target and moderator materials. Mixing the target and the moderator together significantly enhances the resonance absorption. The resonance absorption is enhanced so much that the thermal flux is depressed because fewer neutrons survive resonance absorption and reach the thermal region.

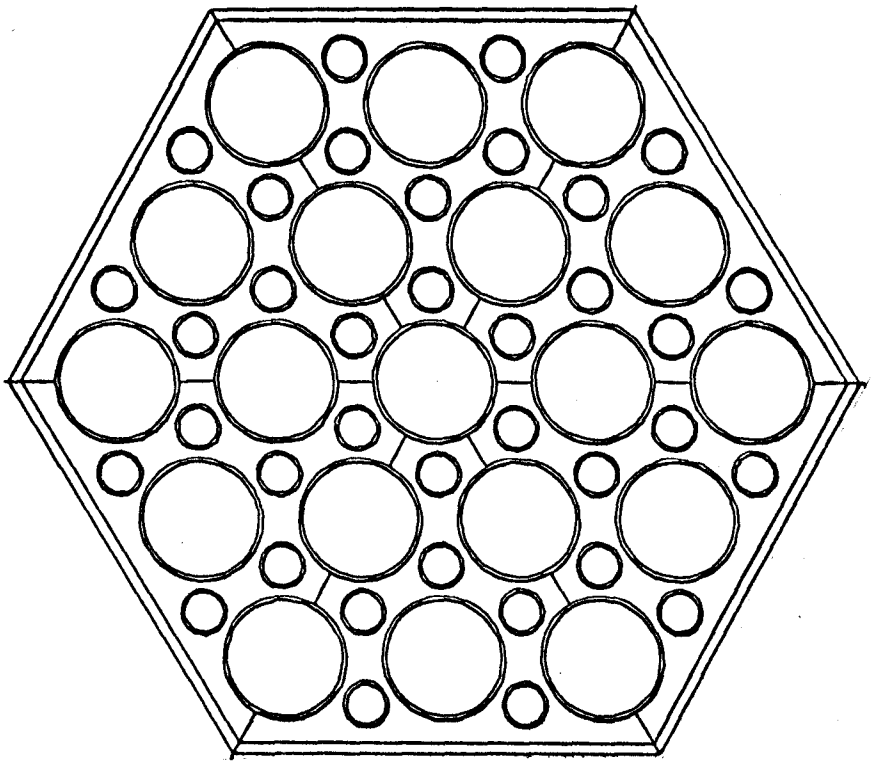

Figure 7.14 Geometry of Example Case 2 (x-y plot at core mid-plane)

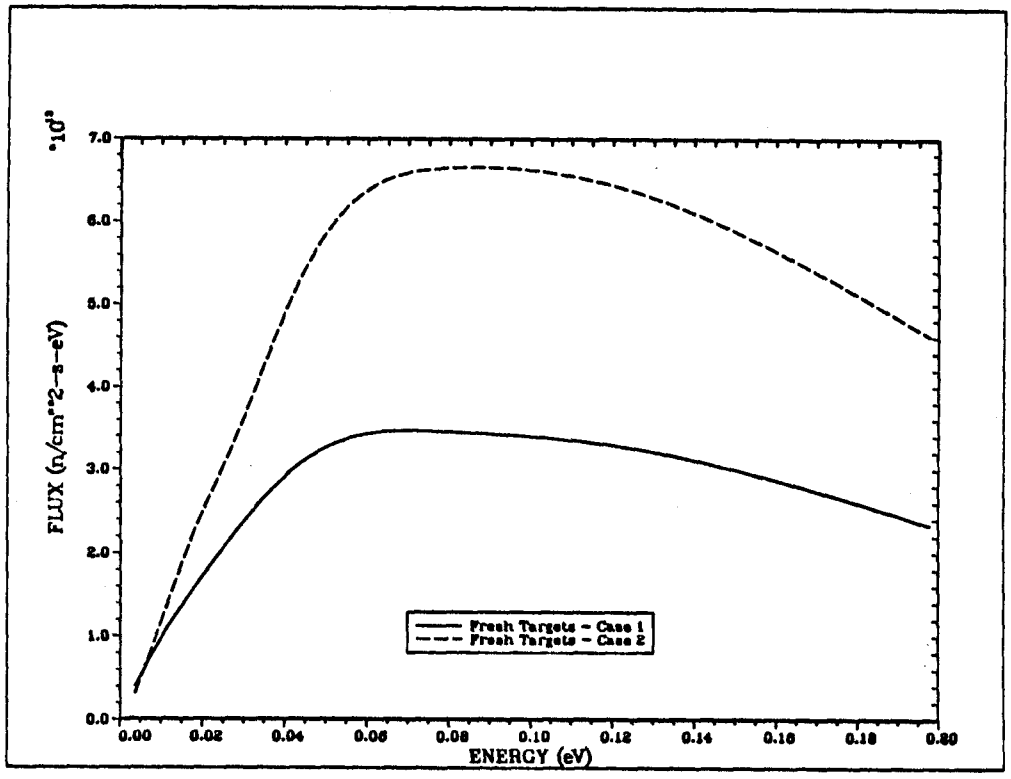

Figure 7.15 Thermal Flux in the Target Pins - Example Cases 1 and 2

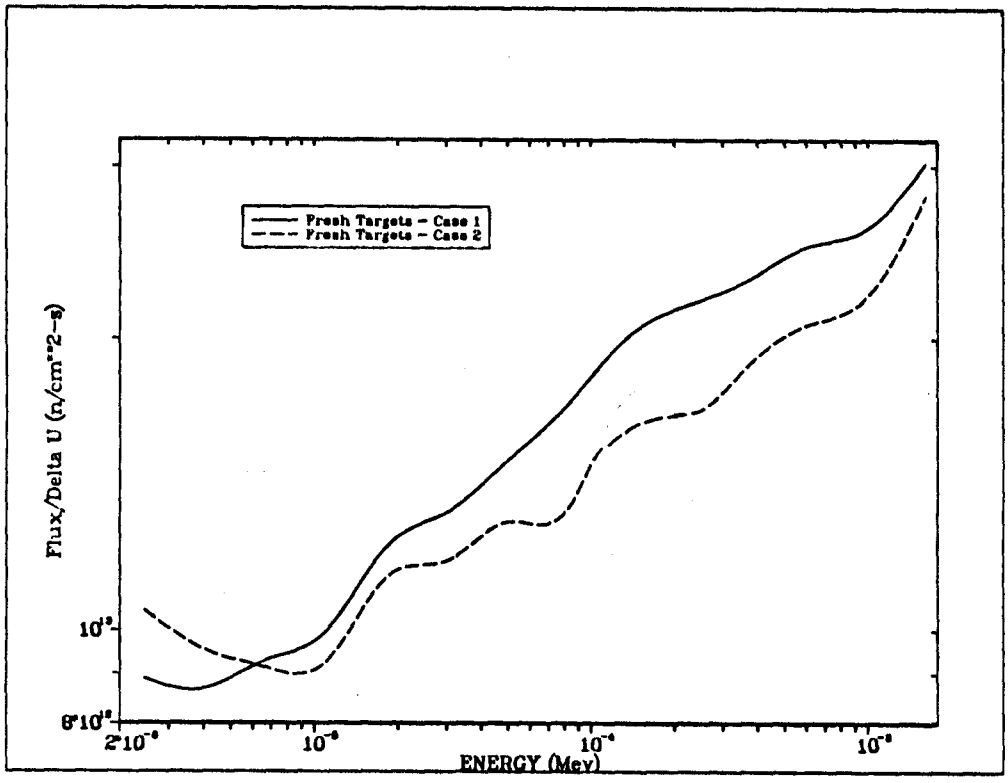

Figure 7.16 Flux Per Unit Lethargy in the Resolved Resonance Region - Example Cases 1 and 2

Figure 7.17 shows the $^{237}Np(n,\gamma)$ reaction rate as calculated by the CHAIN.238DJ code and the "check points" from five intermediate MCNP calculations. Figures 7.18 and 7.19 show similar plots for the $^{237}Np(n,2n)^{236}Pu$ and $^{237}Np(\gamma,n)^{236}Pu$ effective reaction rates. These reactions are very important for ^{238}Pu production systems because of the ^{236}Pu impurity they produce. For all three of these plots, the MCNP calculations at intermediate points validate the reaction rate used by CHAIN.238DJ. One of the intermediate MCNP data points in Figure 7.19 lies significantly off the line, but this is probably a spurious result from the MCNP calculation. It has a fairly large statistical uncertainty, and there is no physical reason for the $^{237}Np(\gamma,n)^{236}Pu$ effective reaction rate to make any sort of strange dip through that part of the plot.

Figure 7.20 shows the plot of the $^{238}Pu(n,\gamma)$ reaction rate in the resolved resonance region. This shows the performance of the C-factor method very well. This reaction rate behaves in a very non-linear

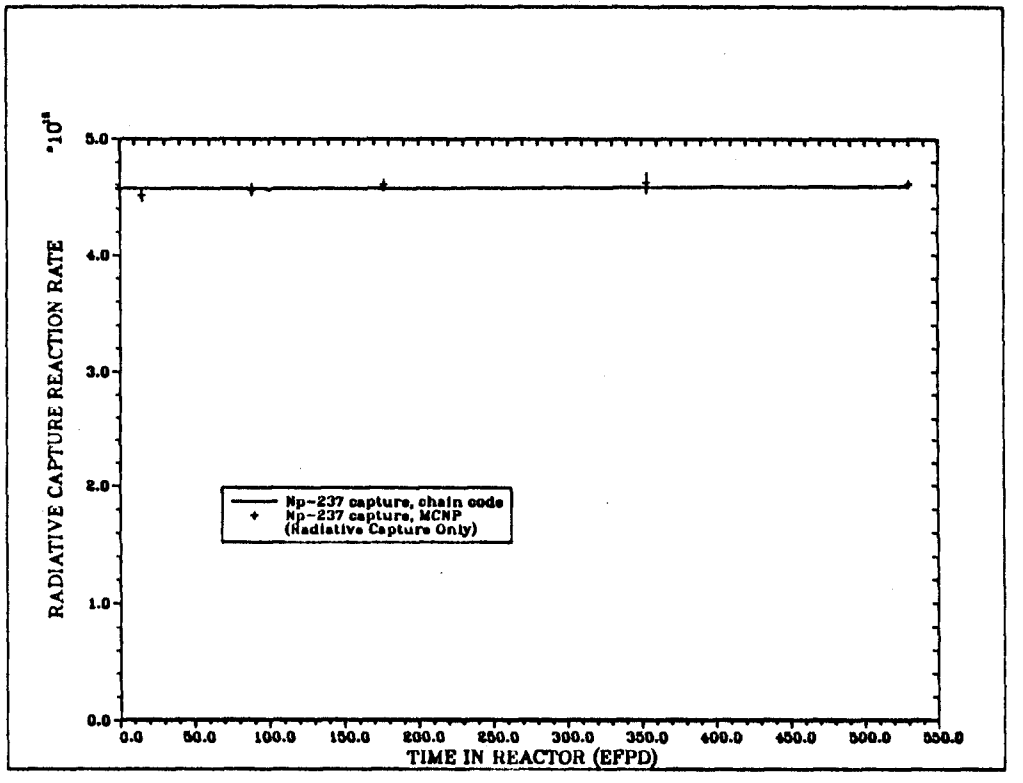

Figure 7.17 Total Microscopic Radiative Neutron Capture Reaction Rate vs Time for Np-237 - Example Case 2

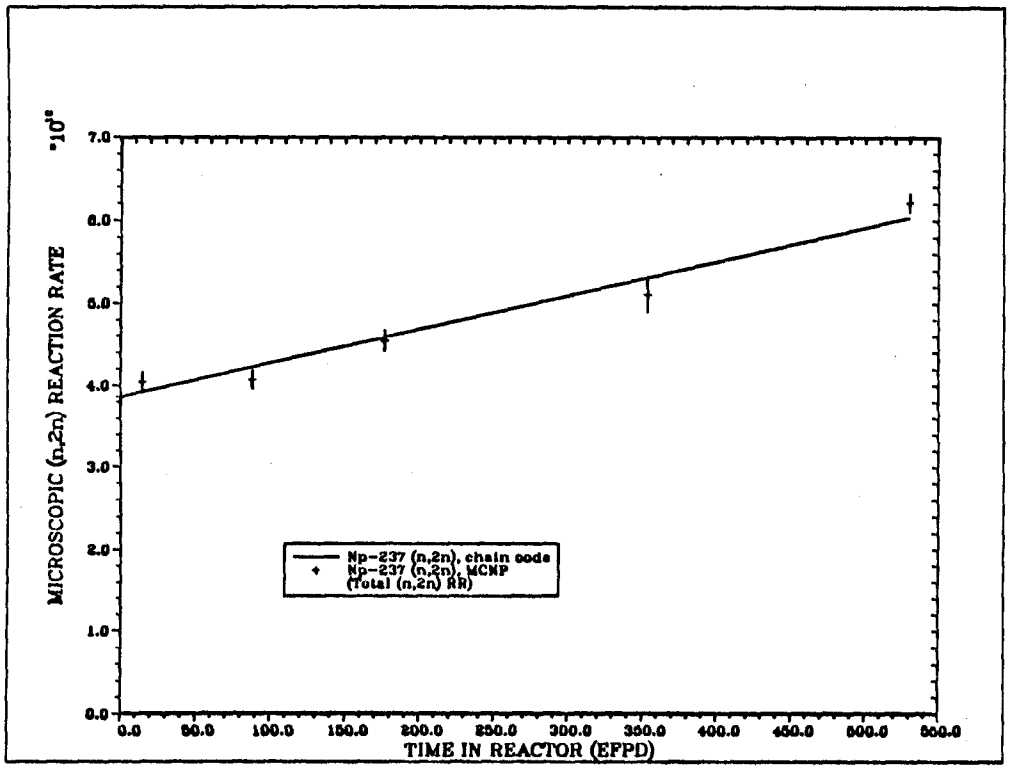

Figure 7.18 Total $^{237}Np(n,2n)^{236}Pu$ Effective Reaction Rate vs Time - Example Case 2

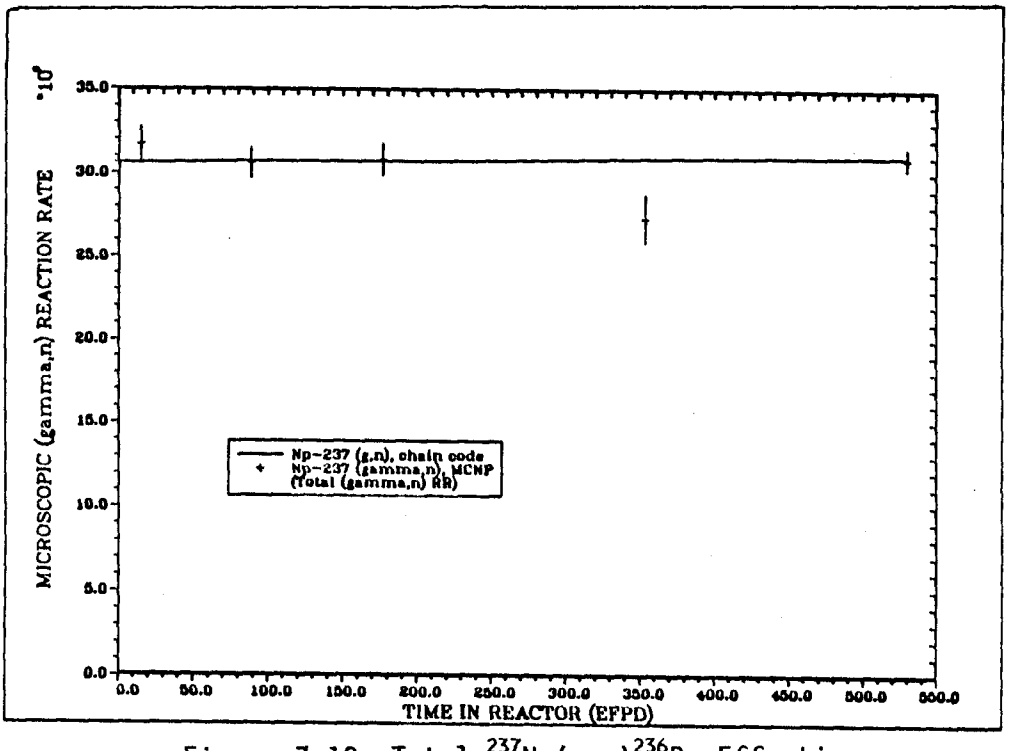

Figure 7.19 Total $^{237}Np(\gamma,n)^{236}Pu$ Effective Reaction Rate vs Time - Example Case 2

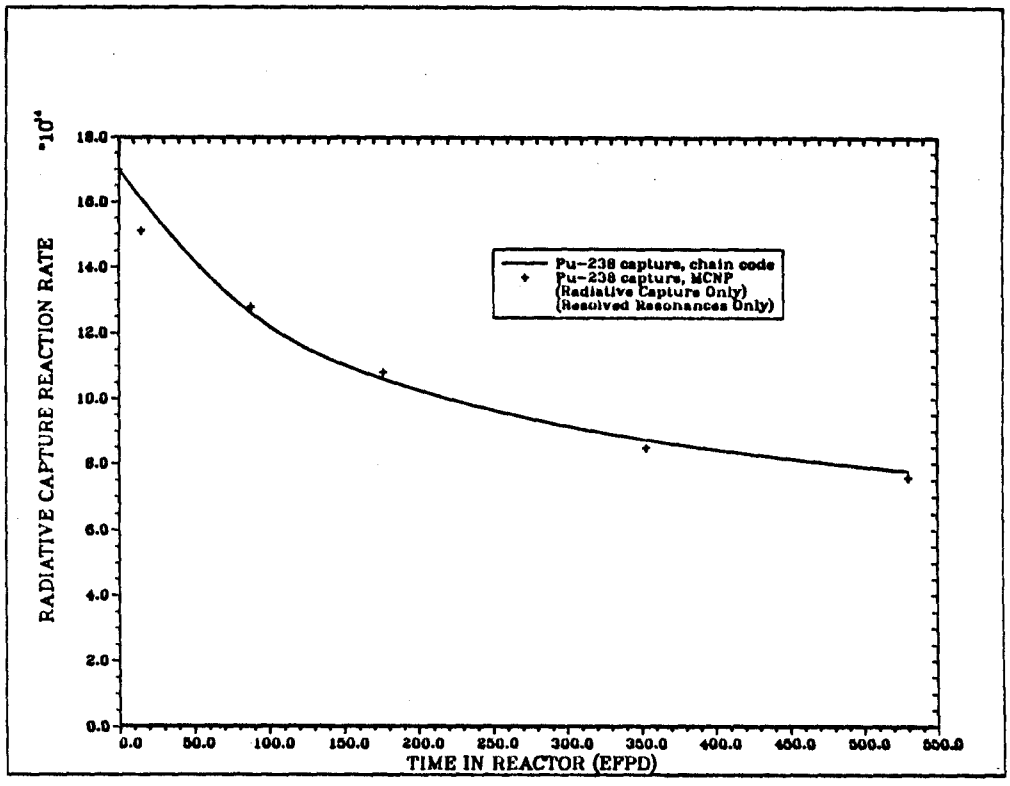

Figure 7.20 Microscopic Radiative Neutron Capture Reaction Rate in the Resolved Resonance Region vs Time for Pu-238 - Example Case 2

fashion, and the C-factor method does an excellent job of predicting this non-linear behavior.

Figures 7.21 through 7.28 show the (n,γ) and (n,f) reaction rate plots for ^{236}Pu, ^{239}Pu, ^{240}Pu, and ^{241}Pu. There appears to be some significant error in the CHAIN.238DJ calculation of these reaction rates. As was done individually for ^{238}Pu and ^{241}Pu in the first example case, a sensitivity study has been completed for the ^{236}Pu reaction rates alone and also for the ^{239}Pu, ^{240}Pu, and ^{241}Pu reaction rates all changed at once. Figures 7.29 through 7.36 show the reaction rates used in the new calculations. Tables 7.4 and 7.5 show the results of the study. The code is not sensitive at all to the two or three percent changes that were made in the ^{236}Pu burnout cross sections. This is because for ^{236}Pu, decay is significantly more important than burnout. The rate of decay is roughly the same as the rate of burnout, but burnout does not occur during the periods of

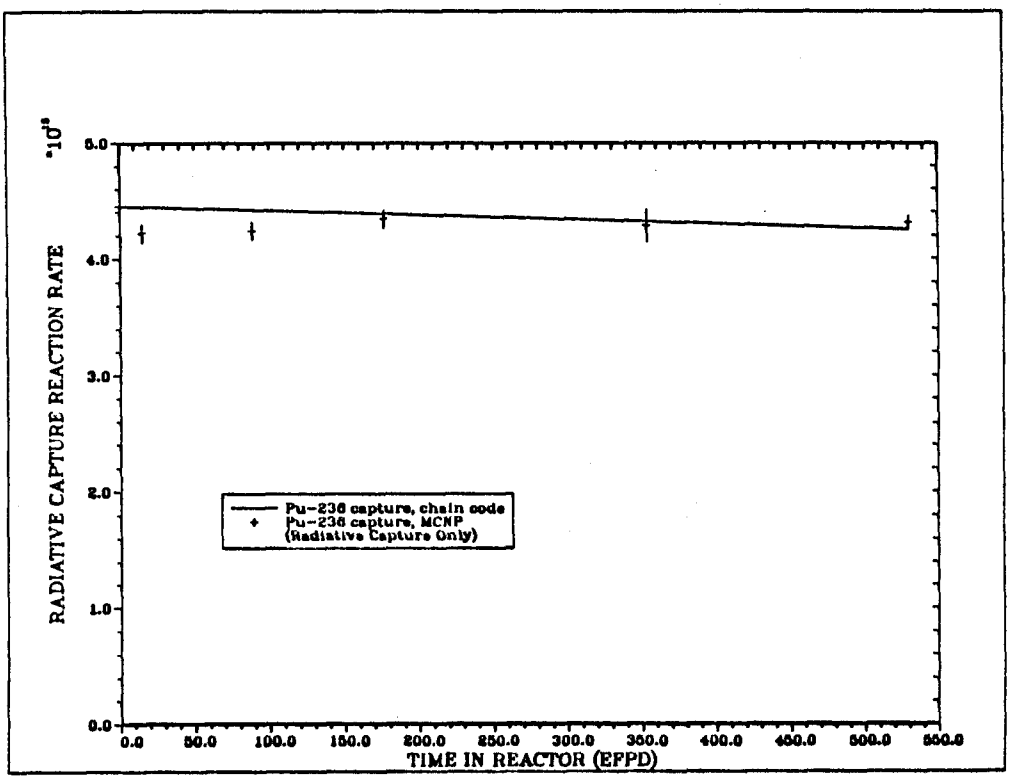

Figure 7.21 Total Microscopic Radiative Neutron Capture Reaction Rate vs Time for Pu-236 - Example Case 2

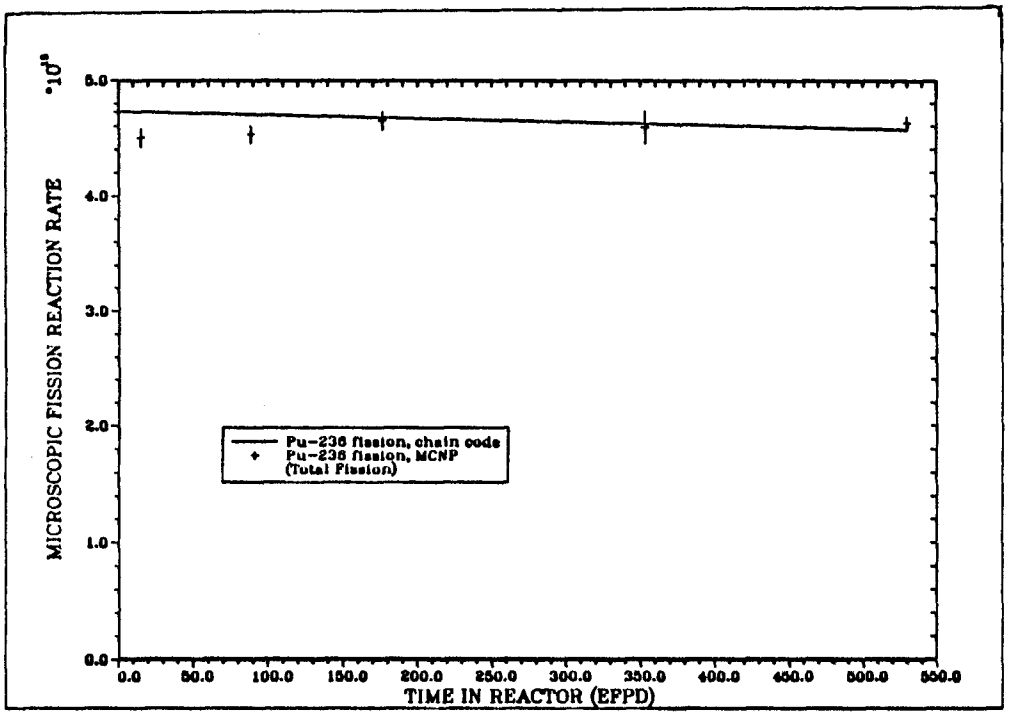

Figure 7.22 Total Microscopic Fission Reaction Rate vs Time for Pu-236 - Example Case 2

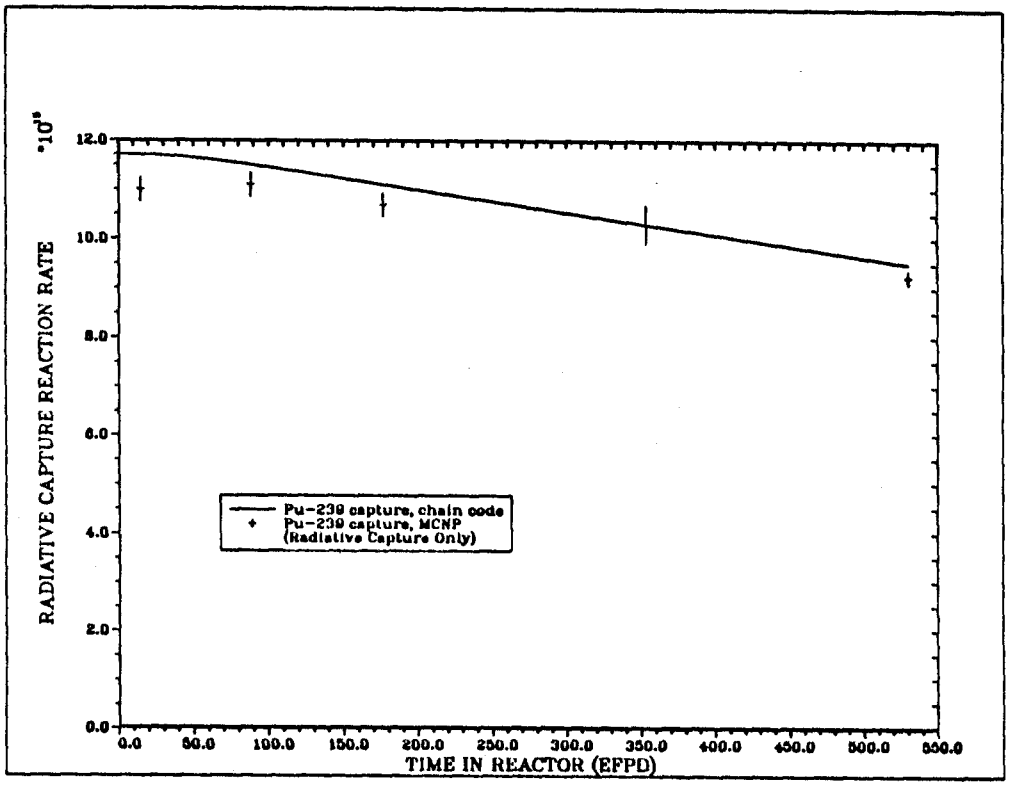

Figure 7.23 Total Microscopic Radiative Neutron Capture Reaction Rate vs Time for Pu-239 - Example Case 2

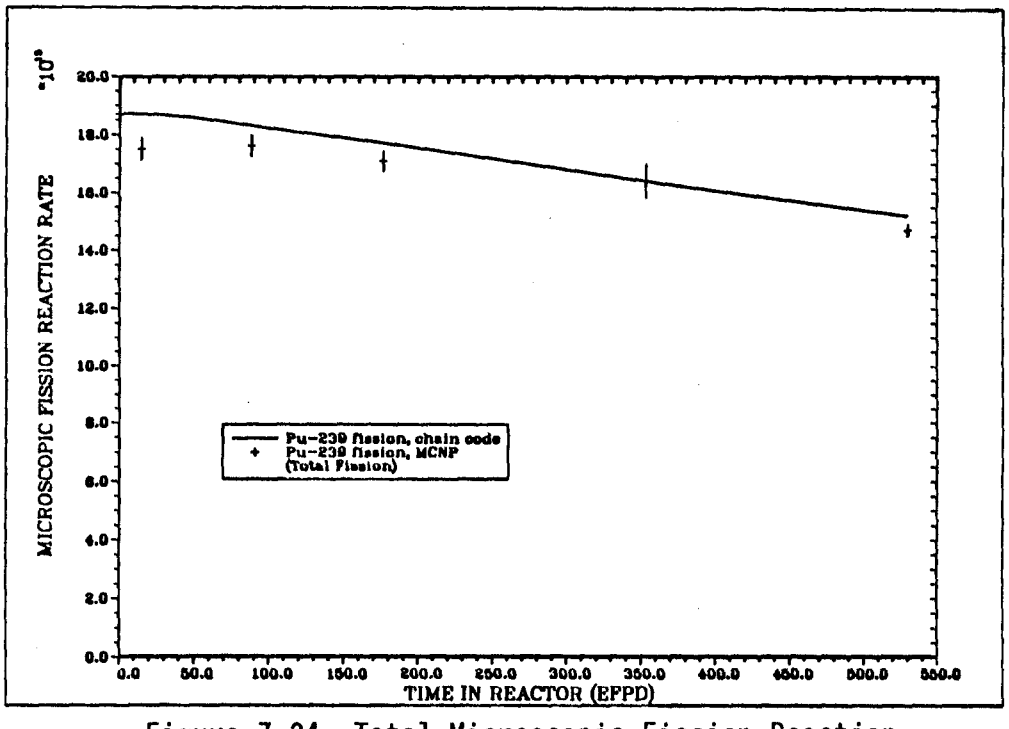

Figure 7.24 Total Microscopic Fission Reaction Rate vs Time for Pu-239 - Example Case 2

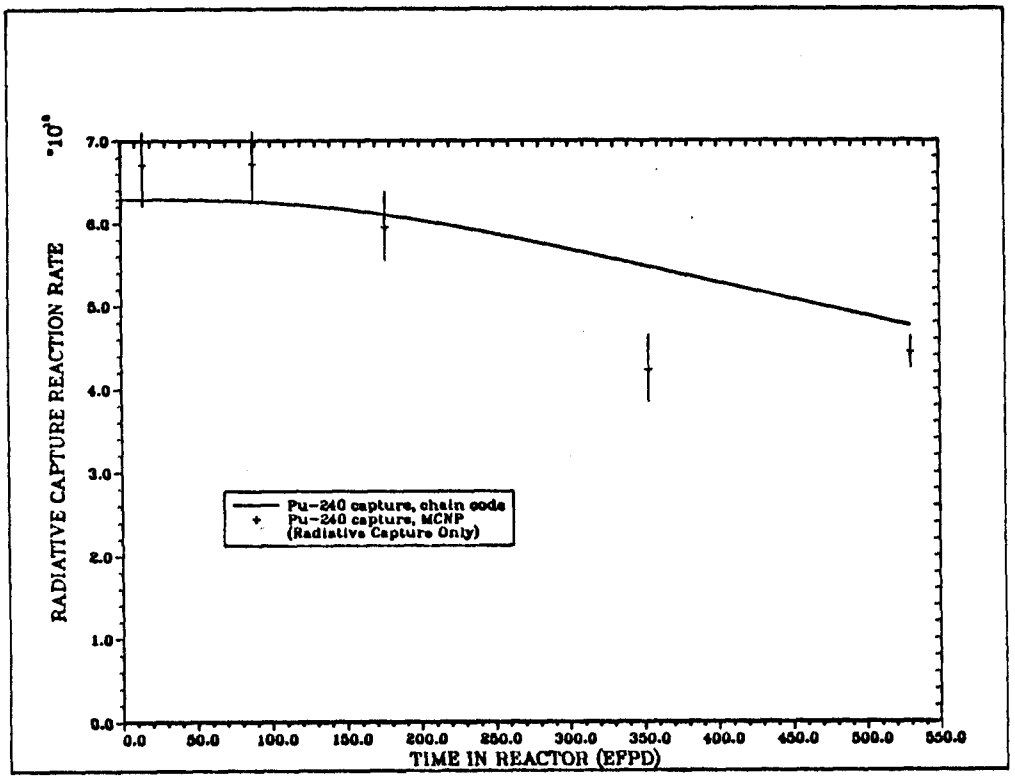

Figure 7.25 Total Microscopic Radiative Neutron Capture Reaction Rate vs Time for Pu-240 - Example Case 2

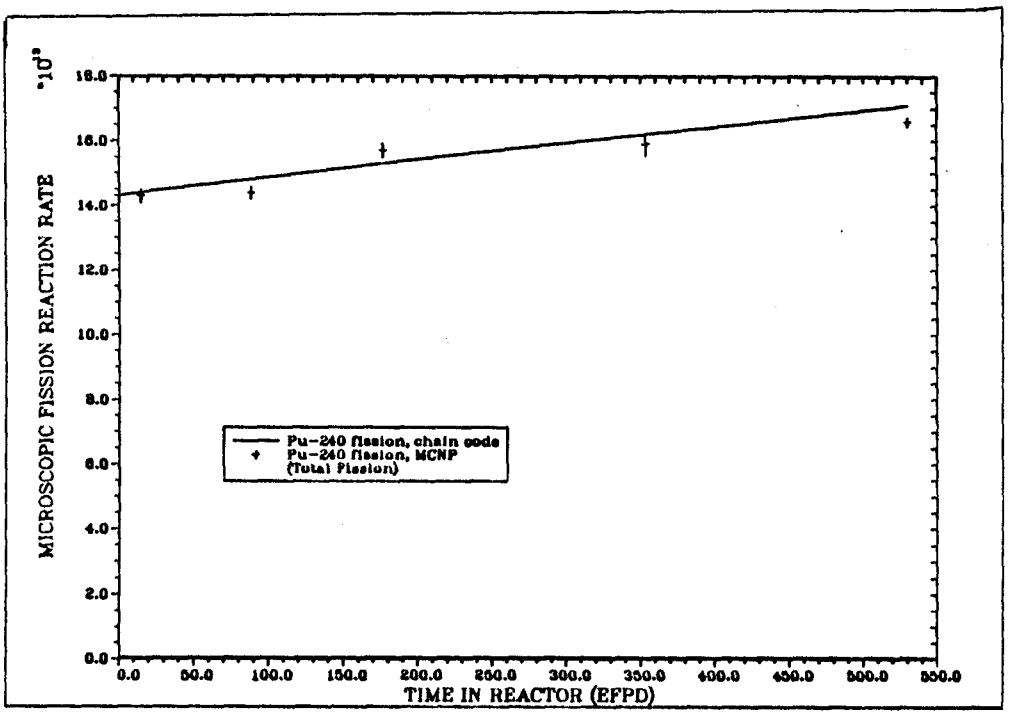

Figure 7.26 Total Microscopic Fission Reaction Rate vs Time for Pu-240 - Example Case 2

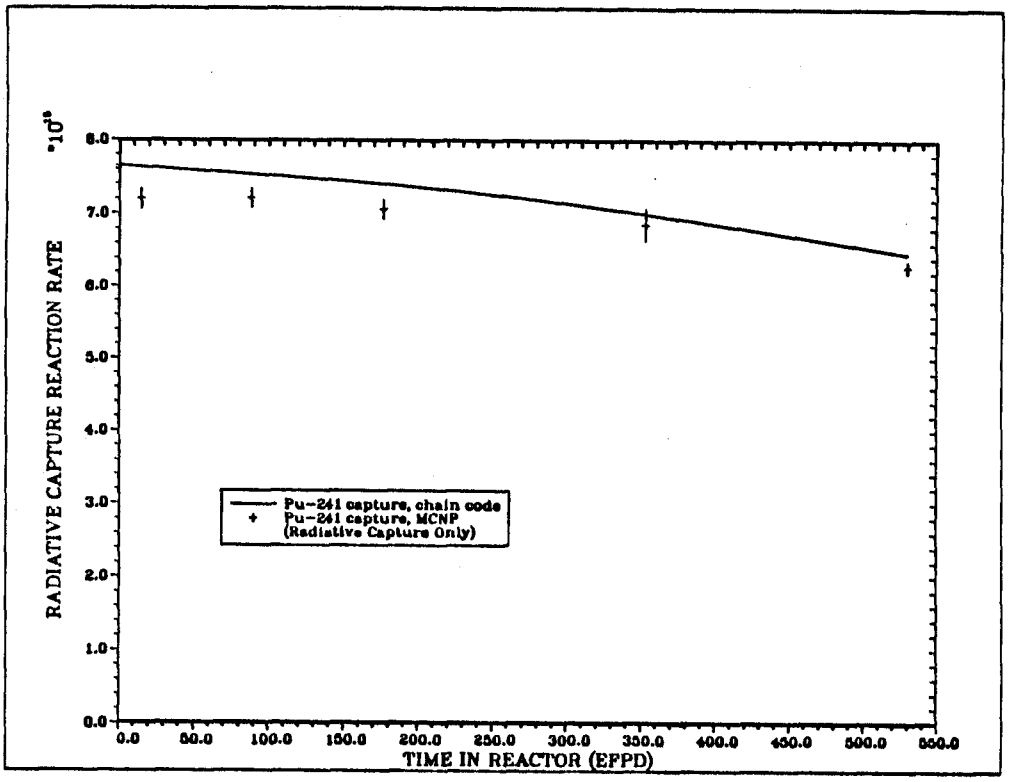

Figure 7.27 Total Microscopic Radiative Neutron Capture Reaction Rate vs Time for Pu-241 - Example Case 2

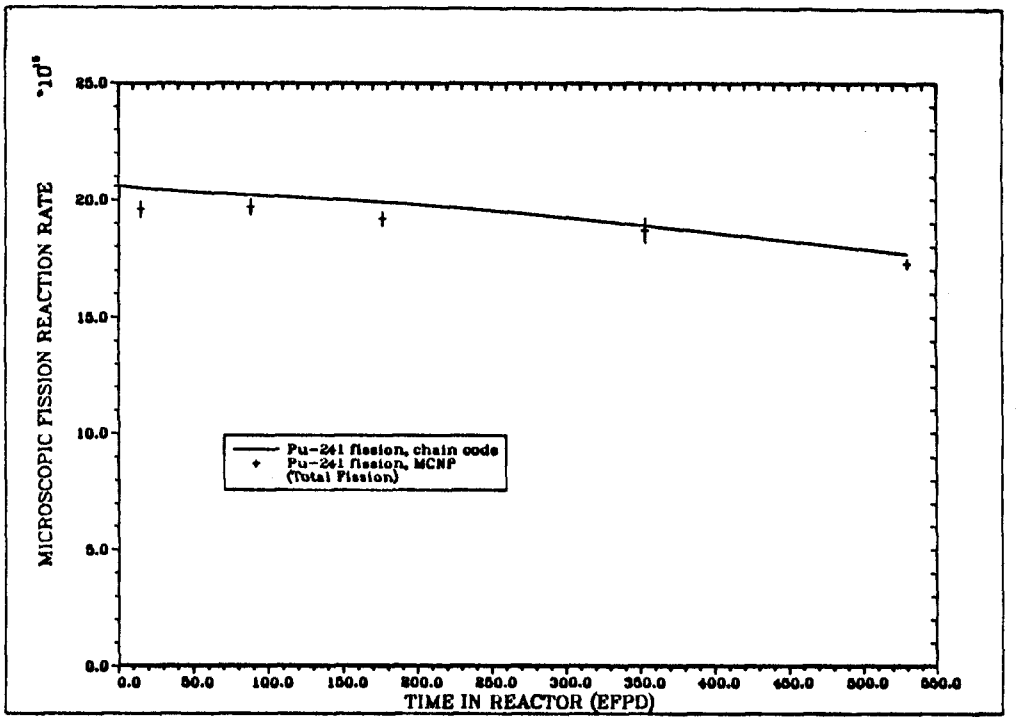

Figure 7.28 Total Microscopic Fission Reaction Rate vs Time for Pu-241 - Example Case 2

reactor shutdown. The final answers given by the code (production, quality, and ^{236}Pu impurity level) are also insensitive to the change in the cross sections of ^{239}Pu, ^{240}Pu, and ^{241}Pu, but this does not necessarily show that the observed changes are always unimportant. The code is used in the initial iterative scheme to determine the EOI target material composition. Five percent errors in the amount of ^{239}Pu or ^{241}Pu in this composition can be more important for their effect on the $^{237}Np(n,2n)$ reaction rate than they are for the results of the CHAIN.238DJ run itself. Though small errors in the amount of these isotopes do not significantly impact the plutonium production or quality levels, they can indirectly impact the ^{236}Pu impurity level. Failure to have the correct amount of these fissile isotopes in the EOI MCNP calculation will cause an erroneous calculation of the $^{237}Np(n,2n)$ reaction rate because the internal fission source in the target pins will not be correct. In this example case the observed differences are still not important because there is so little ^{242}Pu and ^{241}Pu produced that even 10% and 5% errors in their amounts will not significantly impact the $^{237}Np(n,2n)$ reaction rate.

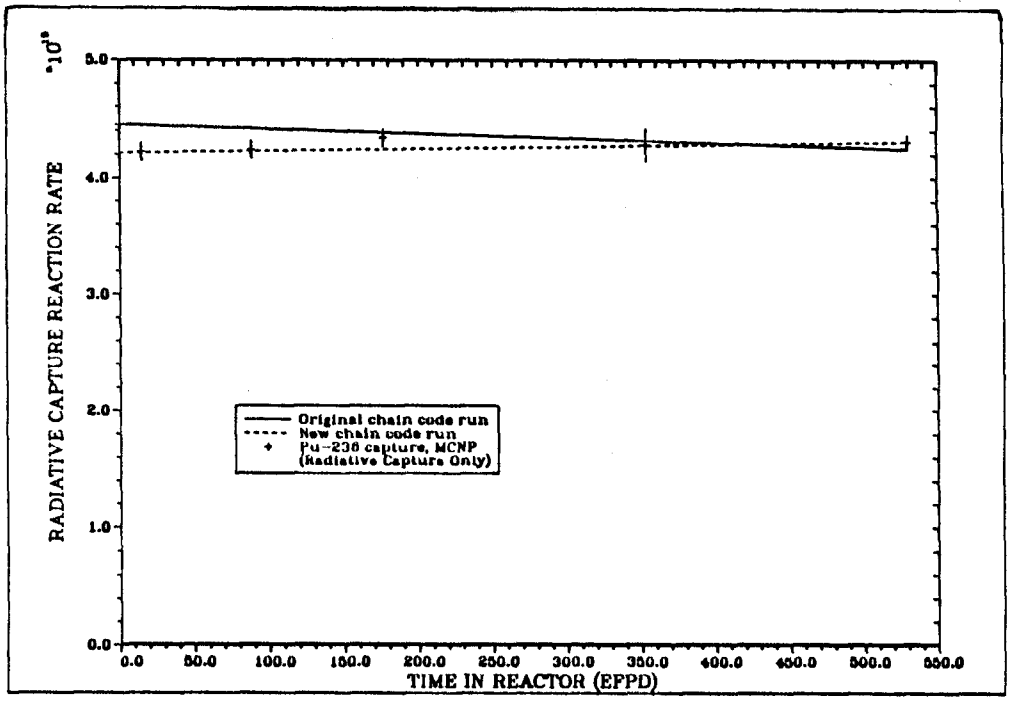

Figure 7.29 New Total Microscopic Radiative Neutron Capture Reaction Rate vs Time for Pu-236 - Example Case 2

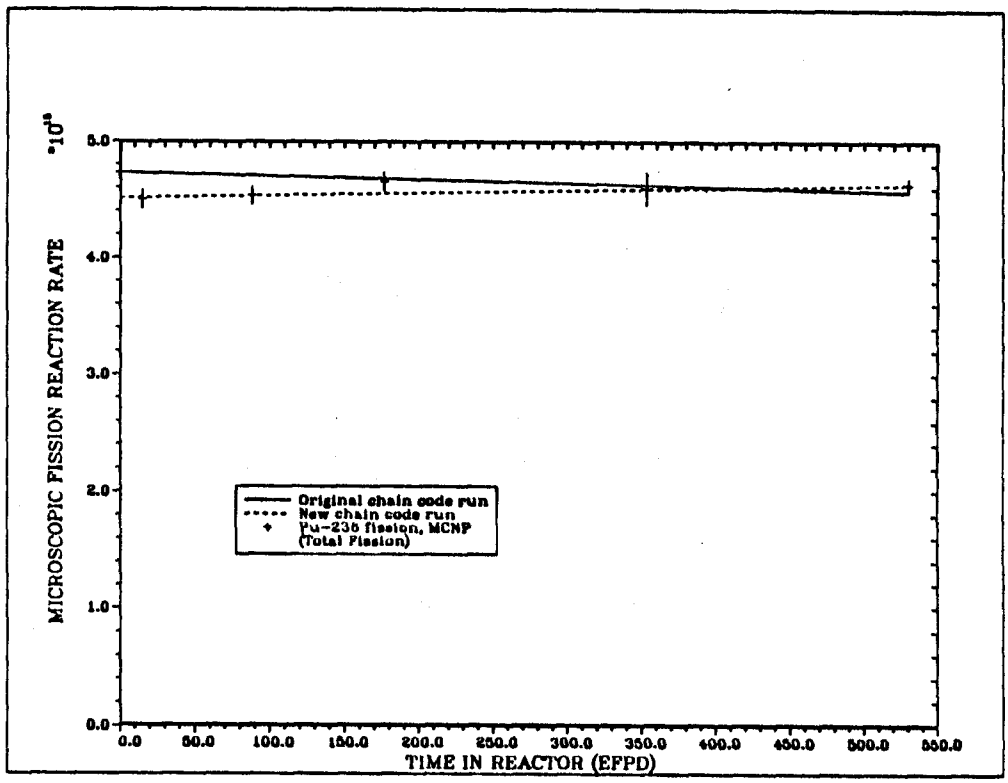

Figure 7.30 New Total Microscopic Fission Reaction Rate vs Time for Pu-236 - Example Case 2

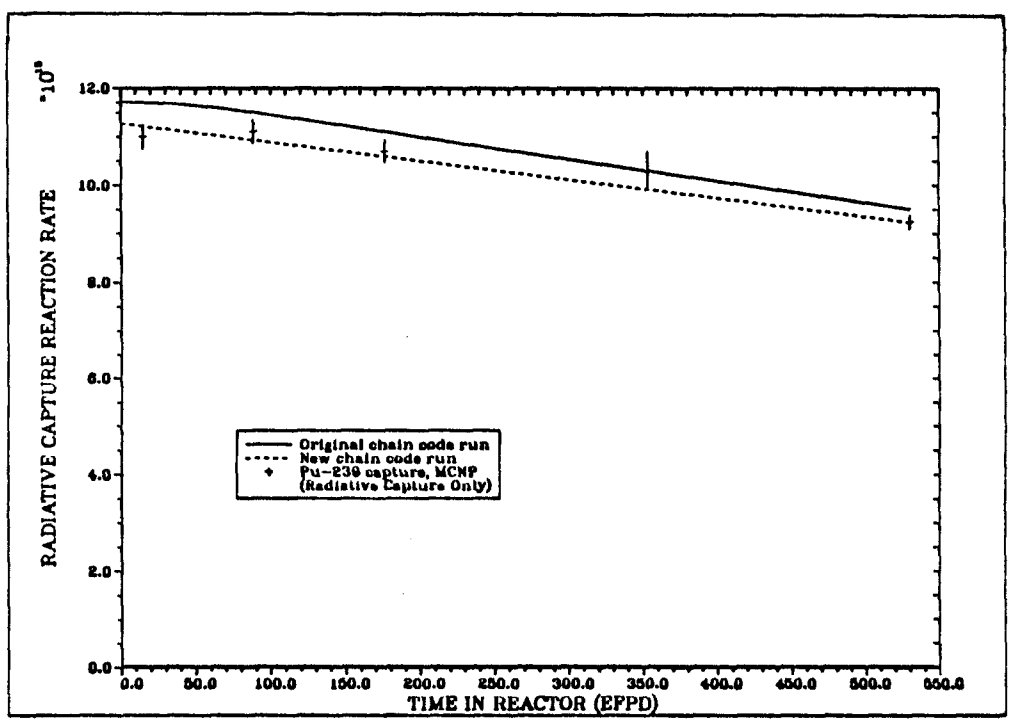

Figure 7.31 New Total Microscopic Radiative Neutron Capture Reaction Rate vs Time for Pu-239 - Example Case 2

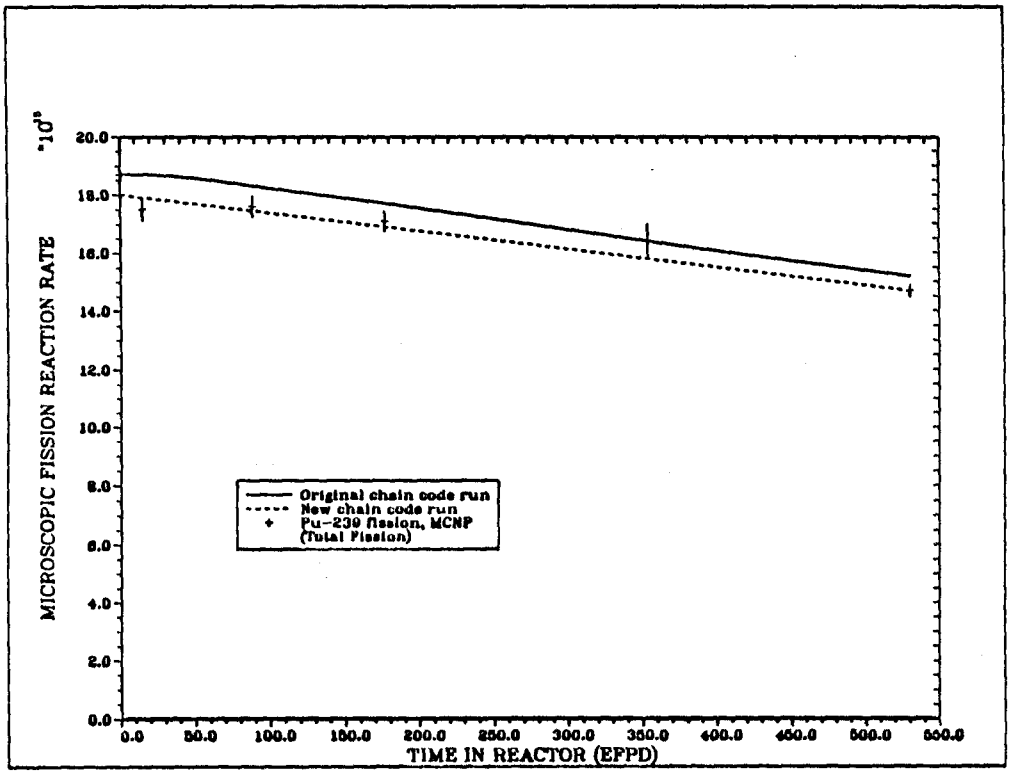

Figure 7.32 New Total Microscopic Fission Reaction Rate vs Time for Pu-239 - Example Case 2

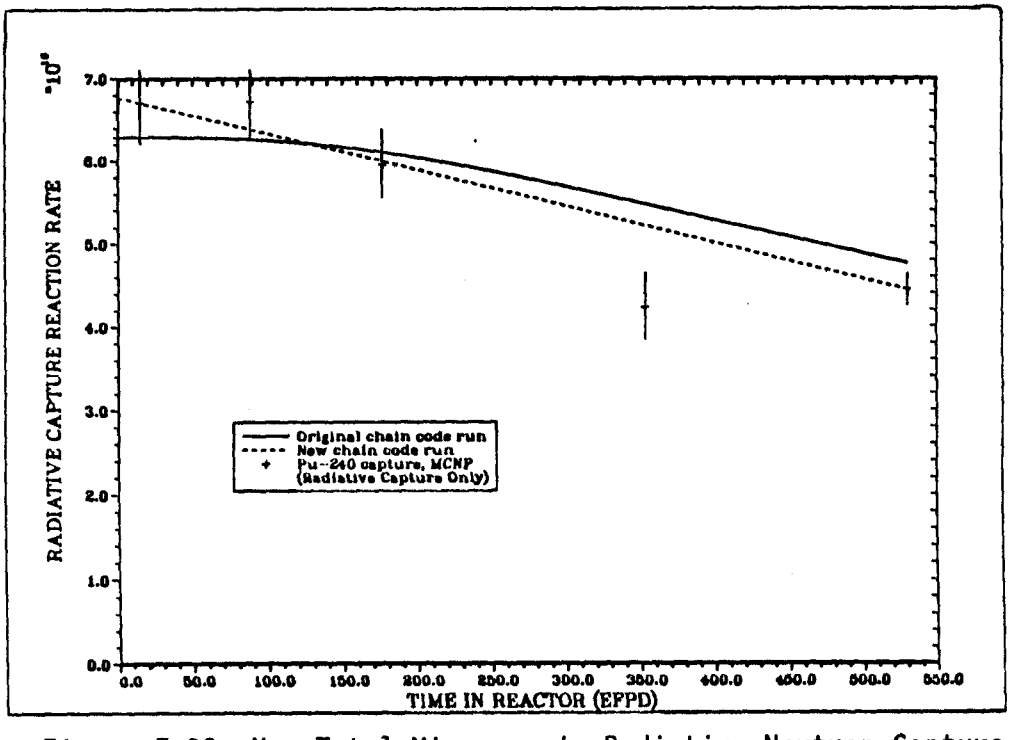

Figure 7.33 New Total Microscopic Radiative Neutron Capture Reaction Rate vs Time for Pu-240 - Example Case 2

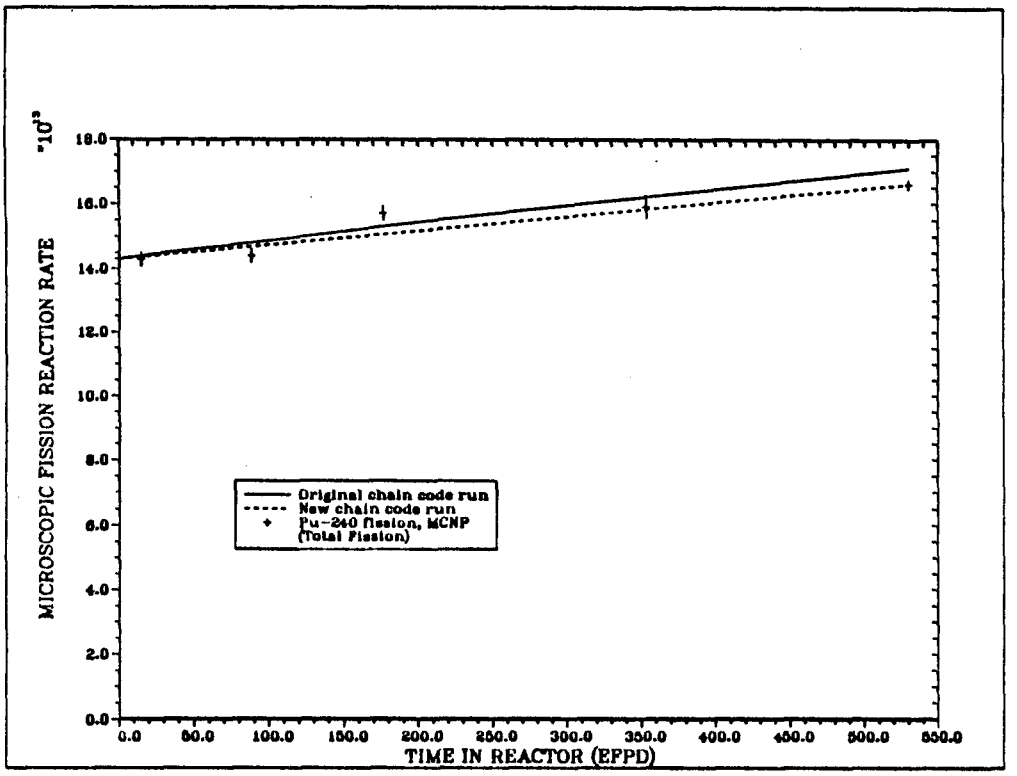

Figure 7.34 New Total Microscopic Fission Reaction Rate vs Time for Pu-240 - Example Case 2

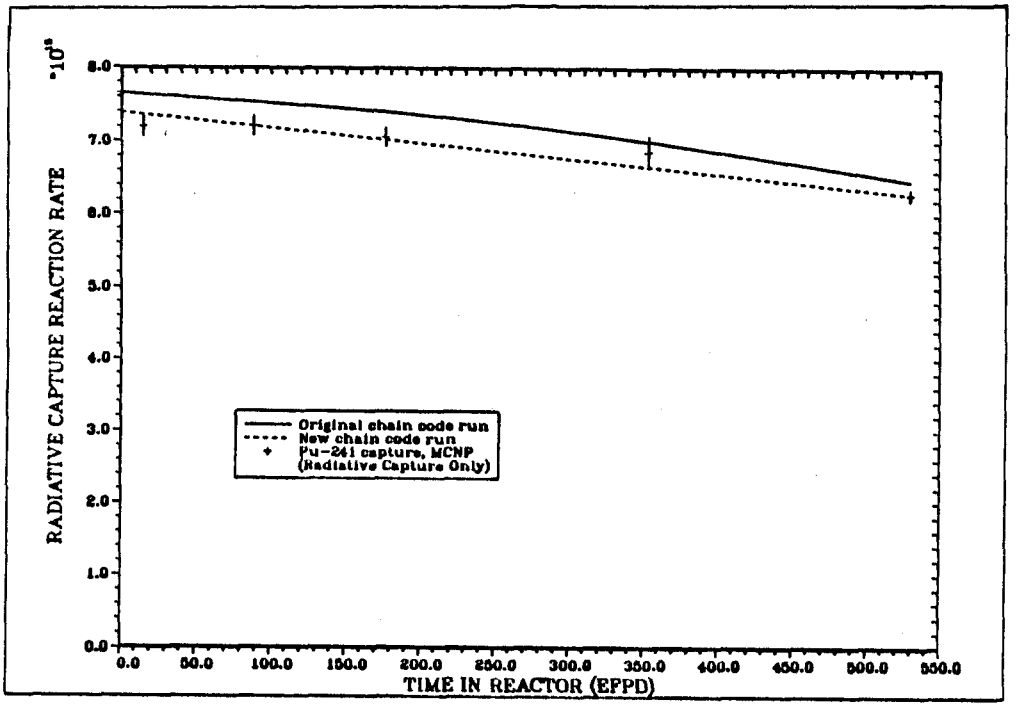

Figure 7.35 New Total Microscopic Radiative Neutron Capture Reaction Rate vs Time for Pu-241 - Example Case 2

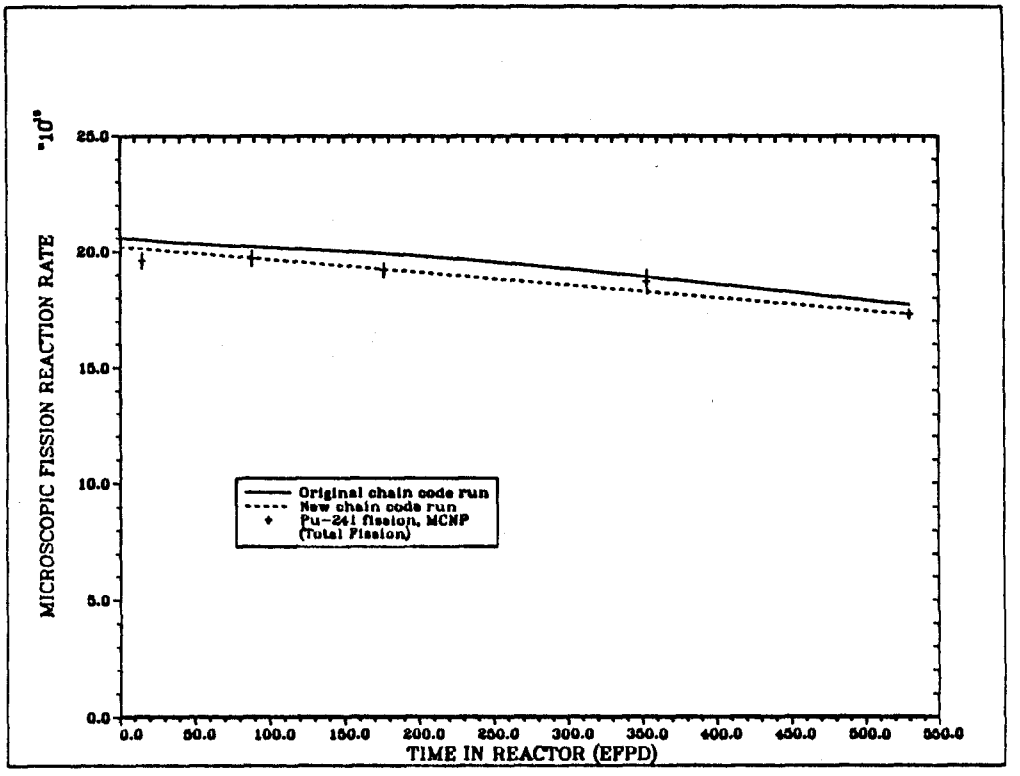

Figure 7.36 New Total Microscopic Fission Reaction Rate vs Time for Pu-241 - Example Case 2

Nuclide	Final Amounts (gram-atoms) at 730 Days (530 EFPD)		
	Results From Original Calculation	Results With New Pu-236 Reaction Rates	Change From Original Calculation
^{237}Np	0.807	0.807	0
^{238}Np	9.70e-4	9.70e-4	0
^{236}Pu	2.19e-6	2.19e-6	< 0.1%
^{238}Pu	0.166	0.166	< 0.1%
^{239}Pu	0.0109	0.0109	< 0.1%
^{240}Pu	1.14e-3	1.14e-3	< 0.1%
^{241}Pu	6.55e-4	6.55e-4	< 0.1%
^{242}Pu	4.63e-5	4.63e-5	< 0.1%
Total Plutonium	0.179	0.179	< 0.1%
^{236}Pu ppm Impurity	12.3 ppm	12.3 ppm	< 0.1%
Quality (^{238}Pu/Pu)	92.9%	92.9%	< 0.1%

Table 7.4 ^{236}Pu Reaction Rate Sensitivity Study - Example Case 2

Nuclide	Final Amounts (gram-atoms) at 730 Days (530 EFPD)		
	Results From Original Calculation	Results With New Pu-239 Pu-240, Pu-241 Reaction Rates	Change From Original Calculation
^{237}Np	0.807	0.807	0
^{238}Np	9.70e-4	9.70e-4	0
^{236}Pu	2.19e-6	2.19e-6	0
^{238}Pu	0.166	0.166	0
^{239}Pu	0.0109	0.0110	+0.9%
^{240}Pu	1.14e-3	1.14e-3	< 0.1%
^{241}Pu	6.55e-4	6.19e-4	-4.5%
^{242}Pu	4.63e-5	4.20e-5	-9.3%
Total Plutonium	0.179	0.179	< 0.1%
^{236}Pu ppm Impurity	12.3 ppm	12.2 ppm	-0.1%
Quality ($^{238}Pu/Pu$)	92.9%	92.8%	-0.8%

Table 7.5 ^{239}Pu, ^{240}Pu, and ^{241}Pu Reaction Rate Sensitivity Study - Example Case 2

7.4 Application to a Heterogeneous Case: Example 3

Figure 7.37 shows a core mid-plane section of the geometry used in the third example case. It features 19 moderator pins (the larger cicles) and 36 target pins (the smaller circles). There is 67.3 kg of $YH_{1.7}$ moderator and 3.03 kg of initial $^{237}NpO_2$ target material per assembly. Given the significantly lighter target loading and the significantly larger moderator loading, this third example case has a softer spectrum and much less self-shielding than the second case had. The ^{237}Np target material burns out more quickly, so the cycle length for this case is reduced to only one year, or 265 EFPD. Figure 7.38 shows a comparison of the thermal flux for this third case with that from example case 2. Figure 7.39 shows a similar comparison of the resonance region flux. This third case obviously has a significantly softer neutron spectrum than either of the first two cases had.

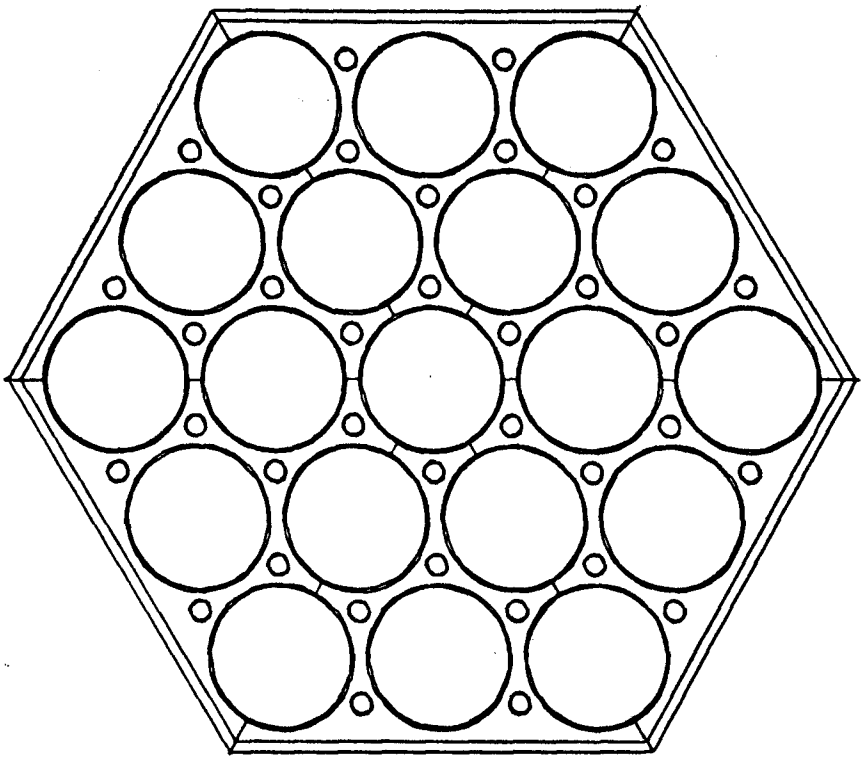

Figure 7.37 Geometry of Example Case 3 (x-y plot at core mid-plane)

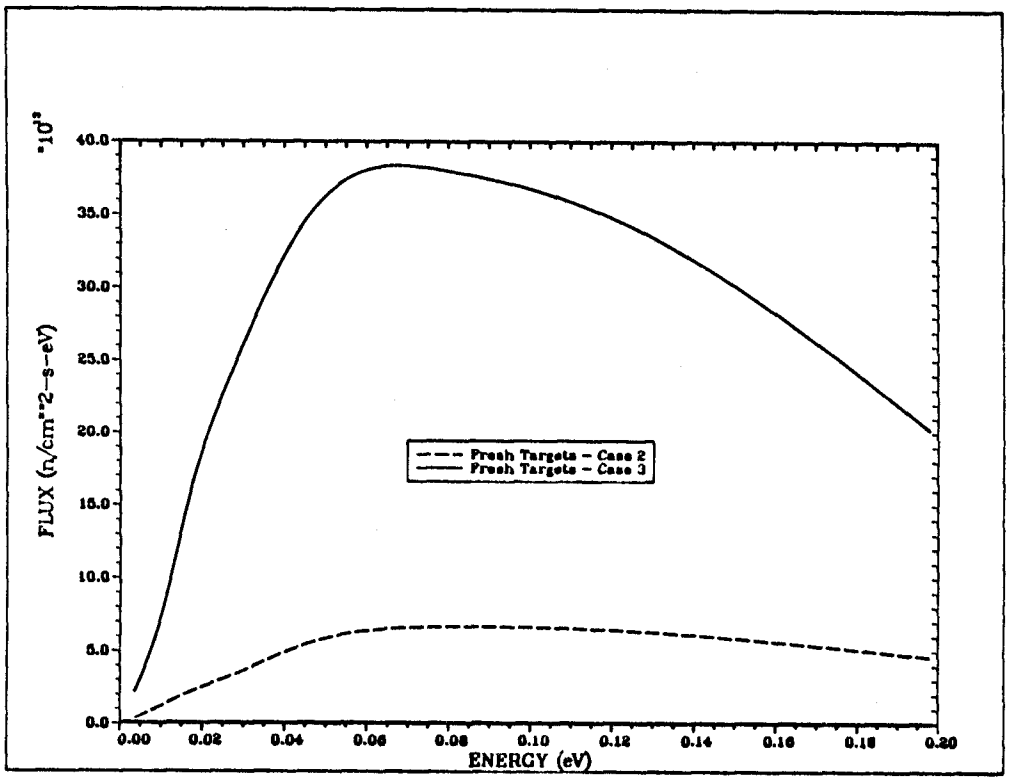

Figure 7.38 Thermal Flux in the Target Pins - Example Cases 2 and 3

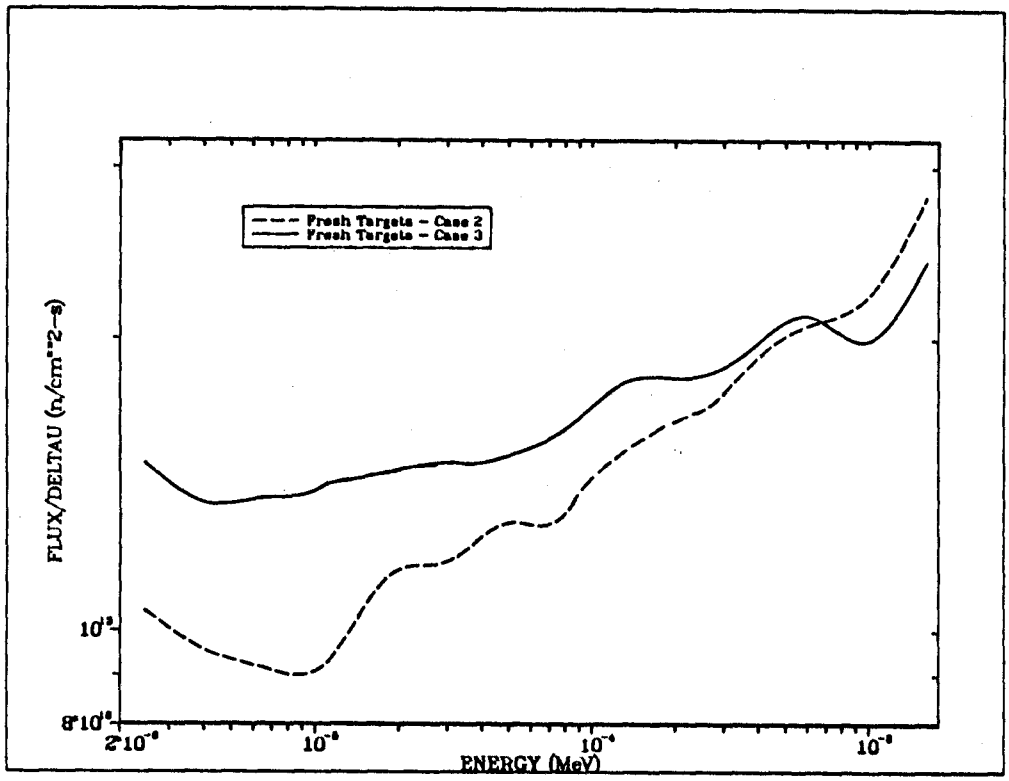

Figure 7.39 Flux Per Unit Lethargy in the Resolved Resonance Region - Example Cases 2 and 3

Figures 7.40 and 7.41 show the $^{237}Np(n,\gamma)$ and $^{238}Pu(n,\gamma)$ reaction rate plots for this case. There is good agreement between the curves for the CHAIN.238DJ reaction rates and the MCNP check points. Other reaction rate plots for this case either show good agreement with the check points or portray the kind of small error that was shown in the first two cases to be not very significant. Figure 7.42 shows the plot for the $^{237}Np(n,2n)$ reaction rate. The intermediate data points generated by MCNP calculations seem to be scattered widely throughout the plot, indicating some very significant error. The root cause of this error is related to equilibrium levels of ^{238}Np.

The half-life of ^{238}Np is 2.117 days, and it has the highest fission cross section of any nuclide in the chain. Because of its large fission cross section, ^{238}Np is an important source of fission neutrons within the target pins. These fission neutrons are born at

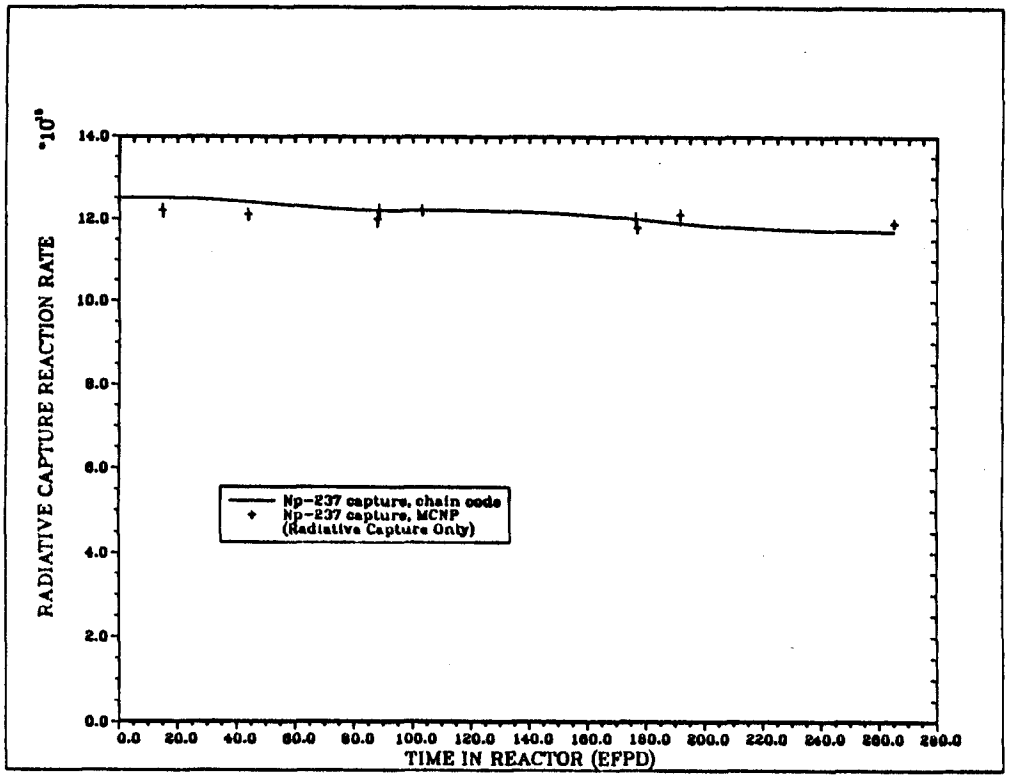

Figure 7.40 Total Microscopic Radiative Neutron Capture Reaction Rate vs Time for Np-237 - Example Case 3

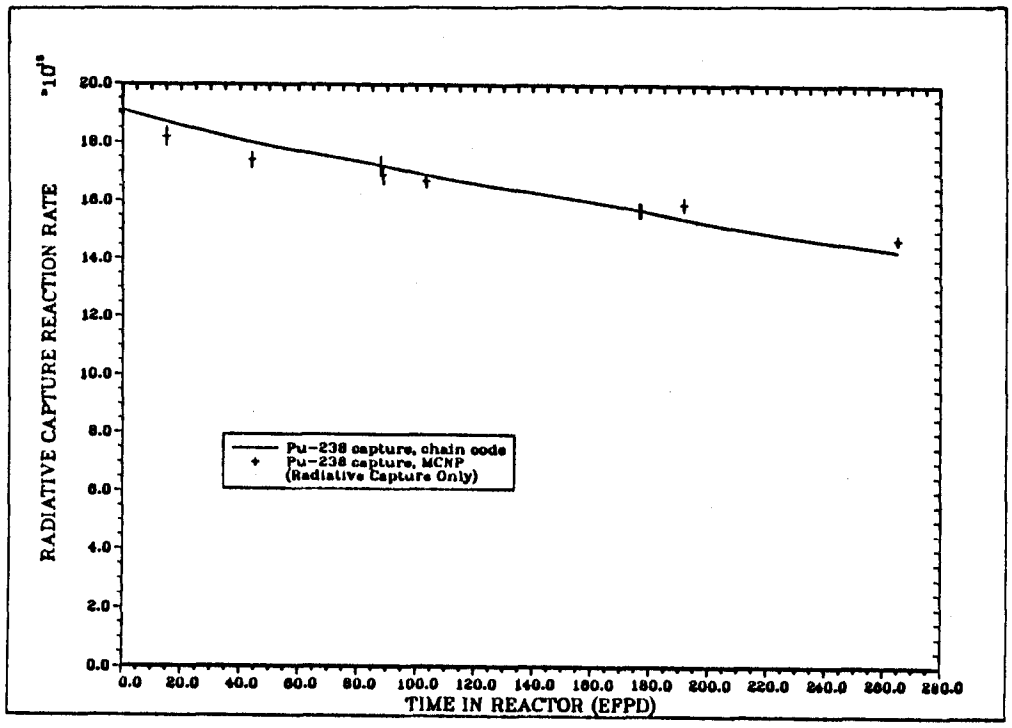

Figure 7.41 Total Microscopic Radiative Neutron Capture Reaction Rate vs Time for Pu-238 - Example Case 3

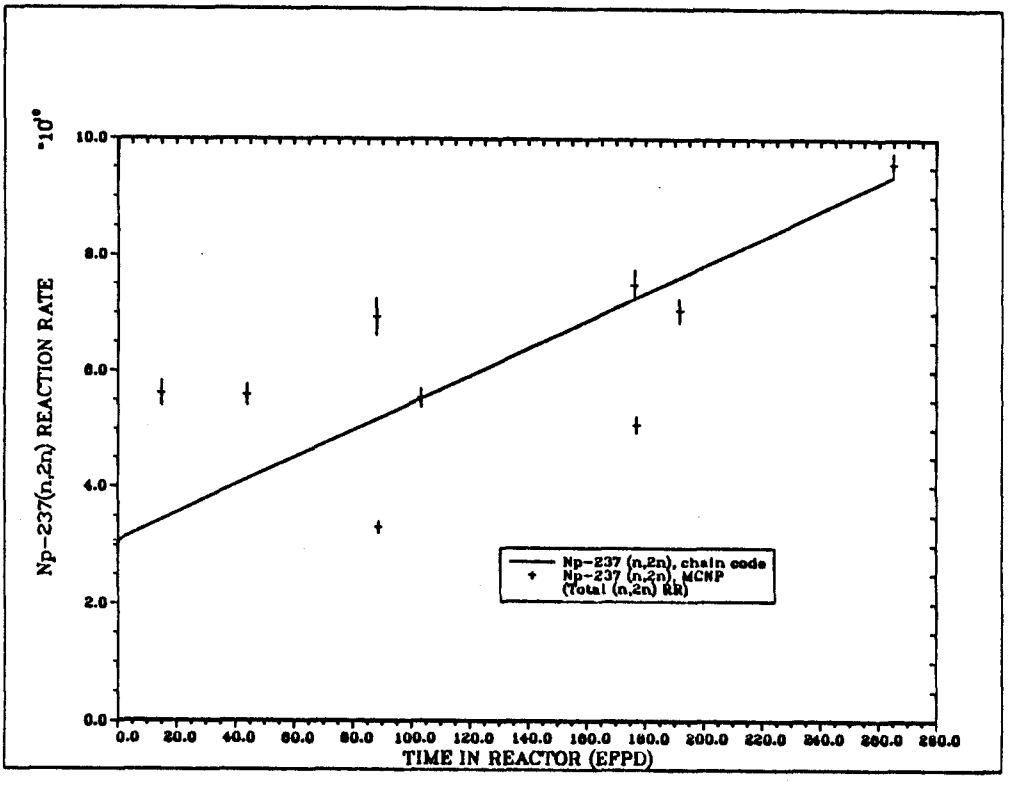

Figure 7.42 Total $^{237}Np(n,2n)^{236}Pu$ Effective Reaction Rate vs Time - Example Case 3

high energies and can cause $^{237}Np(n,2n)$ reactions. Every time the reactor starts up, the ^{238}Np concentration builds rapidly to an equilibrium level within the first ten or fifteen days. Figure 7.43 shows the ^{238}Np concentration as a function of time after initial startup. When the reactor is shut down, the ^{238}Np quickly decays away and is gone before the reactor is started up again. Likewise, when the reactor first starts up, the strength of the ^{238}Np fission neutron source is zero, but in just a few days the ^{238}Np concentration reaches equilibrium as does the fission source that comes from it. At the beginning of each cycle the ^{238}Np concentration, its associated fission source, and the resulting contribution to the $^{237}Np(n,2n)$ reaction rate start at zero, then build rapidly to equilibrium only to drop back to zero again during the next decay period. The actual behavior of the $^{237}Np(n,2n)$ reaction rate is shown as a function of EFPD in Figure 7.44, and as a function of real time in Figure 7.45. The blank areas at about 100 and about 250 days in Figure 7.45

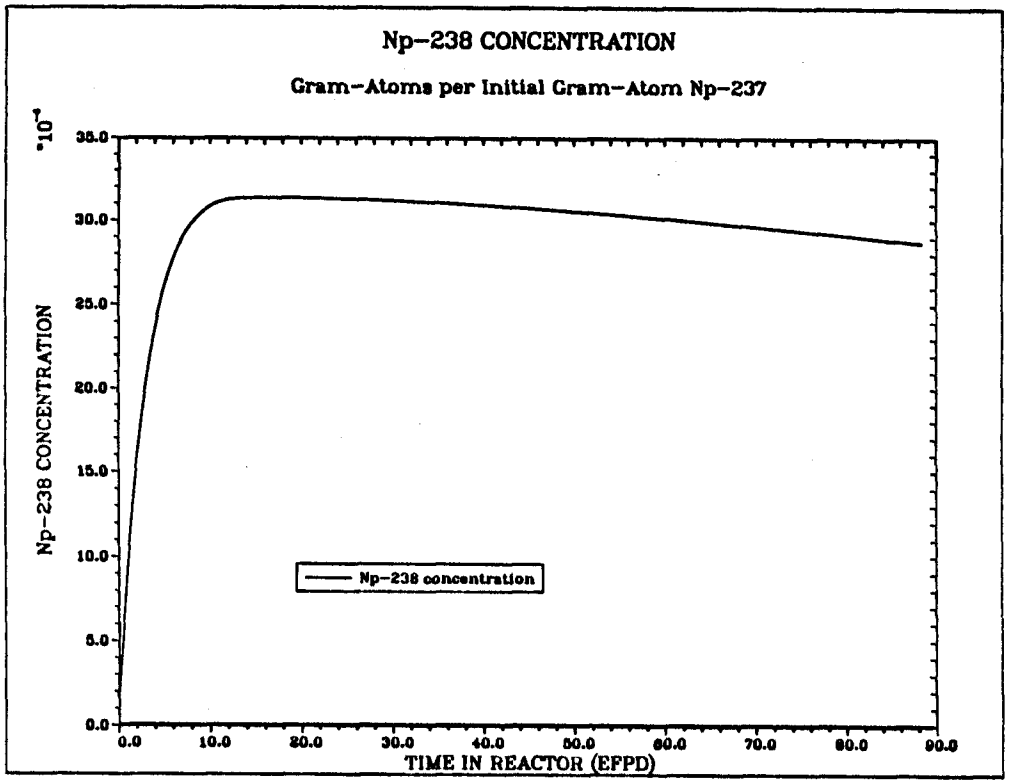

Figure 7.43 ^{238}Np Concentration vs Time - Example Case 3

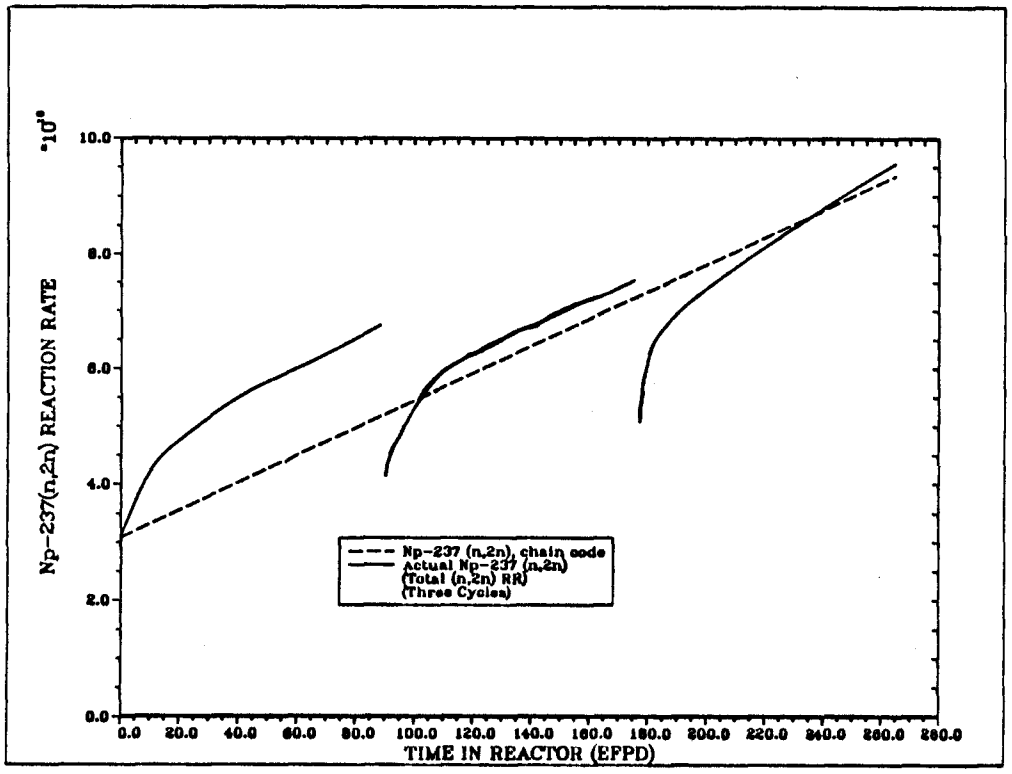

Figure 7.44 Actual Total ^{237}Np(n,2n)^{236}Pu Effective Reaction Rate vs Time (EFPD) - Example Case 3

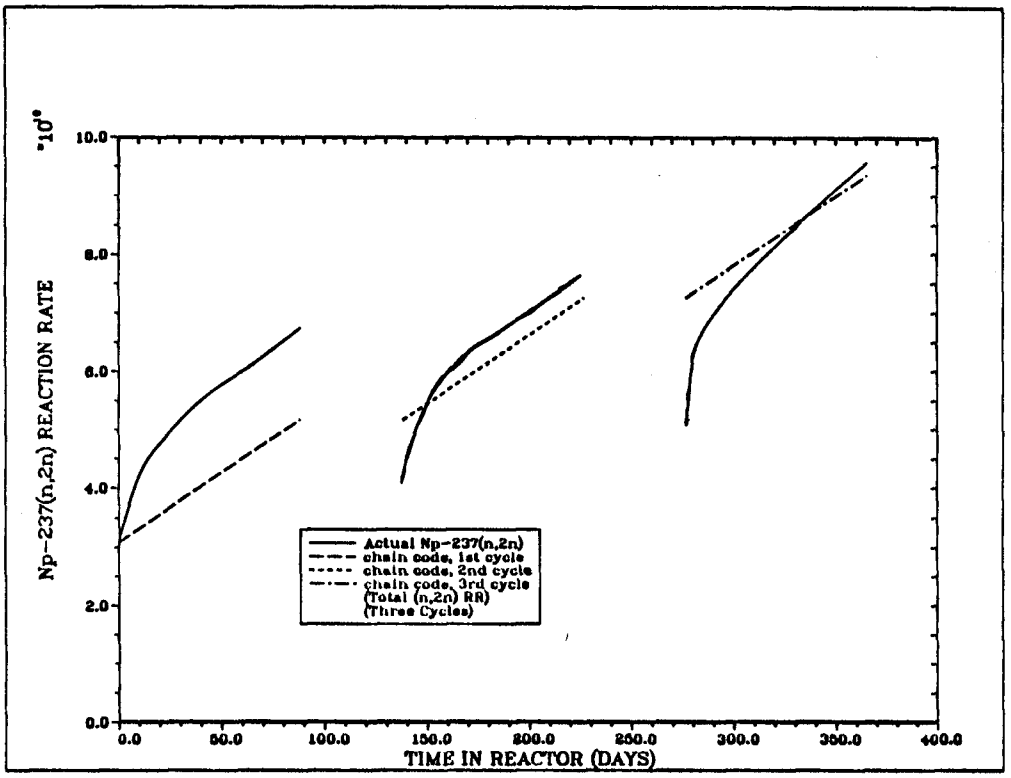

Figure 7.45 Actual Total $^{237}Np(n,2n)^{236}Pu$ Effective Reaction Rate vs Real Time - Example Case 3

represent decay periods when the reactor is shut down and the reaction rates are all zero. Figure 7.46 shows the growth of the total fission rate in the target pins as a function of time. Notice that the fission rate is somewhat dominated by ^{238}Np during the first cycle. During the decay period between 88 and 138 days the ^{238}Np concentration drops to zero, then builds up again. After this point in time, the effect of the equilibrium ^{238}Np concentration becomes too damped to be important because the plutonium isotopes have become dominant of the total fission rate.

This "equilibrium ^{238}Np effect" has a noticeable impact on some of the other reaction rates. Figures 7.47 and 7.48 show the reaction rate plots for $^{237}Np(n,f)$ and $^{240}Pu(n,f)$. These reaction rates are dominated by threshold fission above about 0.5 MeV in neutron energy, so they are affected by the internal fission source. Although these are dominantly high energy reactions, they are not as high energy as the $^{237}Np(n,2n)$ reaction is, so they are not as sensitive to the ^{238}Np

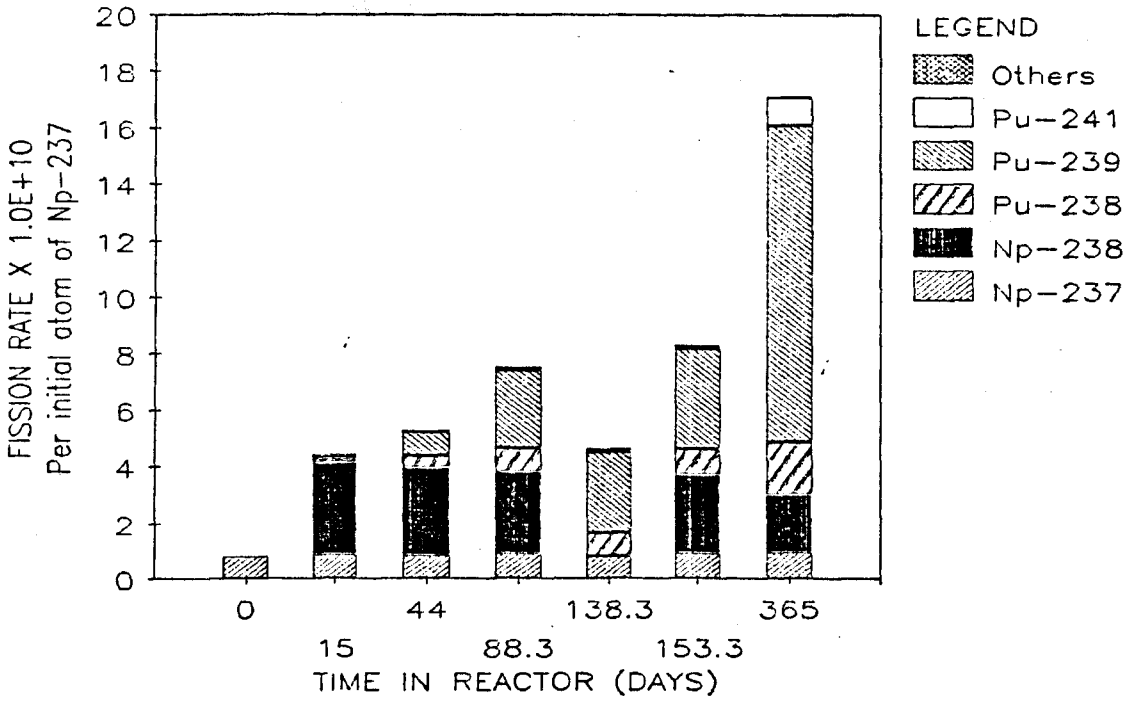

Figure 7.46 Total Fission Rate in the Target Pins vs Time - Example Case 3

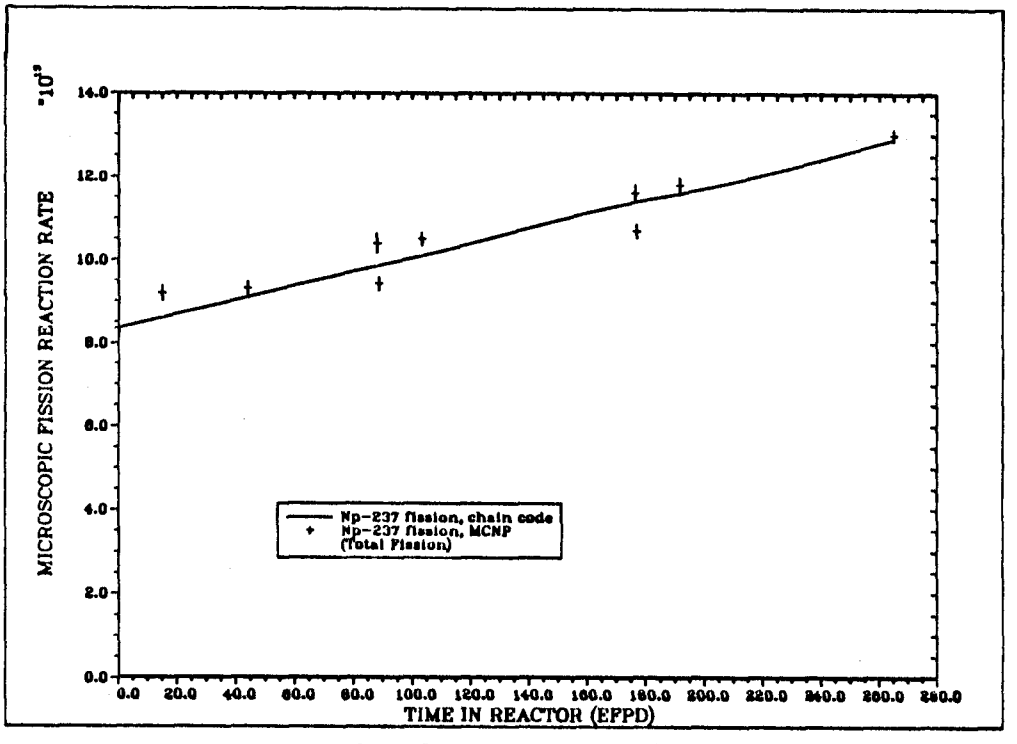

Figure 7.47 Total Microscopic Fission Reaction Rate vs Time for Np-237 - Example Case 3

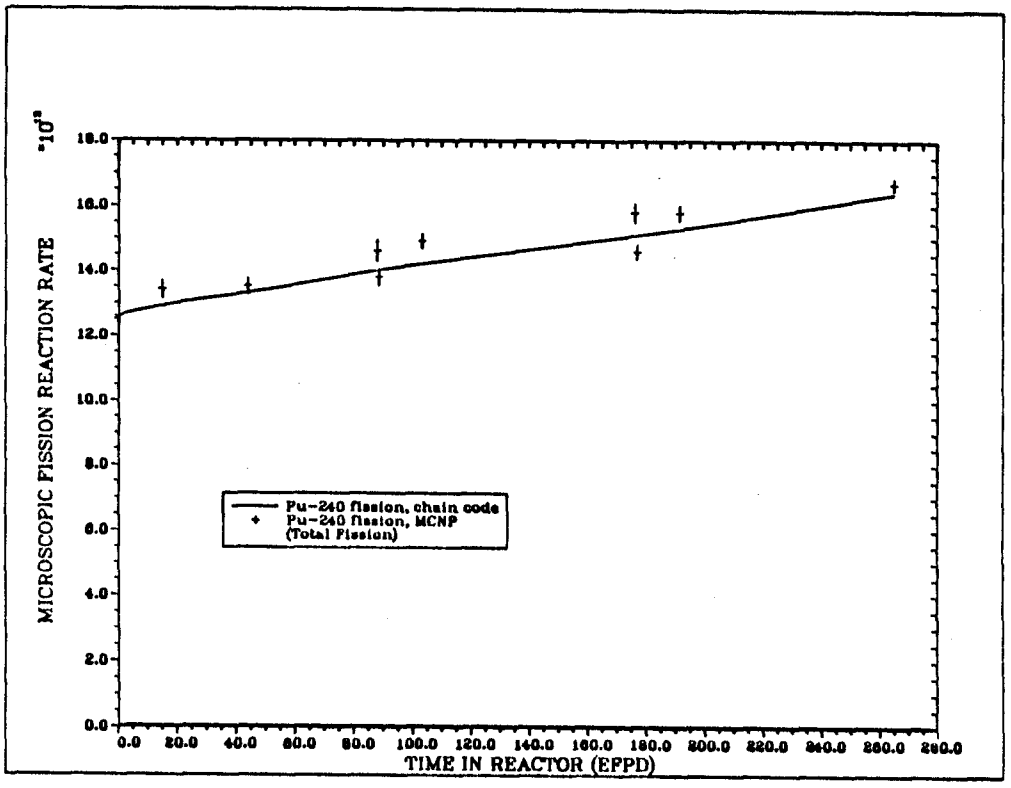

Figure 7.48 Total Microscopic Fission Reaction Rate vs Time for Pu-240 - Example Case 3

equilibrium effect. These fission reaction rates are not as important for the final results as ^{237}Np(n,2n) is, but it is instructive to observe the same ^{238}Np effect in all of them. Figures 7.49 and 7.50 show the actual behavior of these reaction rates as a function of EFPD.

Another aspect of the equilibrium ^{238}Np effect is its impact on the thermal and epithermal reaction rates. This effect is the opposite of that on the high energy reactions in that the equilibrium ^{238}Np level causes a flux drop as opposed to a fission source increase. The effect on the low energy region is much more damped than that on the high energy reaction rates. Figure 7.51 shows a good example of this. It shows the reaction rate plot for ^{241}Pu(n,f). For the first two cycles the reaction rate drops with the onset of equilibrium ^{238}Np. By the third cycle the ^{238}Np effect has become too damped to be observable. As with ^{237}Np(n,f) and ^{240}Pu(n,f), the ^{238}Np

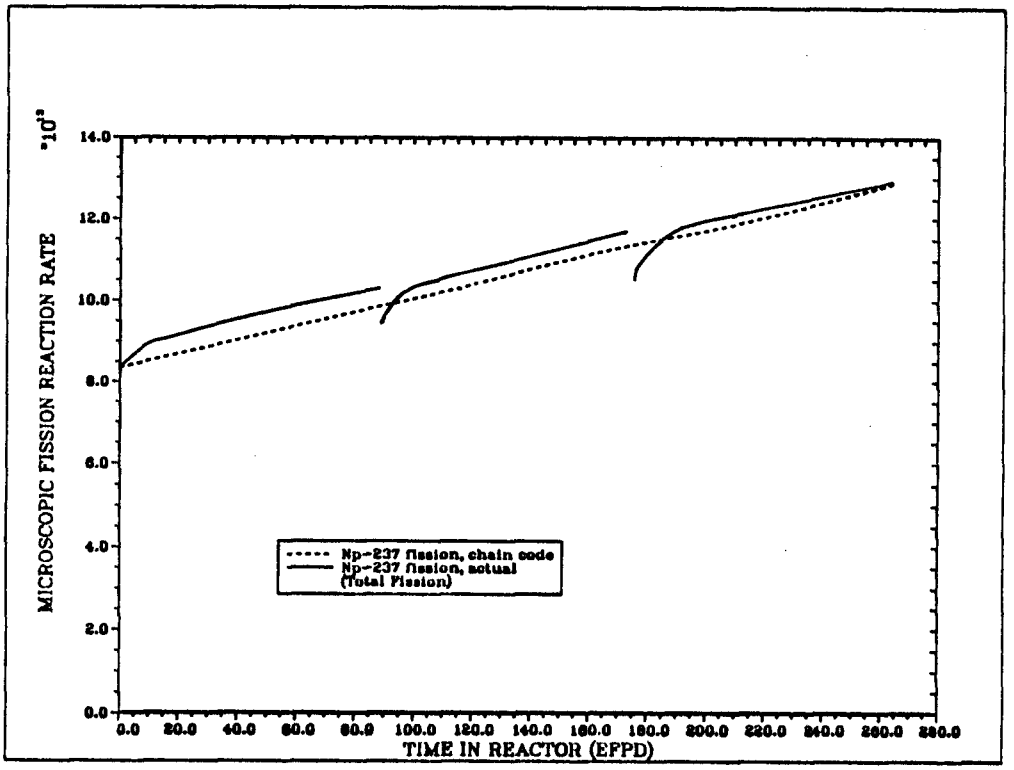

Figure 7.49 Actual Total Microscopic Fission Reaction Rate vs Time for Np-237 - Example Case 3

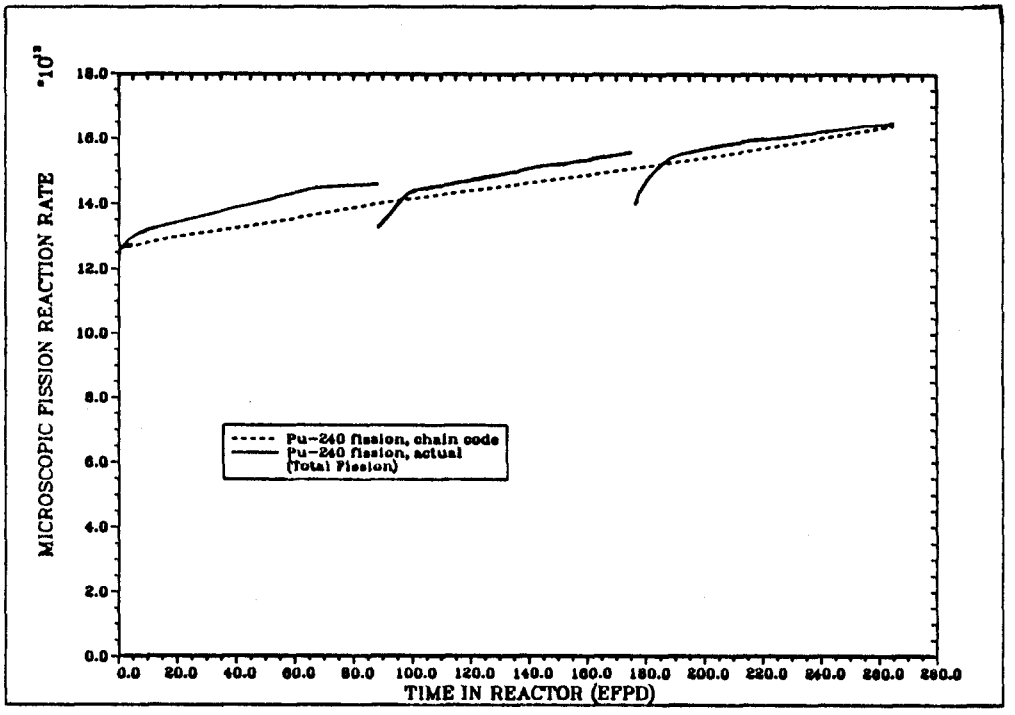

Figure 7.50 Actual Total Microscopic Fission Reaction Rate vs Time for Pu-240 - Example Case 3

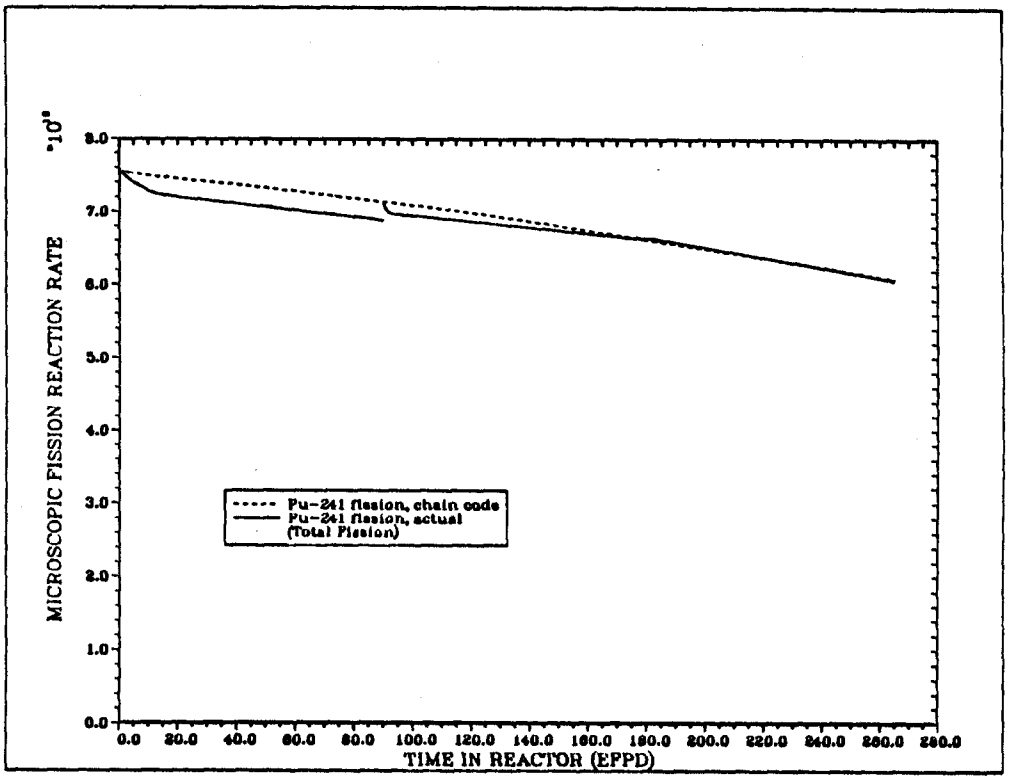

Figure 7.51 Actual Total Microscopic Fission Reaction Rate vs Time for Pu-241 - Example Case 3

effect on $^{241}Pu(n,f)$ is observable, but it is not important for the final answers calculated by the code.

A sensitivity study of the ^{238}Np effect on the $^{237}Np(n,2n)$ reaction rate has been performed. Since the only model available in the CHAIN.238DJ code for treating the $^{237}Np(n,2n)$ reaction rate is the linear interpolation method, there is no way to try to make the reaction rate behave as it does in reality. It is possible, however, to calculate the limit of the error by approximating the reaction rate as shown in Figure 7.52 and using the linear interpolation method. A new calculation with this higher $^{237}Np(n,2n)$ reaction rate resulted in an increase in the final ^{236}Pu impurity level from 9.1 to 9.9 ppm, an increase of 9%. The (n,2n) contribution to the total ppm impurity level increased from 4.2 to 5.0 ppm, an increase of 19%. This is a somewhat extreme upper limit on the error, since all but two of the MCNP intermediate data points are made to lie below the new reaction

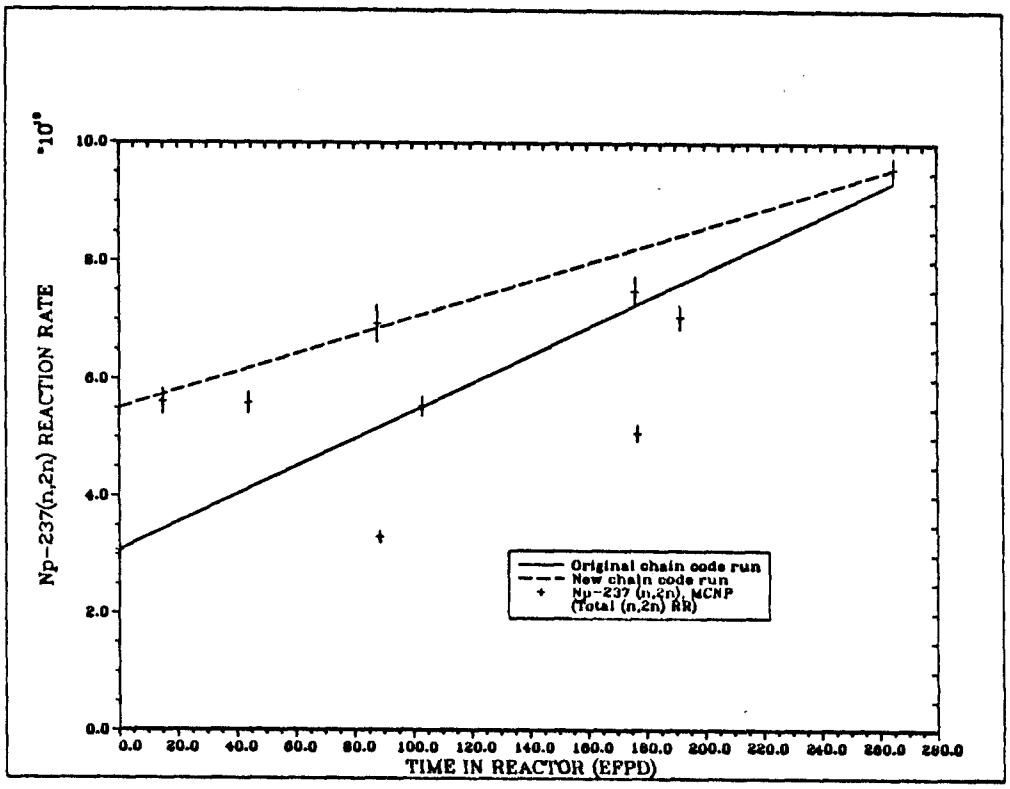

Figure 7.52 New Total $^{237}Np(n,2n)^{236}Pu$ Effective Reaction Rate vs Time (EFPD) - Example Case 3

rate line. Even so, the amount of error is not as bad as one might expect from looking at the scatter in the data points on the plot.

The important error that results from the ^{238}Np effect is in the ^{236}Pu impurity level. The error will be more pronounced for cases where the total irradiation time is relatively short and for cases where the impurity level is more dominated by the (n,2n) reaction. Relatively large errors in the $^{237}Np(n,2n)$ reaction rate early in the irradiation are much less important than the same error would be if it occurred toward the end of the irradiation because the half life of ^{236}Pu is only 2.87 years.

The CHAIN.238DJ code did an accurate job of calculating the plutonium production and quality for this case, but not the ^{236}Pu impurity level. For relatively short irradiations such as in this case the ^{236}Pu impurity level from $^{237}Np(n,2n)$ reactions will not be

calculated correctly without some improvement to the code. A suggestion for an improvement to the CHAIN.238DJ code that might improve the accuracy in situations like this is presented in Section 8.0.

8.0 CONCLUSIONS

The CHAIN.238DJ computer code accurately calculates transmutation in the chain that builds up from irradiation of ^{237}Np. The AKM method of solving the set of differential equations that describe the chain works well for this particular chain, but may not always work well for other chains or on any computer. The C-factor method usually does a good job of modelling the reaction rates that have a non-linear behavior in time. It usually works well as an empirical correlation even when the conditions may not fit the assumptions made in the development of its analytical basis. The most important potential source of error in CHAIN.238DJ calculations is the ^{238}Np equilibrium effect on the $^{237}Np(n,2n)$ reaction rate and the associated production of ^{236}Pu impurity. This problem usually has the greatest potential for causing error if the irradiation period is less than one year.

If it is assumed that the reaction rate and flux data in the input file are correct, the overall uncertainty in the calculations of ^{238}Pu and total plutonium production and of the plutonium quality is almost always less than 5% and is estimated to be usually less than one or two percent. For the ^{236}Pu ppm impurity level, the uncertainty could realistically be as high as 10%, especially for short irradiations with high reaction rates and when the $^{237}Np(n,2n)$ reaction is the dominant contributor to the total impurity level. For most cases when the irradiation period is longer than one year this uncertainty is usually below 5% and may be as low as only one or two percent. Users of the CHAIN.238DJ code should always spend some amount of time checking the reaction rates at intermediate times. It is from this type of checking that the user can arrive at the best estimate of the uncertainties for the case in question.

There are four identifiable upgrades to the code that would be very worthwhile improvements. The first and most important would be to improve the method of modelling the time-dependent $^{237}Np(n,2n)$

reaction rate. A new model could be built into the code to calculate the $^{237}Np(n,2n)$ reaction rate as some base amount plus an additional contribution from the total fission rate of all the nuclides in the chain. The base amount would just be a constant, and the additional contribution from local fission would be directly proportional to the total local fission rate. Figure 8.1 shows how this method would have modelled the $^{237}Np(n,2n)$ reaction rate for the third example case in Section 7.0. An even better model would use the sum of not just the fission rate for each nuclide, but the fission rate multiplied by the effective value of υ.

The second most important potential code upgrade would be to improve the headings and the method of calculating the output in the unit 13 output table. The headings could be more strictly correct, and the calculations of production, quality, and ppm impurity levels could be performed on the basis of weight instead of gram-atoms.

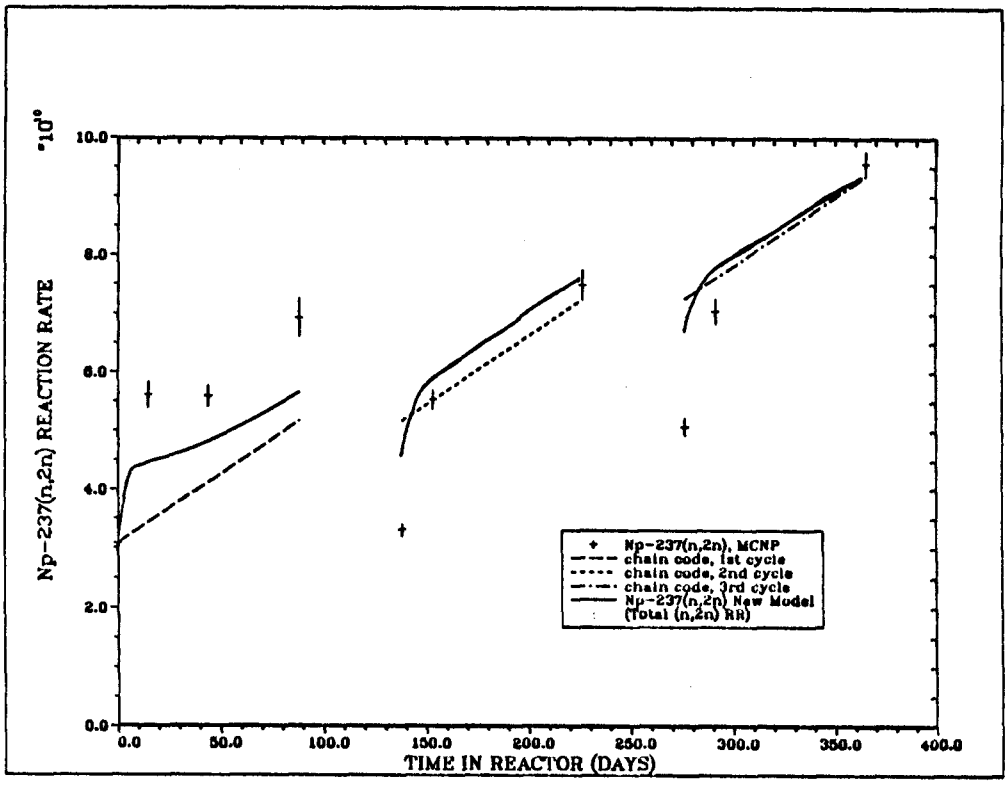

Figure 8.1 Improved Model of the $^{237}Np(n,2n)$ Reaction Rate vs Time for Example Case 3

The code could be upgraded to treat the production of ^{236}Pu impurity from $^{237}Np(n,2n)$ reactions separately from that produced by $^{237}Np(\gamma,n)$ reactions. This would save the user the bother of having to run the code twice to get the separate contribution of each reaction. This would be a fairly simple upgrade, requiring the treatment of ^{236}Pu in two separate array locations, one for (n,2n) and one for (γ,n). Lastly, the code could be upgraded to take into account the overlapping first resonances of ^{239}Pu and ^{241}Pu. The C-factor for ^{241}Pu could be used together with the ^{239}Pu amount instead of just with the ^{241}Pu amount.

For many applications, using only the simple linear interpolation method of treating the reaction rates is sufficient. Table 8.1 shows the results of using only the linear interpolation method compared to using two or three C-factor groups plus a linear interpolation group. This has been done for each of the three example cases from Section 7.0. In each case, the results with only the simple linear interpolation are not significantly different from those with a combination of several C-factors and the linear interpolation model together. The user would be wise not to expend effort building fancy modelling in the input file if the case can be modelled accurately by using simpler methods.

Nuclide	Final Amounts (gram-atoms) After Irradiation Period Given					
	Case 1 After 730 Days (530 EFPD)		Case 2 After 730 Days (530 EFPD)		Case 3 After 365 Days (265 EFPD)	
	With C-factors	Linear Interpolation Only	With C-factors	Linear Interp. Only	With C-factors	Linear Interp. Only
^{237}Np	0.768	0.767	0.807	0.806	0.756	0.755
^{238}Np	0.0012	0.0012	9.70e-4	9.74e-4	2.28e-3	2.30e-3
^{239}Np	-	-	3.28e-7	3.30e-7	2.70e-6	2.72e-6
^{236}Pu	-	-	2.19e-6	2.19e-6	1.98e-6	1.98e-6
^{238}Pu	0.203	0.203	0.166	0.166	0.191	0.192
^{239}Pu	0.0125	0.0127	0.0109	0.0113	0.0198	0.0201
^{240}Pu	9.68e-4	9.94e-4	1.14e-3	1.21e-3	4.47e-3	4.53e-3
^{241}Pu	5.60e-4	5.69e-4	6.55e-4	6.91e-4	1.63e-3	1.67e-3
^{242}Pu	2.84e-5	2.83e-5	4.63e-5	4.78e-5	2.31e-4	2.32e-4
Total Pu	0.217	0.218	0.179	0.179	0.218	0.218
Quality	93.5%	93.4%	92.9%	92.6%	88.0%	87.9%
^{236}Pu ppm	-	-	12.3	12.2	9.1	9.1

Table 8.1 Comparison of a Simple Linear Interpolation Calculation With a Combination C-factor/Linear Interpolation Calculation

REFERENCES

1. Bateman, H., "The Solution of a System of Differential Equations Occurring in the Theory of Radioactive Transformations," Proc. Cambridge Philos. Soc., 15, 423 (1910).

2. Croff, A.G., "A Users Manual for the ORIGEN2 Computer Code," Oak Ridge National Laboratory, Oak Ridge, TN July 1980.

3. Gumprecht, R.O., "Computer Code RIBD," Trans. ANS, Vol. 12, No. 1, p. 141, 1969.

4. England, T.R., "CINDER - A One-Point Depletion and Fission Product Program," Westinghouse Electric Corporation report WADP-TM-334, (1962, Rev. 1964).

5. England, T.R., Wilson, W.B., and Stamatelatos, M.G., "Fission Product Data for Thermal Reactors, Part 2: Users Manual for EPRI-CINDER Code and Data," Los Alamos National Laboratory report LA-6746-MS, (December, 1976).

6. Lietzke, M.P., and Claiborne, H.C., "CRUNCH - An IBM-704 Code for Calculating N Successive First-Order Reactions," ORNL-2958, (October 1960).

7. Schmittroth, F., "Uncertainty Analysis of Fission-Product Decay-Heat Summation Methods," Nuclear Science and Engineering, 59, (1976), 117.

8. Bigelow, J. E., et al., "Production of Transplutonium Elements in the High Flux Isotope Reactor," ACS Symposium Series, No. 161, Oak Ridge National Laboratory, 1981.

9. Duderstadt, J. J. and Hamilton, L.J., Nuclear Reactor Analysis, page 344, Wiley and Sons, 1976.

10. Breismeister, J.F., et. al., "MCNP - A General Monte Carlo Code for Neutron and Photon Transport, Version 3b," LA-7369-M, Rev.2, Los Alamos National Laboratory, Los Alamos, NM 1986.

APPENDIX

APPENDIX A

CHAIN.238DJ Source Code Listing
Example Input File
Example Output Files

```
C
C  Pu-238 Chain Code          6/20/89
C
C  Multiple-region, multiple C-factor, flux ramp,
C  reaction rate ramp approach with decay period.
C
C  Reaction rates read in from unit 5 must
C  be per second, per unit number density.
C
C  Np-237 (n,2n) and (gamma,n) reaction rates
C  read in must go directly to Pu-236, so they
C  must include all branching effects.
C
C  Reaction rates for Np-238, Np-239, Pu-236, and Fsprod are
C  all lumped into the thermal region, where they are ramped.
C
C  Output files:
C       a) Unit 12 contains initial and final amounts at the end of
C          each irradiation period and each decay period, as well
C          as reaction rates at the end of each irradiation period.
C
C       b) Unit 13 contains quality levels, ppm Pu-236 impurity
C          levels, and production levels for Pu-238 at the end
C          of each irradiation period and of each decay period.
C
      CHARACTER*6 NAM(10)
      DIMENSION THALF(10),RRCT1(10),RRFT1(10)
      DOUBLE PRECISION AMTI(10),AMTO(10),ALF(10,10),BTA(10)
      DOUBLE PRECISION A(10,10),AMTII(10)
      DIMENSION RRCT2(10),RRFT2(10)
      DIMENSION CC(10,7),CF(10,7),RRCR1(10,7),RRFR1(10,7)
      DIMENSION FLUX1(10,7),FLUX2(10,7),RRCF1(10,3),RRFF1(10,3)
      DIMENSION RRCF2(10,3),RRFF2(10,3),FINC(10,7),RRICT(10),RRIFT(10)
      DIMENSION RRICF(10,3),RRIFF(10,3),DLAM(10)
      DIMENSION SIGCID(10,7),SIGFID(10,7)
      DIMENSION RRC(10),RRF(10),RRCT(10),RRFT(10),FLUX(10,7)
      DIMENSION RRCF(10,3),RRFF(10,3)
      L=10
      READ(11,99) EFPD
   99 FORMAT(//,10X,1PE9.3,/)
      DO 10 I=1,L
        READ(11,100) NAM(I),AMTI(I),THALF(I),RRCT1(I),RRFT1(I),
     &               RRCT2(I),RRFT2(I)
  100   FORMAT(3X,A6,1X,1PE8.2,1X,1PE9.3,4(1X,1PE8.2))
        RRCT(I)=0.0
        RRFT(I)=0.0
        RRICT(I)=0.0
        RRIFT(I)=0.0
        IF(I.EQ.2.OR.I.EQ.3.OR.I.EQ.4.OR.I.EQ.L) GO TO 10
        DO 13 J=1,7
          READ(11,120) CC(I,J),RRCR1(I,J),CF(I,J),RRFR1(I,J),
     &     FLUX1(I,J),FLUX2(I,J)
  120       FORMAT(10X,1PE8.2,1X,1PE9.3,4(1X,1PE8.2))
            FLUX(I,J)=0.0
            FINC(I,J)=0.0
   13   CONTINUE
        DO 14 J=1,3
          RRCF(I,J)=0.0
          RRFF(I,J)=0.0
          RRICF(I,J)=0.0
          RRIFF(I,J)=0.0
          READ(11,115) RRCF1(I,J),RRFF1(I,J),RRCF2(I,J),RRFF2(I,J)
  115       FORMAT(10X,1PE8.2,1X,1PE9.3,2(1X,1PE8.2))
   14   CONTINUE
```

```
      IF(I.NE.1) GO TO 10
      READ(11,117) RRN2N1,RRN2N2,RRGN1,RRGN2
117   FORMAT(10X,1PE8.2,1X,1PE9.3,/,10X,1PE8.2,1X,1PE9.3)
 10   CONTINUE
      RR2361=RRN2N1+RRGN1
      RR2362=RRN2N2+RRGN2
      WRITE(*,*)
      WRITE(*,*) ' Enter the irradiation time period (days).'
      READ(*,*) TI
      WRITE(*,*) ' Enter the shutdown/decay time period (days).'
      READ(*,*) TD
      WRITE(*,*) ' Enter the number of time periods (integer).'
      READ(*,*) NP
      WRITE(*,*) ' Enter the number of steps in the'
      WRITE(*,*) ' irradiation period (integer).'
      READ(*,*) II
      DELT=TI/II
      DO 20 I=1,L
        DLAM(I)=0.69315/THALF(I)
        IF(THALF(I).GT.1.e+20) DLAM(I)=0.0
        RRICT(I)=(RRCT1(I)-RRCT2(I))/(EFPD*II/TI)
        RRCT(I)=RRCT1(I)-RRICT(I)/2.0
        RRIFT(I)=(RRFT1(I)-RRFT2(I))/(EFPD*II/TI)
        RRFT(I)=RRFT1(I)-RRIFT(I)/2.0
        IF(I.EQ.2.OR.I.EQ.3.OR.I.EQ.4.OR.I.EQ.L) GO TO 20
        DO 25 J=1,7
          IF(FLUX1(I,J).LT.1.) GO TO 25
          FINC(I,J)=(FLUX1(I,J)-FLUX2(I,J))/(EFPD*II/TI)
          FLUX(I,J)=FLUX1(I,J)-FINC(I,J)/2.0
          SIGCID(I,J)=RRCR1(I,J)/FLUX1(I,J)
          SIGFID(I,J)=RRFR1(I,J)/FLUX1(I,J)
          IF(AMTI(I).LT.1.e-15) GO TO 25
          SIGCID(I,J)=(RRCR1(I,J)/FLUX1(I,J))*SQRT(1.+CC(I,J)*AMTI(I))
          SIGFID(I,J)=(RRFR1(I,J)/FLUX1(I,J))*SQRT(1.+CF(I,J)*AMTI(I))
 25     CONTINUE
        DO 22 J=1,3
          IF(RRCF1(I,J).LT.1.e-22.AND.RRFF1(I,J).LT.1.e-22) GO TO 22
          RRICF(I,J)=(RRCF1(I,J)-RRCF2(I,J))/(EFPD*II/TI)
          RRCF(I,J)=RRCF1(I,J)-RRICF(I,J)/2.0
          RRIFF(I,J)=(RRFF1(I,J)-RRFF2(I,J))/(EFPD*II/TI)
          RRFF(I,J)=RRFF1(I,J)-RRIFF(I,J)/2.0
 22     CONTINUE
 20   CONTINUE
      RRI236=(RR2361-RR2362)/(II*EFPD/TI)
      RR236=RR2361-RRI236/2.0
      FAC=86400.
      FAC2=1.e+24
      TIME=0.0
      WRITE(13,145)
145   FORMAT(//,8X,'PLUTONIUM QUALITY, IMPURITY, AND PRODUCTION '
     &'LEVELS:',//,2X,'Time',7X,'Total Plutonium Production',9X,
     &'Pu-238',6X,'Pu-236',/,1X,'(Days)  (Kg total Pu per initial ',
     &'Kg Np-237)  Quality (%)  ppm level',/,1X,'------',2X,35('-'),
     &2X,'-----------',2X,9('-'))
      DO 2000 I=1,NP
        DO 18 N=1,L
          AMTII(N)=AMTI(N)
 18     CONTINUE
        DO 1000 J=1,II
          DO 30 N=1,L
            RRC(N)=0.0
            RRF(N)=0.0
            IF(N.EQ.2.OR.N.EQ.3.OR.N.EQ.4.OR.N.EQ.L) GO TO 33
            DO 31 K=1,7
```

```
            IF(FLUX1(N,K).LT.1.) GO TO 31
            SIGC=SIGCID(N,K)/SQRT(1.+CC(N,K)*AMTI(N))
            SIGF=SIGFID(N,K)/SQRT(1.+CF(N,K)*AMTI(N))
            RRC(N)=RRC(N)+SIGC*FLUX(N,K)
            RRF(N)=RRF(N)+SIGF*FLUX(N,K)
 31       CONTINUE
          DO 32 K=1,3
            RRC(N)=RRC(N)+RRCF(N,K)
            RRF(N)=RRF(N)+RRFF(N,K)
 32       CONTINUE
 33       RRC(N)=RRC(N)+RRCT(N)
          RRF(N)=RRF(N)+RRFT(N)
          BTA(N)=DLAM(N)+((RRF(N)+RRC(N))*FAC)
          IF(N.GE.L) GO TO 30
          ALF(N,N+1)=RRC(N)*FAC
          ALF(N,L)=RRF(N)*FAC
 30     CONTINUE
        ALF(3,4)=0.0
        ALF(4,5)=0.0
        ALF(2,5)=DLAM(2)
        ALF(3,6)=DLAM(3)
        ALF(1,4)=RR236*FAC
        CALL AKM(L,ALF,BTA,AMTI,A)
        CALL TRANX(L,BTA,A,DELT,AMTO)
        IF(J.EQ.II) GO TO 1000
        DO 40 N=1,L
          RRCT(N)=RRCT(N)-RRICT(N)
          RRFT(N)=RRFT(N)-RRIFT(N)
          IF(N.EQ.2.OR.N.EQ.3.OR.N.EQ.4.OR.N.EQ.L) GO TO 43
          DO 41 K=1,7
            FLUX(N,K)=FLUX(N,K)-FINC(N,K)
 41       CONTINUE
          DO 42 K=1,3
            RRCF(N,K)=RRCF(N,K)-RRICF(N,K)
            RRFF(N,K)=RRFF(N,K)-RRIFF(N,K)
 42       CONTINUE
 43       AMTI(N)=AMTO(N)
 40     CONTINUE
        RR236=RR236-RRI236
1000  CONTINUE
      TIME=TIME+TI
      WRITE(12,150) TIME,TIME
 150  FORMAT(///,20X,'OUTPUT AT ',F6.1,' DAYS',//,39X,'Reaction ',
     & 'rates at ',F6.1,' days:',/,10X,'Initial',4X,'Final',10X,
     & 'Total',5X,'Total',3X,'Resonance  Resonance',/,1X,'Nuclide',
     & 2X,'Amount     Amount',8X,'Fission   Capture',
     & 3X,'Fission    Capture',/,
     & ' -------  --------  --------',5X,4(2X,'--------'))
      PUTOT=0.0
      DO 35 N=1,L
        RRCR=0.0
        RRFR=0.0
        IF(N.EQ.2.OR.N.EQ.3.OR.N.EQ.4.OR.N.EQ.L) GO TO 27
        DO 23 K=1,7
          IF(FLUX1(N,K).LT.1.) GO TO 23
          SIGC=SIGCID(N,K)/SQRT(1.+CC(N,K)*AMTO(N))
          SIGF=SIGFID(N,K)/SQRT(1.+CF(N,K)*AMTO(N))
          RRCR=RRCR+SIGC*(FLUX(N,K)+0.5*FINC(N,K))
          RRFR=RRFR+SIGF*(FLUX(N,K)+0.5*FINC(N,K))
 23     CONTINUE
 27     WRITE(12,160) NAM(N),AMTII(N),AMTO(N),RRF(N),RRC(N),
     &  RRFR,RRCR
 160    FORMAT(1X,A6,3X,1PE8.2,2X,E8.2,5X,4(2X,E8.2))
        IF(N.LE.3.OR.N.GE.L) GO TO 35
```

```
          PUTOT=PUTOT+AMTO(N)
   35   CONTINUE
        QUAL=(AMTO(5)/PUTOT)*1.e+02
        PPM=(AMTO(4)/PUTOT)*1.e+06
        WRITE(13,170) TIME,PUTOT,QUAL,PPM
  170   FORMAT(1X,F6.1,16X,1PE8.2,18X,0PF4.1,8X,F4.1)
        DO 45 N=1,L
          BTA(N)=DLAM(N)
          AMTI(N)=AMTO(N)
          DO 46 J=1,L
            ALF(N,J)=0.0
   46     CONTINUE
   45   CONTINUE
        ALF(2,5)=DLAM(2)
        ALF(3,6)=DLAM(3)
        CALL AKM(L,ALF,BTA,AMTI,A)
        CALL TRANX(L,BTA,A,TD,AMTO)
        TIME=TIME+TD
        WRITE(12,155) TIME
  155   FORMAT(///,14X,'OUTPUT AT ',F6.1,' DAYS',//,20X,'Initial    ',
     &  'Final',/,11X,'Nuclide  Amount     Amount',/,11X,'--------',
     &  2X,'--------  --------')
        PUTOT=0.0
        DO 50 N=1,L
          WRITE(12,165) NAM(N),AMTI(N),AMTO(N)
  165     FORMAT(11X,A6,1X,2(2X,1PE8.2))
          IF(N.LE.3.OR.N.GE.L) GO TO 50
          PUTOT=PUTOT+AMTO(N)
   50   CONTINUE
        QUAL=(AMTO(5)/PUTOT)*100.0
        PPM=(AMTO(4)/PUTOT)*1.e+06
        WRITE(13,170) TIME,PUTOT,QUAL,PPM
        DO 55, N=1,L
          RRCT(N)=RRCT(N)-RRICT(N)
          RRFT(N)=RRFT(N)-RRIFT(N)
          IF(N.EQ.2.OR.N.EQ.3.OR.N.EQ.4.OR.N.EQ.L) GO TO 58
          DO 56 K=1,7
            FLUX(N,K)=FLUX(N,K)-FINC(N,K)
   56     CONTINUE
          DO 57 K=1,3
            RRCF(N,K)=RRCF(N,K)-RRICF(N,K)
            RRFF(N,K)=RRFF(N,K)-RRIFF(N,K)
   57     CONTINUE
   58     AMTI(N)=AMTO(N)
   55   CONTINUE
        RR236=RR236-RRI236
 2000 CONTINUE
      END
      SUBROUTINE TRANX(L,BTA,A,T,AMTO)
C
C  This subroutine uses the A(k,m) values (A), the time increment (T),
C  the beta values (BTA), and the chain length (L), to calculate the
C  nuclide amounts at the end of the time step (AMTO).
C
      DOUBLE PRECISION BTA(10),A(10,10),AMTO(10)
      DIMENSION EXPBT(10)
      EPS=1.e-16
      EPM=100.
      DO 1 M=1,L
        AMTO(M)=0.
        EXPBT(M)=0.
        FAC=BTA(M)*T
        IF(FAC.GT.EPM) GO TO 1
        EXPBT(M)=EXP(-FAC)
```

```
        IF(FAC.LT.EPS) EXPBT(M)=1.-FAC
    1   CONTINUE
        DO 2 N=1,L
          DO 2 M=1,N
            AMTO(N)=AMTO(N)+A(N,M)*EXPBT(M)
    2   CONTINUE
        RETURN
        END
        SUBROUTINE AKM(L,ALF,BTA,S0,A)
C
C   This subroutine uses the beta values (BTA), the alpha values (ALF),
C   the chain length (L), and the nuclide amounts (SO), to calculate
C   all of the A(k,m) values (A) for the chain.
C
        DOUBLE PRECISION ALF(10,10),BTA(10),A(10,10),S0(10)
        DO 1 M=1,L
          A(M,M)= S0(M)
          IF (M .EQ. 1) GO TO 2
          M1= M- 1
          DO 3 I=1,M1
 3        A(M,M)= A(M,M)- A(M,I)
 2        IF (M .EQ. L) GO TO 1
          KL= M+ 1
          DO 4 K=KL,L
            SX= 0.
            K1= K- 1
            DO 5 I=M,K1
 5          SX= SX+ ALF(I,K)* A(I,M)
            EPS=1.E-10
            BTKM=(BTA(K)-BTA(M))
            ABTKM=ABS(BTKM)
            IF (ABTKM.LT.EPS) PRINT 100
 100        FORMAT(' BETAS EQUAL')
            IF (ABTKM.LT.EPS) STOP 1
            A(K,M)= SX/BTKM
 4        CONTINUE
 1      CONTINUE
        RETURN
        END
```

```
Ending burned reaction rates are at  530.0 EFPD"s

          5.300E+02

1 Np-237 1.00E+00 7.816E+08 1.09E-09 0.00E+00 8.20E-10 0.00E+00
         2.11E+00 6.066E-10 1.90E-01 0.00E-14 7.25E+12 6.52E+12
         5.00E+03 2.601E-10 5.00E+00 0.00E-14 3.85E+12 3.53E+12
         7.25E+01 1.398E-09 1.55E-01 0.00E-13 5.10E+13 5.36E+13
         1.00E+00 0.000E+00 1.00E+00 0.00E+00 0.00E+00 0.00E+00
         1.00E+00 0.000E+00 1.00E+00 0.00E+00 0.00E+00 0.00E+00
         1.00E+00 0.000E+00 1.00E+00 0.00E+00 0.00E+00 0.00E+00
         1.00E+00 0.000E+00 1.00E+00 0.00E+00 0.00E+00 0.00E+00
         1.21E-09 1.055E-10 1.28E-09 1.30E-10
         0.00E+00 0.000E+00 0.00E+00 0.00E+00
         0.00E+00 0.000E+00 0.00E+00 0.00E+00
         3.86E-14 6.042E-14  (n,2n)  fresh,burned
         3.06E-14 3.086E-14  (gamma,n)  fresh,burned
2 Np-238 0.00E+00 2.117E+00 1.31E-09 3.04E-08 1.13E-09 2.66E-08
3 Np-239 0.00E+00 2.355E+00 1.00E-24 1.00E-24 1.00E-24 1.00E-24
4 Pu-236 0.00E+00 1.041E+03 4.45E-09 4.73E-09 4.31E-09 4.63E-09
5 Pu-238 0.00E+00 3.205E+04 2.97E-09 9.03E-11 2.24E-09 6.79E-11
         1.51E+01 4.840E-10 1.50E+01 1.60E-11 1.24E+13 1.26E+13
         7.41E+01 6.300E-10 2.98E+01 3.93E-11 1.86E+13 1.98E+13
         1.82E+01 5.944E-10 1.53E+01 1.21E-10 2.66E+13 2.78E+13
         0.00E+00 0.000E+00 0.00E+00 0.00E+00 0.00E+00 0.00E+00
         0.00E+00 0.000E+00 0.00E+00 0.00E+00 0.00E+00 0.00E+00
         0.00E+00 0.000E+00 0.00E+00 0.00E+00 0.00E+00 0.00E+00
         0.00E+00 0.000E+00 0.00E+00 0.00E+00 0.00E+00 0.00E+00
         5.14E-10 4.381E-10 5.44E-10 4.89E-10
         0.00E+00 0.000E+00 0.00E+00 0.00E+00
         0.00E+00 0.000E+00 0.00E+00 0.00E+00
6 Pu-239 0.00E+00 8.806E+06 6.63E-10 1.70E-09 4.60E-10 1.17E-09
         4.49E+01 8.954E-09 4.11E+01 1.42E-08 2.79E+13 2.48E+13
         0.00E+00 1.723E-09 0.00E+00 2.06E-09 5.57E+13 5.89E+13
         1.00E+00 0.000E+00 1.00E+00 0.00E+00 0.00E+00 0.00E+00
         1.00E+00 0.000E+00 1.00E+00 0.00E+00 0.00E+00 0.00E+00
         0.00E+00 0.000E+00 0.00E+00 0.00E+00 0.00E+00 0.00E+00
         0.00E+00 0.000E+00 0.00E+00 0.00E+00 0.00E+00 0.00E+00
         0.00E+00 0.000E+00 0.00E+00 0.00E+00 0.00E+00 0.00E+00
         3.76E-10 7.510E-10 4.00E-10 8.18E-10
         0.00E+00 0.000E+00 0.00E+00 0.00E+00
         0.00E+00 0.000E+00 0.00E+00 0.00E+00
7 Pu-240 0.00E+00 2.397E+06 2.45E-09 4.75E-13 1.83E-09 3.55E-13
         1.00E+03 5.789E-08 9.99E+02 1.05E-11 2.68E+13 2.71E+13
         9.40E+01 2.407E-09 2.82E+01 1.88E-11 1.02E+14 1.08E+14
         1.00E+00 0.000E+00 1.00E+00 0.00E+00 0.00E+00 0.00E+00
         1.00E+00 0.000E+00 1.00E+00 0.00E+00 0.00E+00 0.00E+00
         0.00E+00 0.000E+00 0.00E+00 0.00E+00 0.00E+00 0.00E+00
         0.00E+00 0.000E+00 0.00E+00 0.00E+00 0.00E+00 0.00E+00
         0.00E+00 0.000E+00 0.00E+00 0.00E+00 0.00E+00 0.00E+00
         1.16E-10 1.135E-10 1.20E-10 1.38E-10
         0.00E+00 0.000E+00 0.00E+00 0.00E+00
         0.00E+00 0.000E+00 0.00E+00 0.00E+00
```

```
 8 Pu-241 0.00E+00 5.241E+03 1.23E-09 3.56E-09 8.92E-10 2.59E-09
          6.19E+02 4.242E-09 5.83E+02 1.05E-08 1.97E+13 1.72E+13
          5.30E+01 1.743E-09 1.03E+01 4.75E-09 4.25E+13 4.49E+13
          1.00E+00 0.000E+00 1.00E+00 0.00E+00 0.00E+00 0.00E+00
          1.00E+00 0.000E+00 1.00E+00 0.00E+00 0.00E+00 0.00E+00
          0.00E+00 0.000E+00 0.00E+00 0.00E+00 0.00E+00 0.00E+00
          0.00E+00 0.000E+00 0.00E+00 0.00E+00 0.00E+00 0.00E+00
          0.00E+00 0.000E+00 0.00E+00 0.00E+00 0.00E+00 0.00E+00
          4.36E-10 1.738E-09 4.56E-10 1.83E-09
          0.00E+00 0.000E+00 0.00E+00 0.00E+00
          0.00E+00 0.000E+00 0.00E+00 0.00E+00
 9 Pu-242 0.00E+00 1.374E+08 1.54E-08 8.90E-11 1.49E-08 1.10E-10
          1.00E+00 0.000E+00 1.00E+00 0.00E+00 0.00E+00 0.00E+00
          1.00E+00 0.000E+00 1.00E+00 0.00E+00 0.00E+00 0.00E+00
          0.00E+00 0.000E+00 0.00E+00 0.00E+00 0.00E+00 0.00E+00
          0.00E+00 0.000E+00 0.00E+00 0.00E+00 0.00E+00 0.00E+00
          0.00E+00 0.000E+00 0.00E+00 0.00E+00 0.00E+00 0.00E+00
          0.00E+00 0.000E+00 0.00E+00 0.00E+00 0.00E+00 0.00E+00
          0.00E+00 0.000E+00 0.00E+00 0.00E+00 0.00E+00 0.00E+00
          0.00E+00 0.000E+00 0.00E+00 0.00E+00
          0.00E+00 0.000E+00 0.00E+00 0.00E+00
          0.00E+00 0.000E+00 0.00E+00 0.00E+00
10 Fsprod 0.00E+00 9.999E+25 0.00E+00 0.00E+00 0.00E+00 0.00E+00

  Reaction rates are in units of
  (reactions-cc)/(sec-atom)


 I NAM(I) AMTI(I) THALF(I)  RRCT1(I) RRFT1(I)   RRCT2(I)   RRFT2(I)
          CC(I,J) RRCR1(I,J) CF(I,J) RRFR1(I,J) FLUX1(I,J) FLUX2(I,J)
          RRCF1(I,J) RRFF1(I,J) RRCF2(I,J) RRFF2(I,J)
```

OUTPUT AT 100.0 DAYS

Nuclide	Initial Amount	Final Amount	Reaction rates at 100.0 days: Total Fission	Total Capture	Resonance Fission	Resonance Capture
Np-237	1.00E+00	9.60E-01	1.10E-10	4.57E-09	0.00E+00	2.30E-09
Np-238	0.00E+00	1.15E-03	2.97E-08	1.28E-09	0.00E+00	0.00E+00
Np-239	0.00E+00	4.31E-07	1.00E-24	1.00E-24	0.00E+00	0.00E+00
Pu-236	0.00E+00	5.62E-07	4.71E-09	4.42E-09	0.00E+00	0.00E+00
Pu-238	0.00E+00	3.63E-02	6.72E-10	4.54E-09	1.38E-10	1.19E-09
Pu-239	0.00E+00	6.79E-04	1.82E-08	1.14E-08	1.58E-08	1.04E-08
Pu-240	0.00E+00	2.02E-05	1.48E-10	6.23E-08	2.94E-11	5.99E-08
Pu-241	0.00E+00	2.70E-06	2.02E-08	7.50E-09	1.50E-08	5.90E-09
Pu-242	0.00E+00	3.54E-08	9.30E-11	1.53E-08	0.00E+00	0.00E+00
Fsprod	0.00E+00	1.35E-03	0.00E+00	0.00E+00	0.00E+00	0.00E+00

OUTPUT AT 140.0 DAYS

Nuclide	Initial Amount	Final Amount
Np-237	9.60E-01	9.60E-01
Np-238	1.15E-03	2.36E-09
Np-239	4.31E-07	3.33E-12
Pu-236	5.62E-07	5.47E-07
Pu-238	3.63E-02	3.75E-02
Pu-239	6.79E-04	6.79E-04
Pu-240	2.02E-05	2.02E-05
Pu-241	2.70E-06	2.68E-06
Pu-242	3.54E-08	3.54E-08
Fsprod	1.35E-03	1.35E-03

OUTPUT AT 240.0 DAYS

Nuclide	Initial Amount	Final Amount	Reaction rates at 240.0 days: Total Fission	Total Capture	Resonance Fission	Resonance Capture
Np-237	9.60E-01	9.22E-01	1.15E-10	4.57E-09	0.00E+00	2.34E-09
Np-238	2.36E-09	1.10E-03	2.90E-08	1.24E-09	0.00E+00	0.00E+00
Np-239	3.33E-12	4.04E-07	1.00E-24	1.00E-24	0.00E+00	0.00E+00
Pu-236	5.47E-07	1.04E-06	4.69E-09	4.40E-09	0.00E+00	0.00E+00
Pu-238	3.75E-02	7.08E-02	6.59E-10	4.22E-09	1.19E-10	9.96E-10
Pu-239	6.79E-04	2.35E-03	1.74E-08	1.09E-08	1.51E-08	9.92E-09
Pu-240	2.02E-05	1.26E-04	1.52E-10	5.96E-08	2.91E-11	5.72E-08
Pu-241	2.68E-06	3.30E-05	1.97E-08	7.32E-09	1.48E-08	5.78E-09
Pu-242	3.54E-08	8.86E-07	9.69E-11	1.52E-08	0.00E+00	0.00E+00
Fsprod	1.35E-03	3.07E-03	0.00E+00	0.00E+00	0.00E+00	0.00E+00

OUTPUT AT 280.0 DAYS

Nuclide	Initial Amount	Final Amount
Np-237	9.22E-01	9.22E-01
Np-238	1.10E-03	2.27E-09
Np-239	4.04E-07	3.11E-12
Pu-236	1.04E-06	1.02E-06
Pu-238	7.08E-02	7.18E-02
Pu-239	2.35E-03	2.35E-03
Pu-240	1.26E-04	1.26E-04
Pu-241	3.30E-05	3.29E-05
Pu-242	8.86E-07	8.86E-07
Fsprod	3.07E-03	3.07E-03

OUTPUT AT 380.0 DAYS

			Reaction rates at 380.0 days:			
Nuclide	Initial Amount	Final Amount	Total Fission	Total Capture	Resonance Fission	Resonance Capture
Np-237	9.22E-01	8.86E-01	1.19E-10	4.57E-09	0.00E+00	2.39E-09
Np-238	2.27E-09	1.06E-03	2.83E-08	1.21E-09	0.00E+00	0.00E+00
Np-239	3.11E-12	3.77E-07	1.00E-24	1.00E-24	0.00E+00	0.00E+00
Pu-236	1.02E-06	1.46E-06	4.67E-09	4.37E-09	0.00E+00	0.00E+00
Pu-238	7.18E-02	1.02E-01	6.52E-10	3.98E-09	1.08E-10	8.89E-10
Pu-239	2.35E-03	4.61E-03	1.65E-08	1.04E-08	1.43E-08	9.42E-09
Pu-240	1.26E-04	3.32E-04	1.56E-10	5.52E-08	2.85E-11	5.29E-08
Pu-241	3.29E-05	1.24E-04	1.91E-08	7.07E-09	1.43E-08	5.59E-09
Pu-242	8.86E-07	5.04E-06	1.01E-10	1.51E-08	0.00E+00	0.00E+00
Fsprod	3.07E-03	5.25E-03	0.00E+00	0.00E+00	0.00E+00	0.00E+00

OUTPUT AT 420.0 DAYS

Nuclide	Initial Amount	Final Amount
Np-237	8.86E-01	8.86E-01
Np-238	1.06E-03	2.18E-09
Np-239	3.77E-07	2.91E-12
Pu-236	1.46E-06	1.42E-06
Pu-238	1.02E-01	1.03E-01
Pu-239	4.61E-03	4.61E-03
Pu-240	3.32E-04	3.32E-04
Pu-241	1.24E-04	1.23E-04
Pu-242	5.04E-06	5.04E-06
Fsprod	5.25E-03	5.25E-03

OUTPUT AT 520.0 DAYS

Reaction rates at 520.0 days:

Nuclide	Initial Amount	Final Amount	Total Fission	Total Capture	Resonance Fission	Resonance Capture
Np-237	8.86E-01	8.51E-01	1.24E-10	4.58E-09	0.00E+00	2.43E-09
Np-238	2.18E-09	1.02E-03	2.75E-08	1.17E-09	0.00E+00	0.00E+00
Np-239	2.91E-12	3.53E-07	1.00E-24	1.00E-24	0.00E+00	0.00E+00
Pu-236	1.42E-06	1.81E-06	4.65E-09	4.34E-09	0.00E+00	0.00E+00
Pu-238	1.03E-01	1.32E-01	6.50E-10	3.77E-09	1.00E-10	8.18E-10
Pu-239	4.61E-03	7.21E-03	1.57E-08	9.83E-09	1.36E-08	8.93E-09
Pu-240	3.32E-04	6.29E-04	1.60E-10	5.03E-08	2.78E-11	4.82E-08
Pu-241	1.23E-04	2.91E-04	1.84E-08	6.76E-09	1.37E-08	5.33E-09
Pu-242	5.04E-06	1.57E-05	1.05E-10	1.50E-08	0.00E+00	0.00E+00
Fsprod	5.25E-03	7.92E-03	0.00E+00	0.00E+00	0.00E+00	0.00E+00

OUTPUT AT 560.0 DAYS

Nuclide	Initial Amount	Final Amount
Np-237	8.51E-01	8.51E-01
Np-238	1.02E-03	2.09E-09
Np-239	3.53E-07	2.72E-12
Pu-236	1.81E-06	1.77E-06
Pu-238	1.32E-01	1.33E-01
Pu-239	7.21E-03	7.21E-03
Pu-240	6.29E-04	6.29E-04
Pu-241	2.91E-04	2.89E-04
Pu-242	1.57E-05	1.57E-05
Fsprod	7.92E-03	7.92E-03

OUTPUT AT 660.0 DAYS

Reaction rates at 660.0 days:

Nuclide	Initial Amount	Final Amount	Total Fission	Total Capture	Resonance Fission	Resonance Capture
Np-237	8.51E-01	8.17E-01	1.29E-10	4.58E-09	0.00E+00	2.47E-09
Np-238	2.09E-09	9.81E-04	2.68E-08	1.14E-09	0.00E+00	0.00E+00
Np-239	2.72E-12	3.29E-07	1.00E-24	1.00E-24	0.00E+00	0.00E+00
Pu-236	1.77E-06	2.12E-06	4.64E-09	4.32E-09	0.00E+00	0.00E+00
Pu-238	1.33E-01	1.59E-01	6.50E-10	3.59E-09	9.44E-11	7.68E-10
Pu-239	7.21E-03	9.99E-03	1.49E-08	9.35E-09	1.29E-08	8.48E-09
Pu-240	6.29E-04	1.00E-03	1.64E-10	4.58E-08	2.71E-11	4.38E-08
Pu-241	2.89E-04	5.33E-04	1.75E-08	6.42E-09	1.31E-08	5.05E-09
Pu-242	1.57E-05	3.55E-05	1.09E-10	1.49E-08	0.00E+00	0.00E+00
Fsprod	7.92E-03	1.11E-02	0.00E+00	0.00E+00	0.00E+00	0.00E+00

OUTPUT AT 700.0 DAYS

Nuclide	Initial Amount	Final Amount
Np-237	8.17E-01	8.17E-01
Np-238	9.81E-04	2.01E-09
Np-239	3.29E-07	2.54E-12
Pu-236	2.12E-06	2.06E-06
Pu-238	1.59E-01	1.59E-01
Pu-239	9.99E-03	9.99E-03
Pu-240	1.00E-03	1.00E-03
Pu-241	5.33E-04	5.30E-04
Pu-242	3.55E-05	3.55E-05
Fsprod	1.11E-02	1.11E-02

OUTPUT AT 800.0 DAYS

			Reaction rates at 800.0 days:			
Nuclide	Initial Amount	Final Amount	Total Fission	Total Capture	Resonance Fission	Resonance Capture
Np-237	8.17E-01	7.84E-01	1.33E-10	4.59E-09	0.00E+00	2.51E-09
Np-238	2.01E-09	9.44E-04	2.61E-08	1.11E-09	0.00E+00	0.00E+00
Np-239	2.54E-12	3.07E-07	1.00E-24	1.00E-24	0.00E+00	0.00E+00
Pu-236	2.06E-06	2.38E-06	4.62E-09	4.29E-09	0.00E+00	0.00E+00
Pu-238	1.59E-01	1.83E-01	6.51E-10	3.42E-09	9.02E-11	7.31E-10
Pu-239	9.99E-03	1.28E-02	1.42E-08	8.91E-09	1.22E-08	8.07E-09
Pu-240	1.00E-03	1.44E-03	1.68E-10	4.18E-08	2.65E-11	3.99E-08
Pu-241	5.30E-04	8.43E-04	1.67E-08	6.07E-09	1.24E-08	4.76E-09
Pu-242	3.55E-05	6.57E-05	1.13E-10	1.48E-08	0.00E+00	0.00E+00
Fsprod	1.11E-02	1.47E-02	0.00E+00	0.00E+00	0.00E+00	0.00E+00

OUTPUT AT 840.0 DAYS

Nuclide	Initial Amount	Final Amount
Np-237	7.84E-01	7.84E-01
Np-238	9.44E-04	1.94E-09
Np-239	3.07E-07	2.37E-12
Pu-236	2.38E-06	2.32E-06
Pu-238	1.83E-01	1.84E-01
Pu-239	1.28E-02	1.28E-02
Pu-240	1.44E-03	1.44E-03
Pu-241	8.43E-04	8.38E-04
Pu-242	6.57E-05	6.57E-05
Fsprod	1.47E-02	1.47E-02

PLUTONIUM QUALITY, IMPURITY, AND PRODUCTION LEVELS:

Time (Days)	Total Plutonium Production (Kg total Pu per initial Kg Np-237)	Pu-238 Quality (%)	Pu-236 ppm level
100.0	3.70E-02	98.1	15.2
140.0	3.82E-02	98.2	14.3
240.0	7.33E-02	96.6	14.3
280.0	7.43E-02	96.6	13.7
380.0	1.07E-01	95.3	13.6
420.0	1.08E-01	95.3	13.1
520.0	1.40E-01	94.2	13.0
560.0	1.41E-01	94.2	12.6
660.0	1.70E-01	93.2	12.5
700.0	1.71E-01	93.2	12.1
800.0	1.99E-01	92.3	12.0
840.0	1.99E-01	92.4	11.6